GFHybrids
Group of Functional Organic-Inorganic Hybrids

university of aveiro
theoria poiesis praxis

ciceco
centre for research in ceramics & composite materials

Thermometry at the Nanoscale

L. D. Carlos

Physics Department & CICECO
University of Aveiro, Portugal
http://sweet.ua.pt/~lcarlos/

July 18th, XIX Escuela Internacional de Verano Nicolás Cabrera
INTERNATIONAL SUMMER SCHOOL ON FLUORESCENT NANO-PARTICLES IN BIO-MEDICINE

ahcravo

university of aveiro
theoria poiesis praxis

ciceco
centre for research in ceramics & composite materials

GFHybrids
Group of Functional Organic-Inorganic Hybrids


Carlos Brites


Patricia Lima


Nuno Silva


Vitor Amaral

icma
INSTITUTO DE CIENCIA DE MATERIALES DE ARAGÓN

UNIVERSIDAD DE ZARAGOZA

CSIC

Instituto de Ciencia de Materiales de Aragón
Universidad de Zaragoza, Spain


A. Millan


F. Palacio

GFHybrids
Group of Functional Organic-Inorganic Hybrids

MAIN GOALS

- General overview of recent examples of luminescent and non-luminescent thermometers working at nanometric scale.

- Performance of self-referencing Eu^{3+}/Tb^{3+} luminescent molecular thermometers based on functional hybrid materials combining:
  - Self-referencing that allows absolute measurements
  - $1\%\cdot K^{-1}$ maximum temperature sensitivity in the physiological gamut
  - High photostability for long-term use
  - Flexibility to be processed as thin films for mapping large areas
  - Multifunctionality (hosted in silica-coated magnetic NPs)

OUTLINE

- I. Why thermometry at sub-micron scale? Which is need for?
- II. Temperature sensing at microscale
- II. Sensing/mapping at a submicron scale
- III. Eu/Tb luminescent nanothermometer I
  - Breakthrough
  - Design & characterization
  - Performance and spatial resolution
- IV. Eu/Tb luminescent nanothermometers operating at physiological temperatures
- V. Conclusions and outlook

NJC
New Journal of Chemistry
A journal for new directions in chemistry
www.rsc.org/njc
Volume 35 | Number 6 | June 2011 | Pages 1149–1336

www.rsc.org/njc
New J. Chem. 2011, 35, 1177-1183
PERSPECTIVE

Lanthanide-based luminescent molecular thermometers†

Carlos D. S. Brites,[a] Patricia P. Lima,[a] Nuno J. O. Silva,[a] Angel Millán,[b] Vitor S. Amaral,[a] Fernando Palacio[b] and Luís D. Carlos*[a]

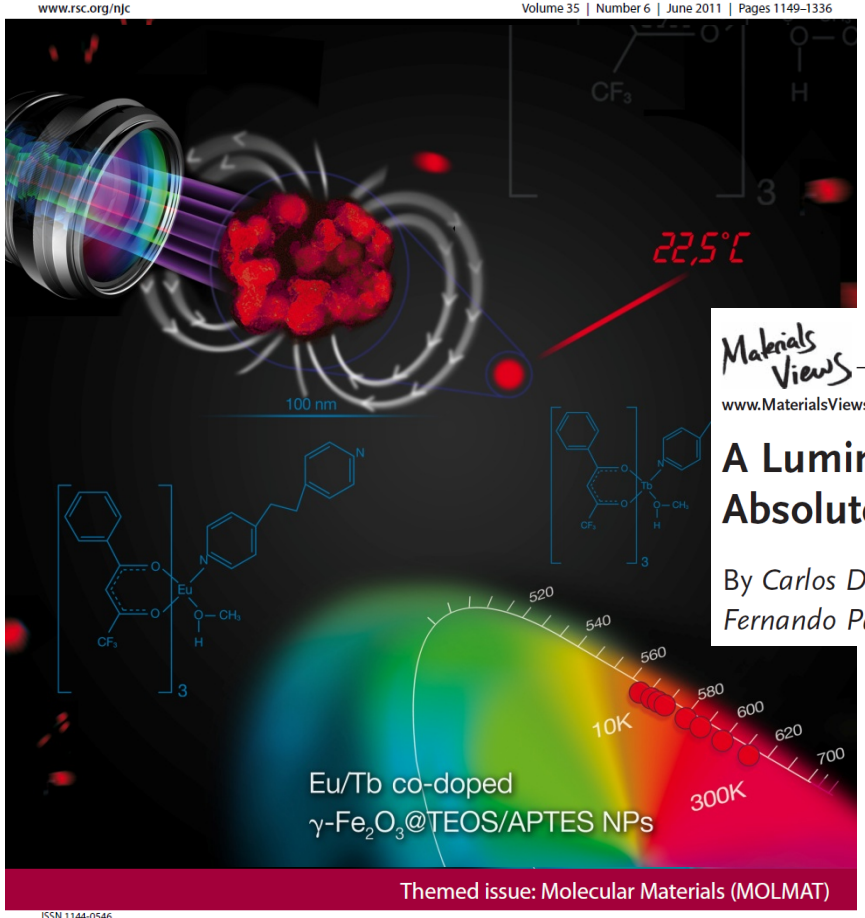

ISSN 1144-0546
RSC Publishing
International Year of CHEMISTRY 2011
1144-0546(2011)35:6;1-I

Materials Views
www.MaterialsViews.com
Adv. Mater. 2010, 22, 4499–4504
ADVANCED MATERIALS
www.advmat.de

A Luminescent Molecular Thermometer for Long-Term Absolute Temperature Measurements at the Nanoscale

By *Carlos D. S. Brites, Patricia P. Lima, Nuno J. O. Silva, Angel Millán, Vitor S. Amaral, Fernando Palacio,* and Luís D. Carlos**

L. D. Carlos *et al.*, ***Chem. Soc. Rev.*** 2011, 40, 536–549, *Tutorial Review (Hybrid Materials themed issue)*

Nanoscale

Cite this: DOI: 10.1039/c2nr30663h

www.rsc.org/nanoscale

REVIEW

Thermometry at the nanoscale

Carlos D. S. Brites,[a] Patricia P. Lima,[a] Nuno J. O. Silva,[a] Angel Millán,[b] Vitor S. Amaral,[a] Fernando Palacio*[b] and Luís D. Carlos*[a]

Received 19th March 2012, Accepted 26th April 2012
DOI: 10.1039/c2nr30663h

Nanoscale

Cite this: *Nanoscale*, 2012, **4**, 4301

www.rsc.org/nanoscale

REVIEW

Luminescence nanothermometry†

Daniel Jaque*[a] and Fiorenzo Vetrone*[b]

Received 30th March 2012, Accepted 14th May 2012
DOI: 10.1039/c2nr30764b

Minireviews

O. S. Wolfbeis et al.

Angew. Chem. Int. Ed. 2011, 50, 4546 DOI: 10.1002/anie.201006835

Upconverting Nanoparticles

Upconverting Nanoparticles for Nanoscale Thermometry

*Lorenz H. Fischer, Gregory S. Harms, and Otto S. Wolfbeis**

I. Why thermometry at sub-micron scale? Which is the need for?

- Temperature measurements are crucial in countless scientific investigations and technological developments, 75%–80% of the sensor market throughout the world.

- Current technological demands (microelectronics, microoptics, photonics, microfluidics, nanomedicine) have reached a point such that the use of conventional thermometry is not able to make measurements when **spatial resolution** decreases to the submicron scale (*e.g.* in intracellular temperature fluctuations and temperature mapping of microcircuits and microfluids).

Spatial resolution: minimum distance to move in order to get ***ΔT (temperature change) > S*** (relative sensitivity, **figure of merit**)

$$S = \frac{\frac{d\Delta}{dT}}{\Delta}$$

parameter to be measured

J. Lee & N. A. Kotov, ***Nano Today***, 2007, 2, 48; K.M. McCabe & M. Hernandez, ***Pediatr. Res.***, 2010, 67, 469.

- Sensing temperature in an accurate way with sub–micron resolution is critical for understanding numerous features of micro and nanoscale electronic devices (thermal transport, heat dissipation, and profiles of heat transfer.

Microdevice for surface-thermometry using SU8/Rh B thin layer

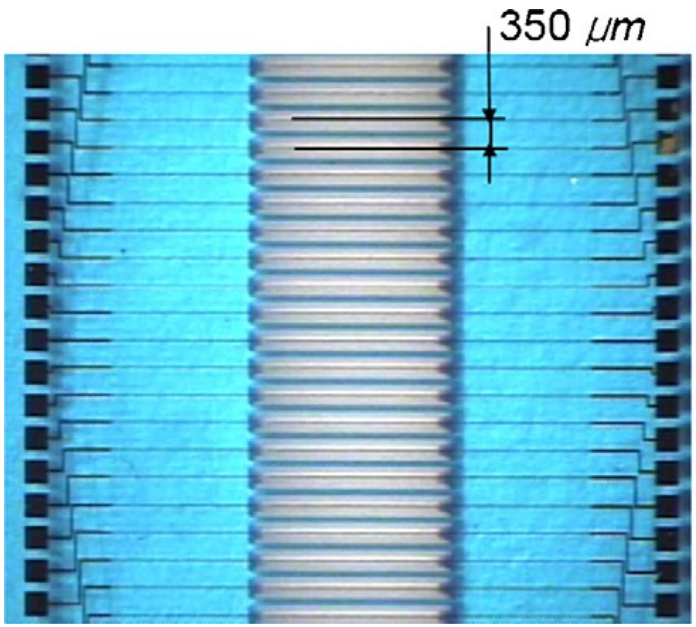

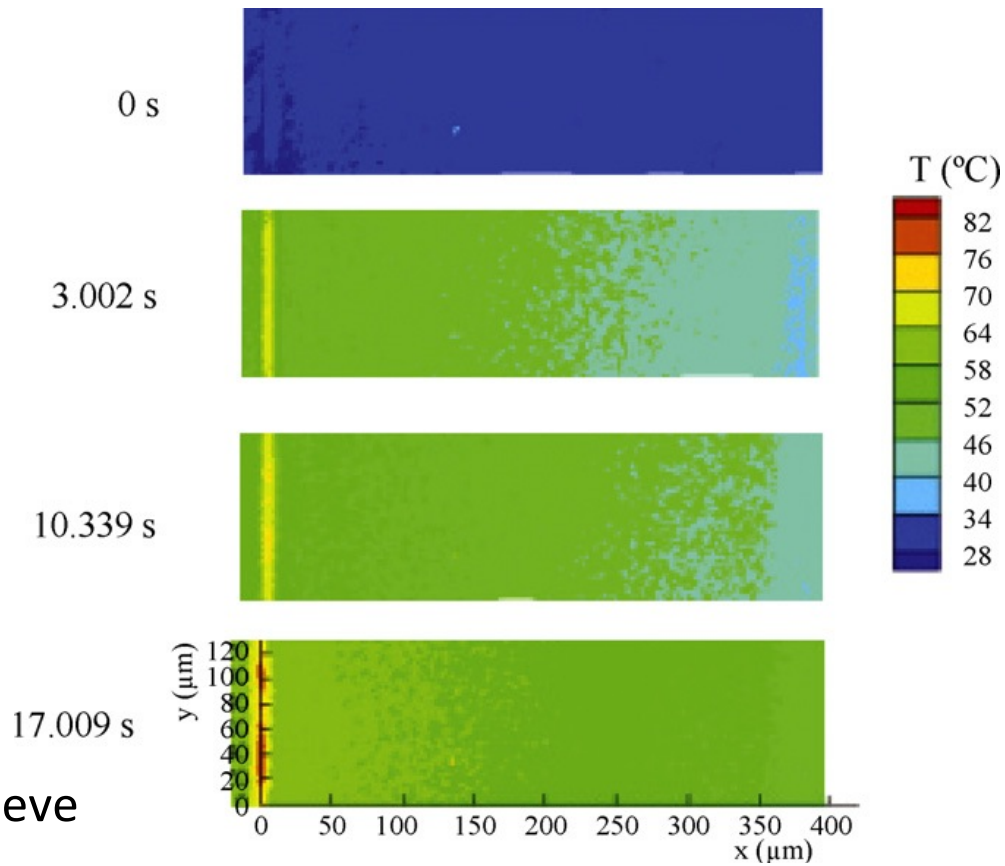

Thin layer spin-coated on the microheaters (heat sources) to achieve microscale heating

W. Jung *et al.*, ***Sens. Actuators A***, 2011, 171, 228

- Miniaturization of electronic and optoelectronic devices and circuits and ever faster switching speeds have increased the importance of localized heating problems and, thus, steady–state and transient characterization of temperature distributions is central for performance and reliability analysis

Scanning Thermal Microscopy

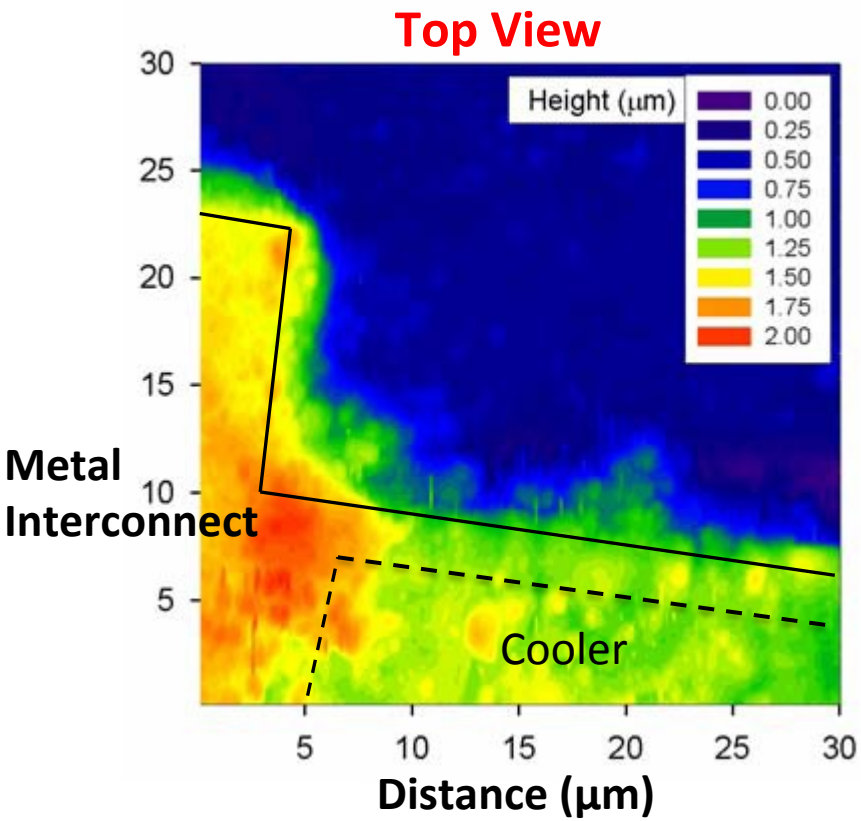

High resolution thermal and topography maps are generated with a very small thermocouple on the tip of the AFM scanner very

nano-sized cantilever tip designed for topographic and thermal measurements on microrefrigerator sample.

J. Christofferson *et al.*, ***J. Electron. Packaging***, 2008, 130, 041101

- The precise mapping of the temperature of living cells, especially cancer cells (***higher*** temperature than those of ***normal tissues*** due to the increased metabolic activity) strongly improves the perception of their pathology and physiology

optimization of premature diagnosis and therapeutic processes (*e.g.* in hyperthermal tumour treatment and photodynamic therapy)

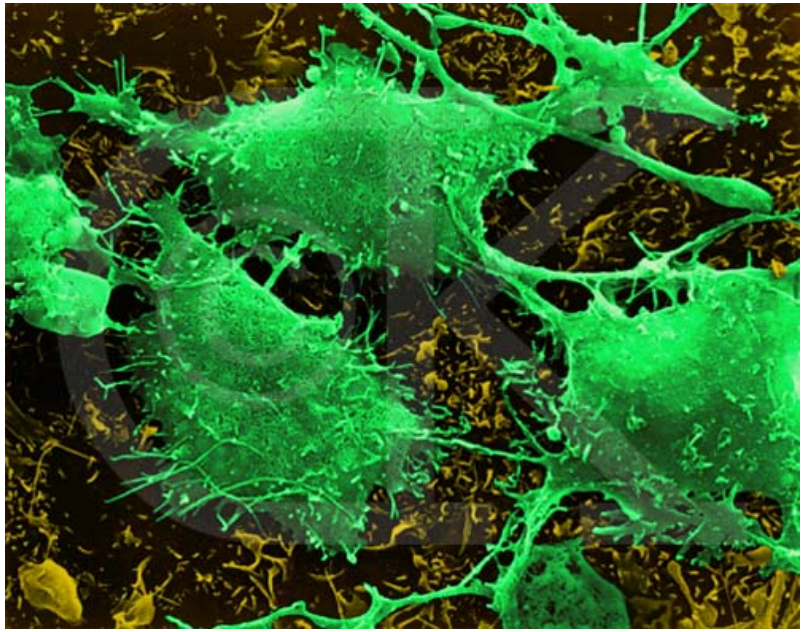

Electron Microscope Photos of Brain Cancer Cells
(http://www.alternative-cancer.net/Cell_photos.htm)

C. L. Wang *et al.*, ***Cell. Res.***, 2011, 21, 1517

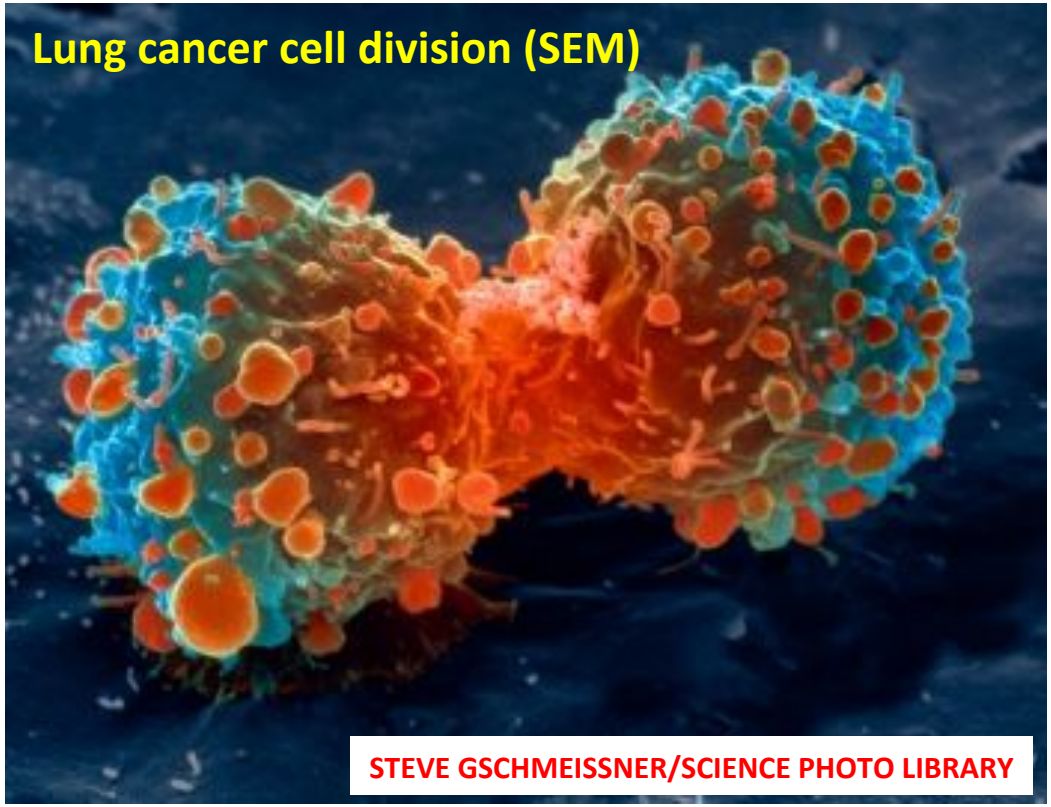

http://www.sciencephoto.com/set/1336

- The temperature of living cells is modified during every cellular activity (cell division, gene expression, enzyme reaction and changes in metabolic activity) leading to acute variation of intracellular temperatures.

The most popular approach to nanothermometers has been the miniaturization of the geometrical size of conventional thermometers.

- Luminescent thermometers based on temperature–dependent emission intensity and/or lifetime of dye–sensitized polymer dots, QDs, and Ln^{3+}–doped NPs;
- Nanoscale IR thermometers from metal NPs based on blackbody radiation;
- Scanning thermal microscopes based on Ln^{3+}–doped NPs;
- Nanoscale thermocouples fabricated from point contact junctions;
- Liquid– and solid–in–tube nanothermometers fabricated from nanotubes and based on temperature–dependent thermal expansion of liquids;
- Coulomb blockade nanothermometers from nanosized superconductor–insulator–metal tunnel junctions based on the Coulomb blockade of tunneling
- Complex structured nanothermometers from MEMS based on temperature–dependent resonator quality factor or Fermi–level shift.

C.D.S. Brites *et al.*, ***Nanoscale***, 2012, in press (DOI: 10.1039/c2nr30663h)

The well known example of expansion of Ga inside a CNT…

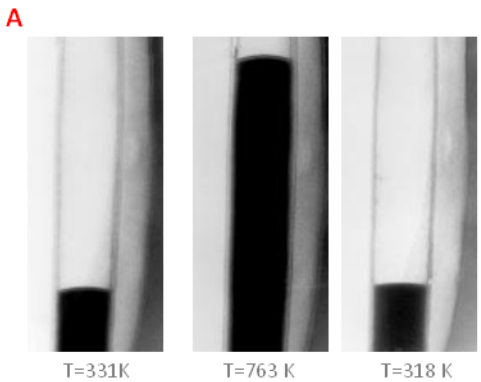

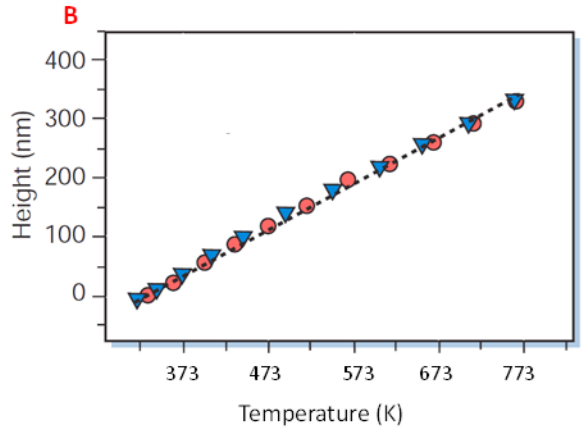

Calibration curve for obtained during heating (red circles) and cooling (blue triangles) stages.

Level of the Ga meniscus increases with the increasing of temperature

Y. H. Gao & Y. Bando, ***Nature***, 2002, 415, 599

Scanning Thermal Microscopy

A related technique based on *ac* heating of the resistive probe and monitoring *ac* current uses point contact junctions: measurement of the thermoelectric voltage of a platinum–gold point contact that is function of the local temperature. A Si AFM cantilever with a tip radius of ~20 nm, depositing a double Ti/Pt (5/40 nm) layer on both sides of the cantilever.

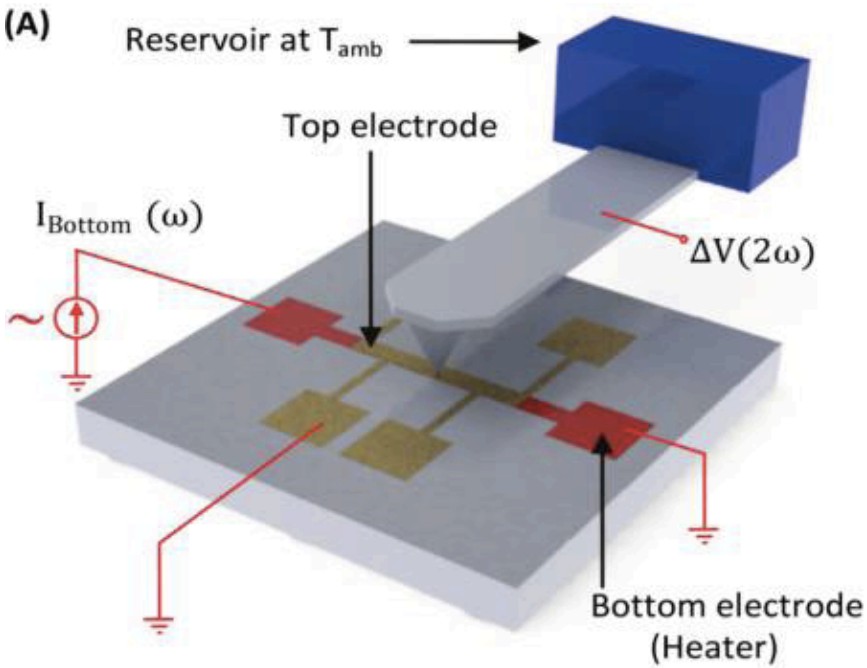

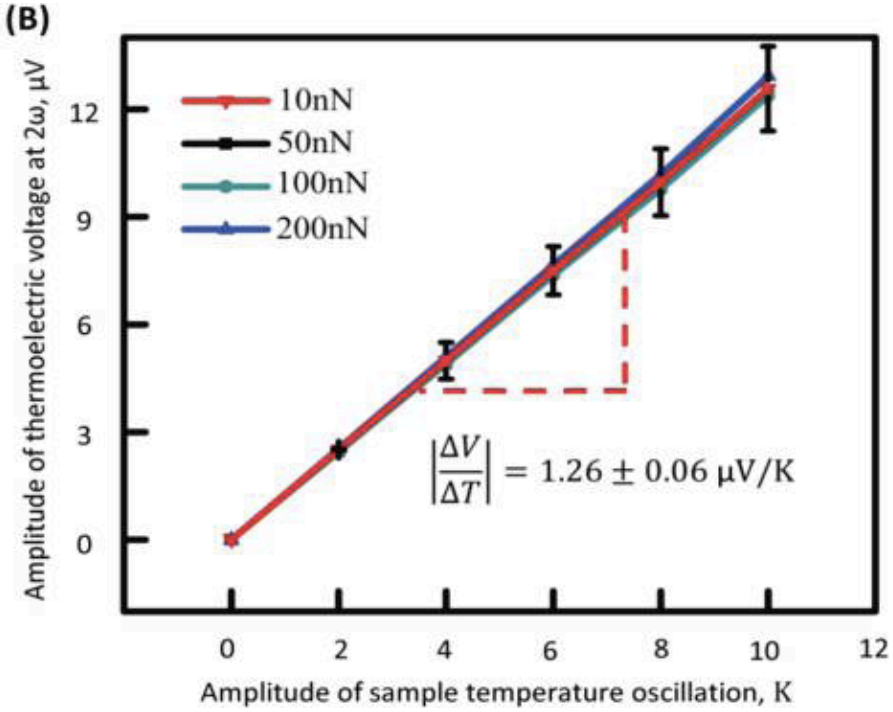

Sadat *et al.*, **Nano Lett.**, 2010, 10 2613

Scanning Thermal Microscopy

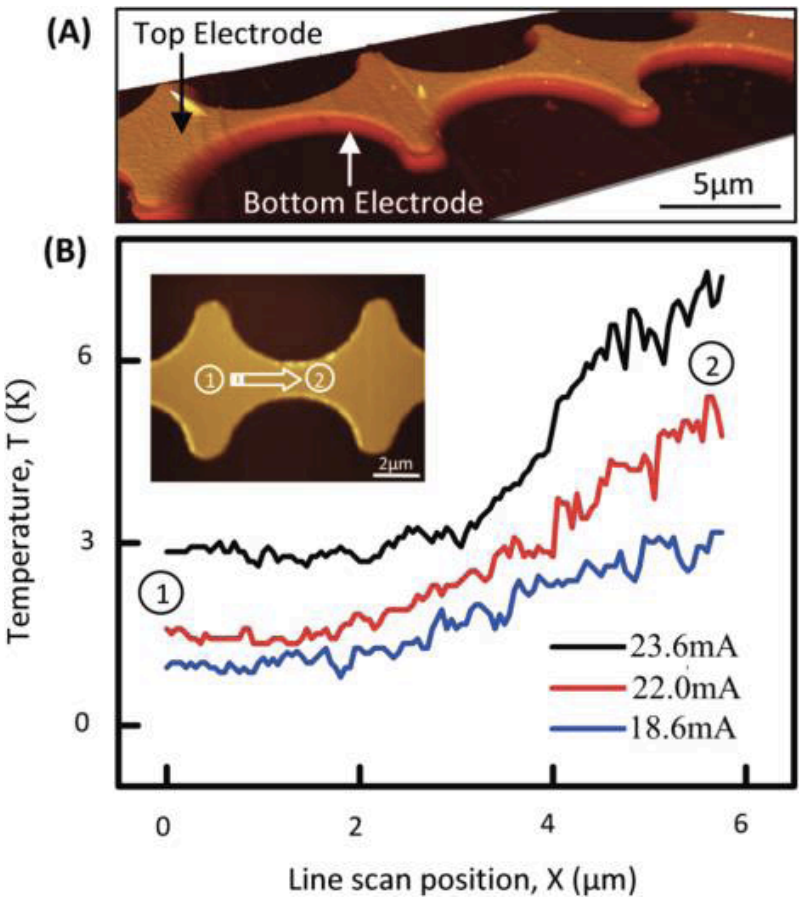

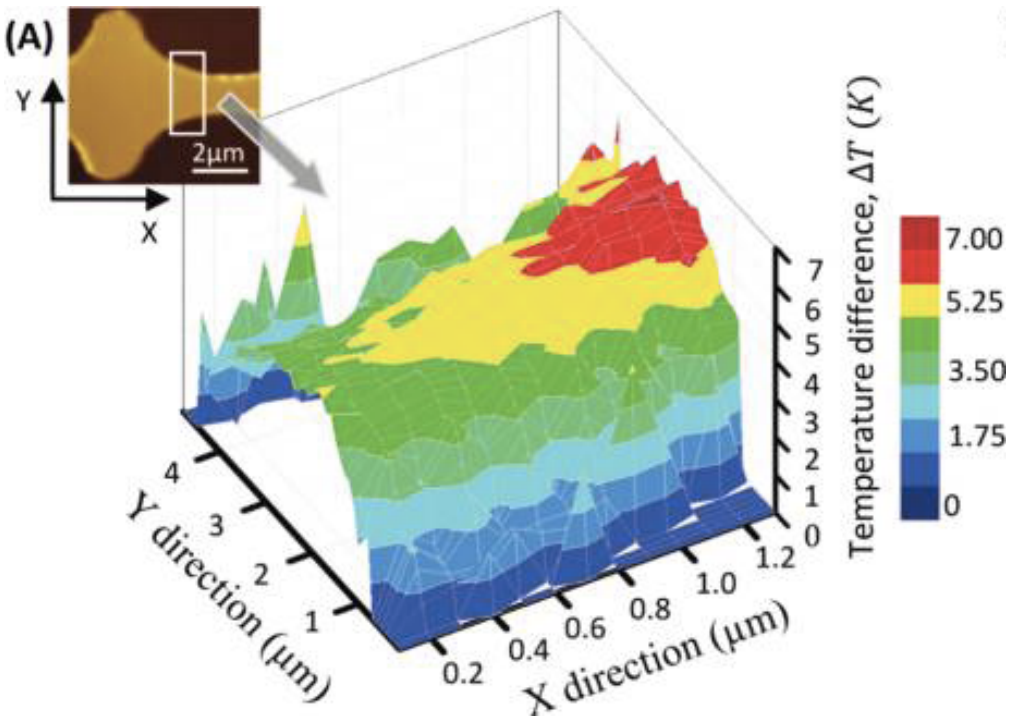

- High–resolution thermometry techniques have been catalogued in many different manners, for instance, depending on whether they make use of electrical or optical signals or based on near– or far–field applications.

- With this very general outline, it is common that the same technique is classified in different ways (scanning thermal microscopy can be either categorized as electrical or near–field thermometric method).

Table 1 Summary of the advantages, disadvantages and general applications of high-resolution electrical, near- and far-field thermal techniques. The typical spatial (δx), temporal (δt) and temperature (δT) resolutions of each method are also included. The table is adapted from those published by Asheghi and Yang[25] and Christofferson *et al.*[26]

High-resolution thermal measurement techniques in micrometer–nanometer range

		Typical resolution				
Method	Principle	δx (μm)	δT (K)	δt (μs)	Advantages	Disadvantages
Infrared thermography	Planck blackbody emission	10	10^{-1}	10	• Well implemented commercial technique	• Detector saturation at high temperatures • Difficulties on the precise estimation of the emissivity of the surface materials
					• Provides temperature image profile of the surface	• Spatial resolution for the temperature detection, which is Rayleigh limited (not all "hot bodies" are perfect blackbodies, in the physical meaning of the term)
Thermoreflectance	Temperature dependence of the reflection	10^{-1}	10^{-2}	10^{-1}	• High thermal and temporal resolution	• Requires the calibration of the reflectivity index • Spatial resolution limited by the diffraction limit
					• Quantitative and qualitative measurement	• Thermoreflectance coefficient is not available for every material and depends on excitation wavelength and thickness of the optical layer
Raman	Inelastic scattering of monochromatic light	1	10^{-1}	10^{6}	• No sample preparation needed • Works in solids and liquids	• Highly time-consuming technique implying image point analysis as slow as 0.5 point s^{-1}
					• Small volumes (<1 μm diameter) can be probed	• Low signal and crosstalk with fluorescent molecules

C.D.S. Brites *et al.*, ***Nanoscale***, 2012, in press (DOI: 10.1039/c2nr30663h)

Micro-thermocouple	Seebeck effect	10^{2}	10^{-1}	10	• Precise temperature calibration • Spatial resolution (at one dimension) of 25 nm	• The thermometer is separated from the active region of the device limiting, at very short timescales, the access to it • Additional fabrication effort required • Voltage reflections and capacitive coupling limit the timescale for transient thermometry of the device
Fluorescence thermography	Temperature dependence of quantum efficiency/ lifetime/intensity	10^{-1}	10^{-2}	10	• Diverse experimental techniques to measure temperature • High temperature sensitivity • Ratiometric algorithms are independent of illumination source	• Photobleaching limits the long-term intensity and lifetime determination • High-expensive excitation sources and detectors to measure temperature using lifetime-based algorithms
Near-field scanning optical microscopy	Use near field to improve optical resolution	10^{-2}	10^{-1}	10	• Spatial resolution below the Rayleigh limit (100 nm)	• Depends on the surface characteristics • Only access to surface temperature • Slow temperature acquisition • Vacuum and/or cryogenic temperatures required
Liquid crystal thermography	Crystal phase transitions (change colour)	10	10^{-1}	10^{2}	• Diverse materials available commercially for different temperature ranges • Fully integrated with electronic devices	• Yields a semi-quantitative temperature map, unless a detailed calibration is performed • A layer of the probe must be placed over the sample • Not compatible with liquid systems
Scanning thermal microscopy	AFM with thermocouple or Pt thermistor tip	10^{-1}	10^{-1}	10^{2}	• Uses AFM tips to simultaneously measure temperature and determine the surface roughness • Sub-micrometric spatial resolution	• Slow acquisition times • Limited to solid samples • Requires fundamental knowledge of tip-sample heat transfer

Contact Thermometers

- Thermocouples
- Pyrometers
- Filled System Thermometer
- Bimetalic Thermometers

Non-Contact Thermometers

- Raman
- Infrared
- Optical

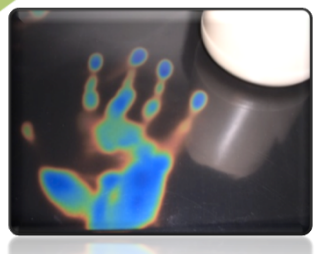

P. R. N. Childs *et al.*, ***Rev. Sci. Instrum.***, 2000, 71, 2959

Contact thermometers

- Measure of temperature by heat flow to a probe, collect information as an electrical signal

Advantages

- Well implemented technology
- Solutions for different temperature ranges
- Low cost temperature sensors
- High reproducibility and reliability

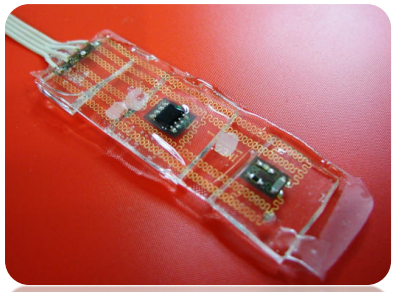

Disadvantages

- Sensor must be placed in contact with the sample
- Sensor often bigger than the sample to measure
- Calibration procedures may be needed
- Not suitable for measurements at scales below 10^{-6}m

Development of new non-contact accurate thermometers with micro and nanometric precision

J. Lee & N. A. Kotov, **Nano Today** 2007, 2, 48

Non-contact thermometers

A large number of molecular systems can be used to sense and measure temperature:

- High-spin/low spin systems
- Biomolecules: proteins, nucleic acids, mRNAs and others
- Thermoresponsive polymer gels
- QDs
- **Ln^{3+} complexes**
- Light-emitting molecules showing temperature-dependent conformations
- Organic dyes

Luminescent non-contact thermometers

- Optical probes (organic dyes, proteins, polymers, QDs, Ln^{3+}) emitting visible or NIR light (*thermochromic materials*)
- band shape
- peak energy & intensity
- excited states lifetimes

Advantages

- Noninvasive and accurate technique that works remotely by way of an optical detection system, even in biological fluids, strong electromagnetic fields and fast-moving objects
- Intensity ratio of two emissions provide self-calibration

Disadvantages

- Some examples use complex analysis of lifetimes or emission quantum yields
- Intensity decreases drastically under continuous excitation (photobleaching): <u>not suitable for long-term monitoring</u> (organic dyes)

Relative sensitivity as figure of merit

$$S = \frac{\frac{d\Delta}{dT}}{\Delta}$$

Temperature dependent parameter whose values were calculated fitting the experimental data graphically reported in literature to polynomial interpolations implemented with MatLab. A cut-off on the relative sensitivity values is assumed when the absolute temperature resolution is below 1 K.

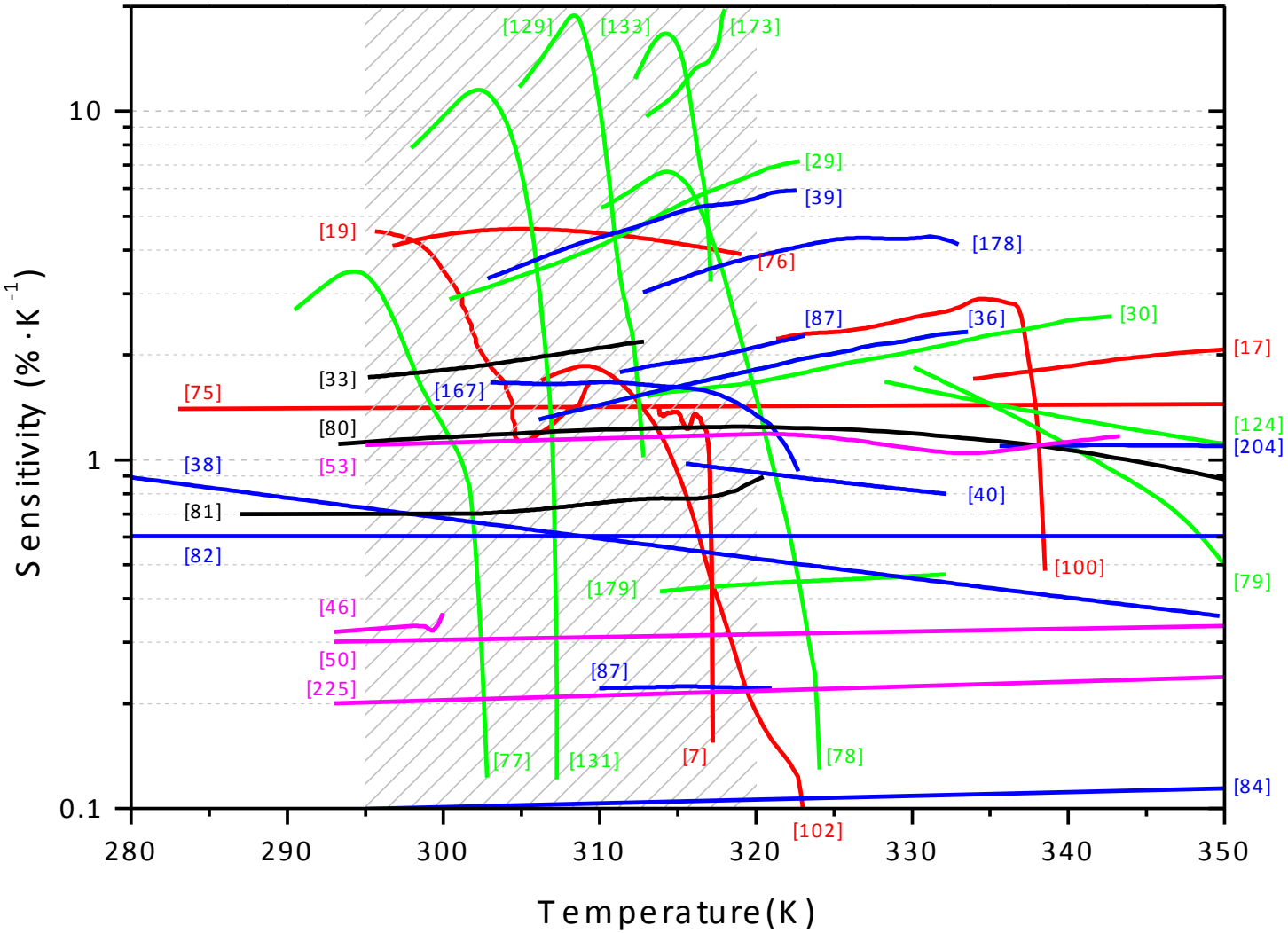

- Dye– (red), polymer– (green), QDs– (black) and Ln^{3+}–based (blue) luminescent thermometers. Non–luminescent thermometers in magenta.

C.D.S. Brites *et al.*, ***Nanoscale***, 2012, in press (DOI: 10.1039/c2nr30663h)

Luminescent ratiometric thermometers

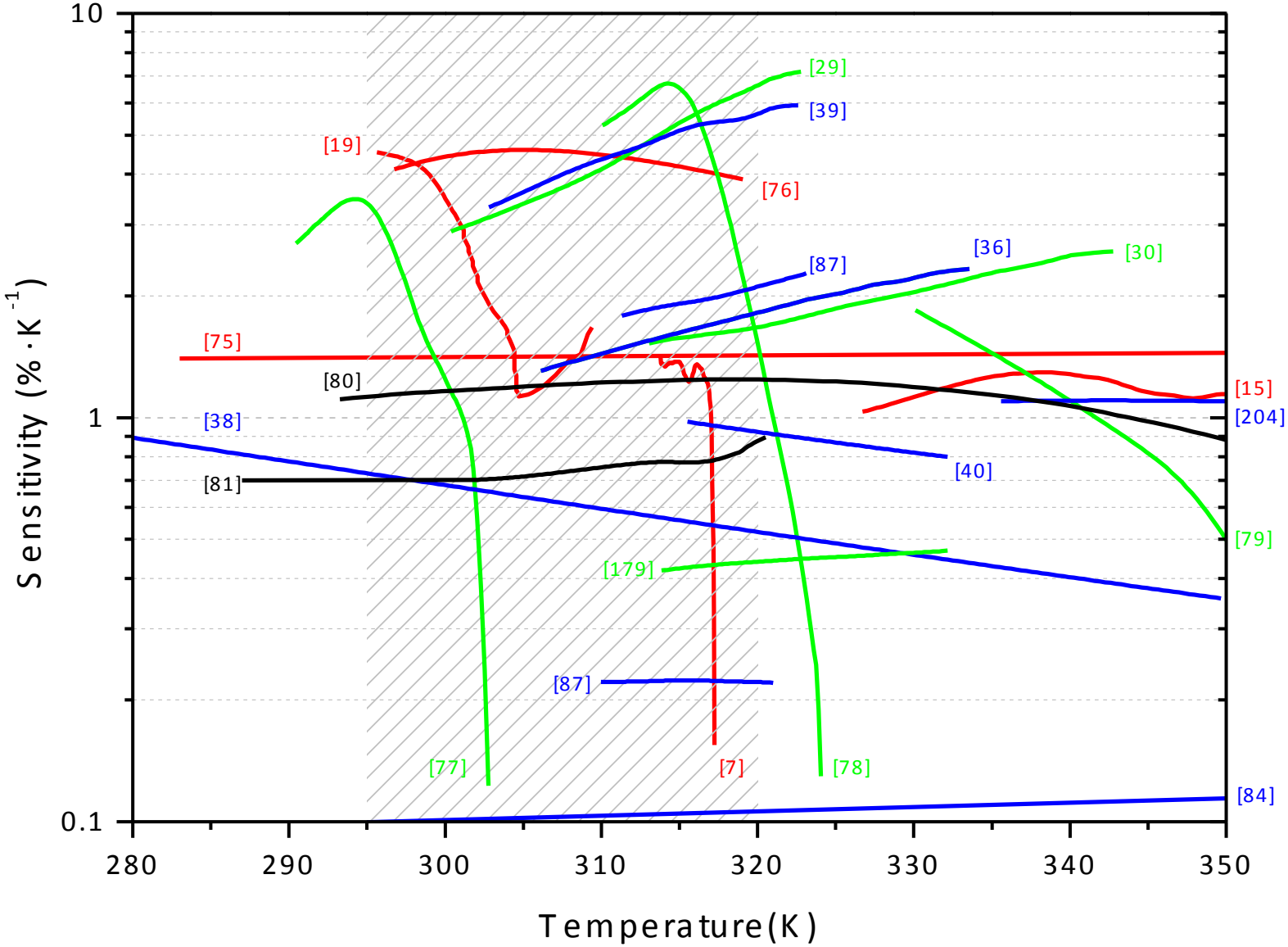

- Dyes (red), polymers (green), QDs (black), Ln^{3+} (blue)

Luminescent thermometers based on rise or decay times

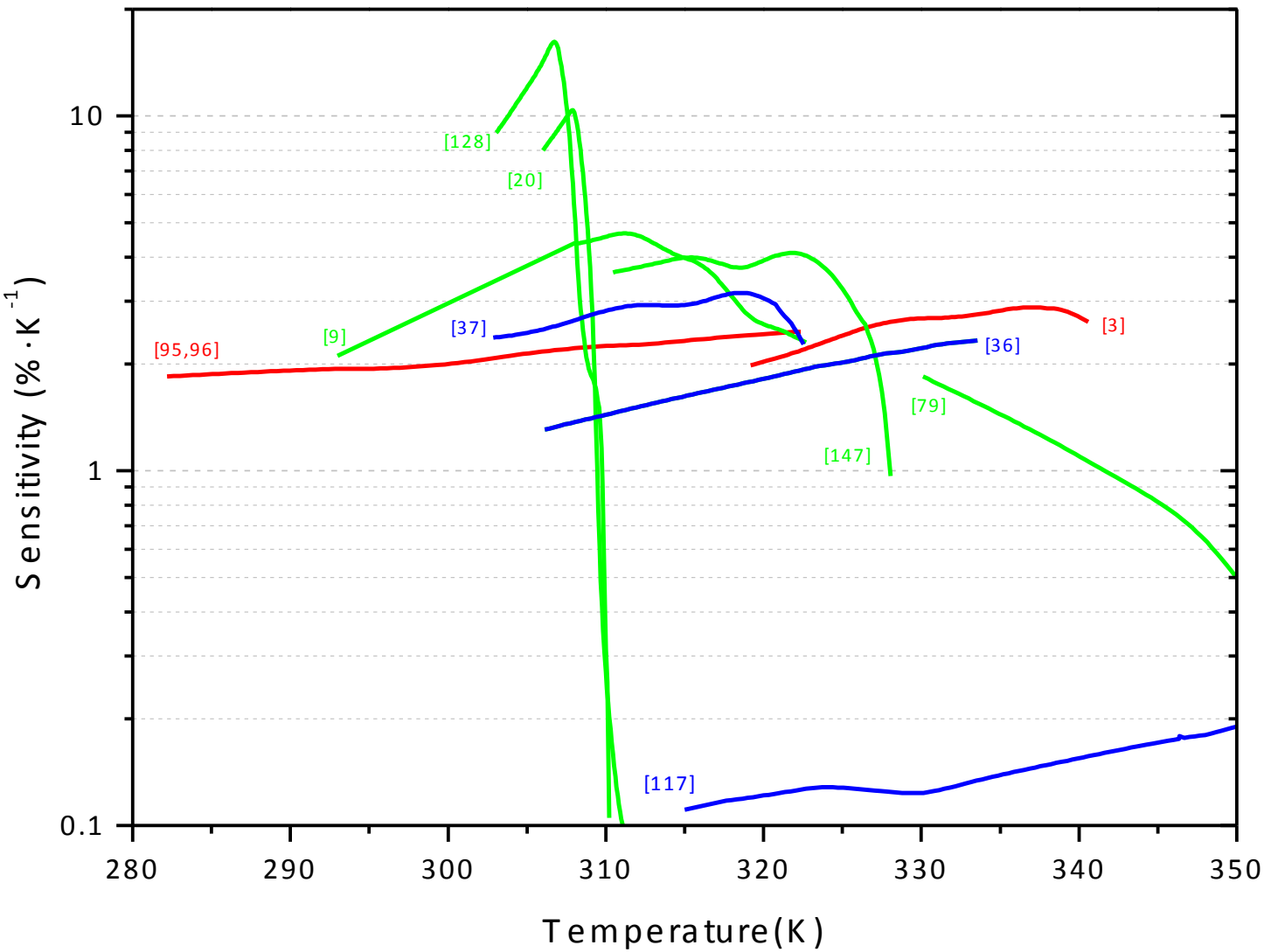

- Dyes (red), polymers (green), Ln^{3+} (blue)

Thermometers displaying spatial resolution <10 µm (dotted lines: non-ratiometric luminescent examples)

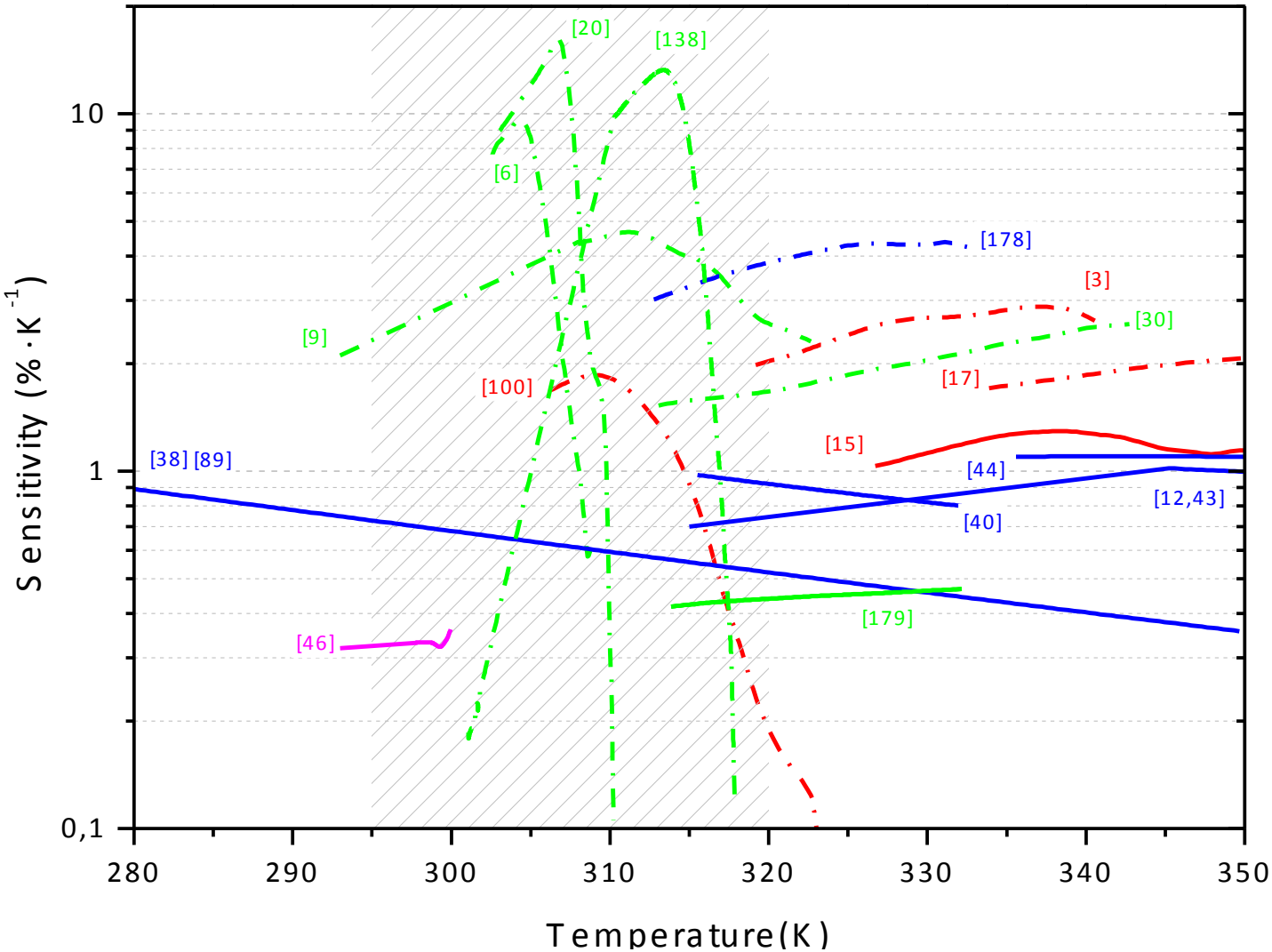

- Dyes (red), polymers (green), Ln^{3+} (blue). Non–luminescent thermometers in magenta.

II. Temperature sensing at microscale (Molecular nanothermometry)

- 2D distribution maps using $^5D_0$ rise-time temporal response in Y_2O_3:Eu

A. Khalid & K. Kontis, ***Meas. Sci. Technol.*** 2009, 20, 025305

- Siloxane hybrid nanoparticles (20-30 nm) incorporating a Eu^{3+} tris(β-diketonate) complex and an Eu^{3+} complex & an organic dye reference

H. S. Peng *et al.*, ***Adv. Mater.*** 2010, 22, 716; *ibid* ***J. Nanopart. Res.***, 2010, 12, 2729

- Scanning thermal microscope with Er^{3+}/Yb^{3+} co-doped fluoride glass or PbF_2 nanoparticles glued at the tip extremity

E. Saïdi *et al.*, ***Nanotechnology*** 2009, 20, 115703.L. Aigouy *et al.*, ***J. Appl. Phys.*** 2009, 106, 4301

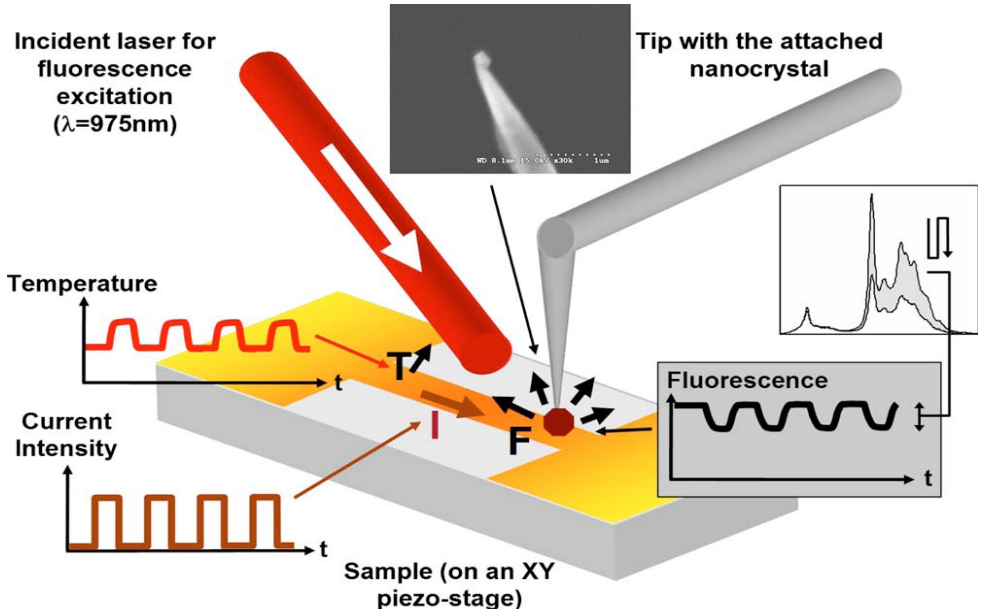

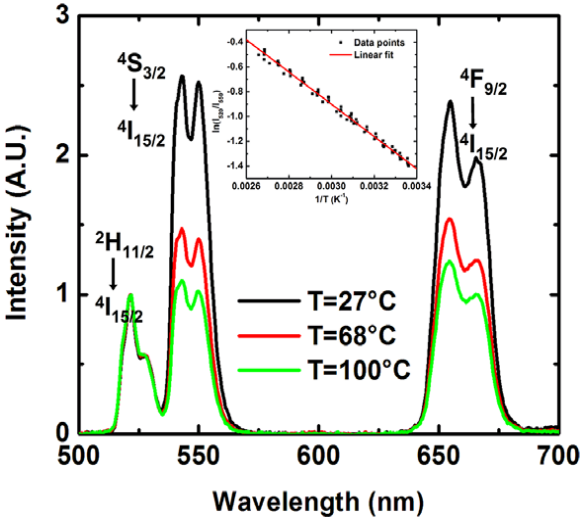

Cellular thermometers

- UC in $NaYF_4:Er^{3+},Yb^{3+}$ NPs (**ratiometric**)

F. Vetrone *et al.*, ***ACS Nano***, 2010, 4, 3254; Angew. Chem. Int. Edit., 2011, 50, 4546-4551.

- With an organic dye as the temperature probe (non-ratiometric)

C. Gota *et al.*, ***J. Am. Chem. Soc.*** 2009, 131, 2766

Thermoresponsive polymer

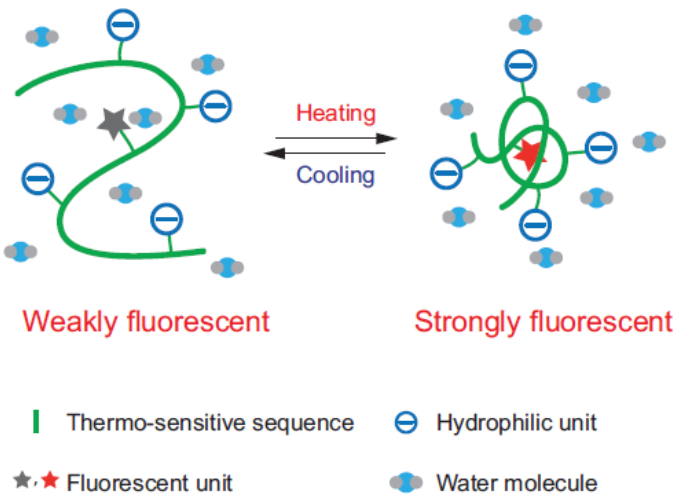

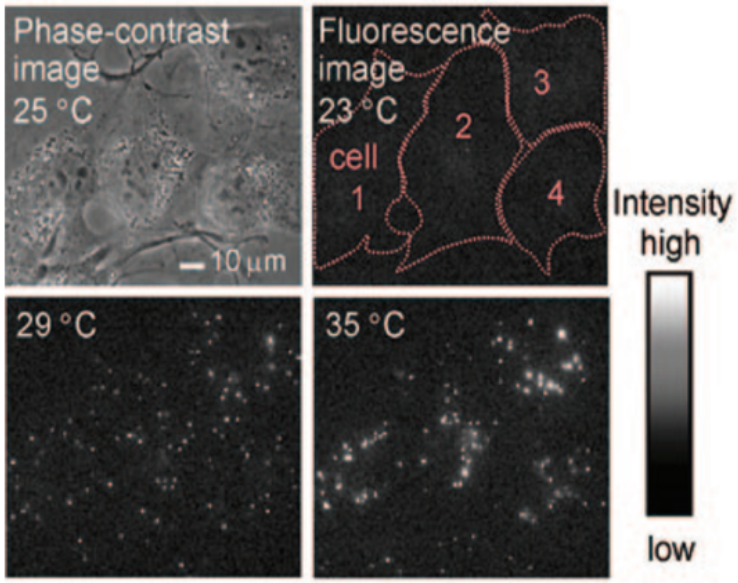

- Resolution of 0.3-0.5 K
- No intracellular temperature distribution

- Large size (>62 nm)
- Low hydrophilicity, hindered dispersion throughout the cell.

- Involving QDs as the temperature probe (**non-ratiometric**)

H. Huang *et al.*, ***Nat. Nanotechnol.*** 2010, 5, 602

$MnFe_2O_4$ NPs (6 nm) targeted to specific proteins on the plasma membrane of Human embryonic kidney cells (HEK 293) and heated by a RF magnetic field (***40 MHz, 8.4 G***) between 30 and 46 °C.

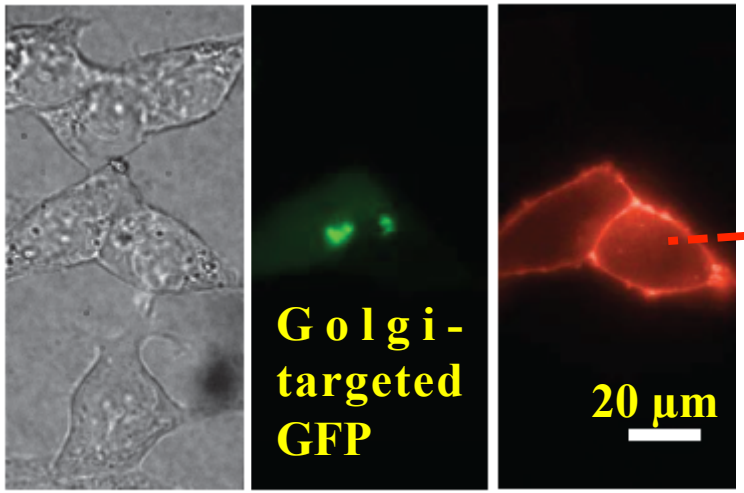

DyLight549 conjugated to the streptavidin-coated NPs, exclusively localized on the plasma membrane of the expressing cells

Microscopy images: group of HEK 293 cells, two of which are expressing Golgi-targeted GFP and the biotinylated membrane protein AP-CFP-TM.

After application of the RF magnetic field (hatched box)

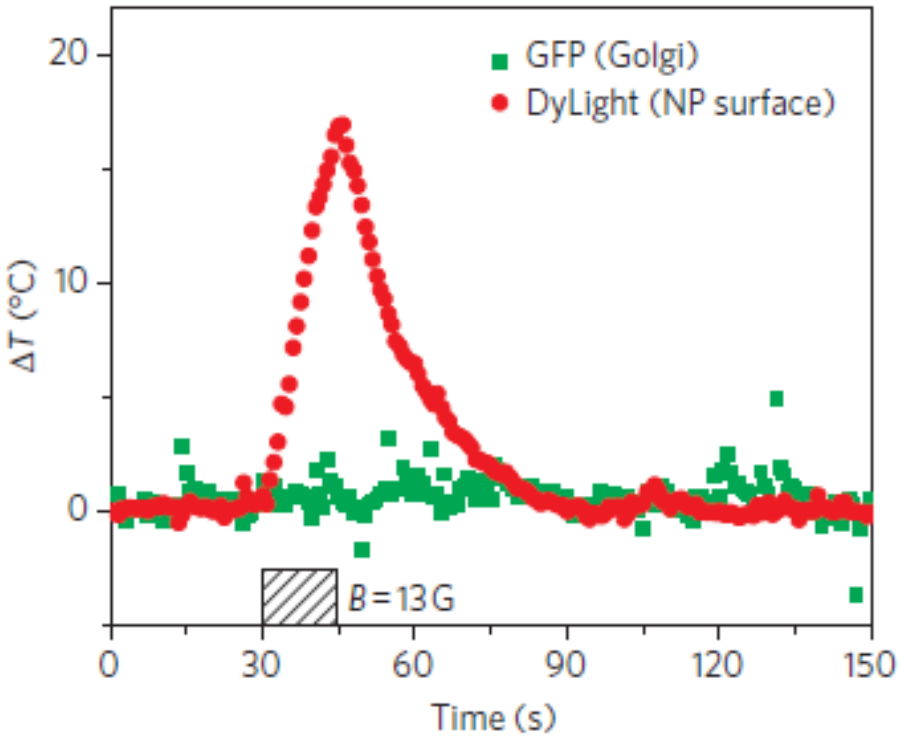

RF magnetic field-induced NP heating ***is sufficient*** to **trigger the opening of TRPV1 ion channels in cells**.

Neuronal signalling was demonstrated **triggering behavioural** responses in worms (*C. elegans*).

- The local temperature increases at the plasma membrane (red, decrease in DyLight549 fluorescence intensity)
- Remained constant at the Golgi apparatus (green, fluorescence intensity of Golgi-targeted GFP).

Heat generated locally in the plasma membrane without cytoplasmic heating

Fluorescent polymer internalized in living COS7 cells

(first effective intracellular temperature mapping)

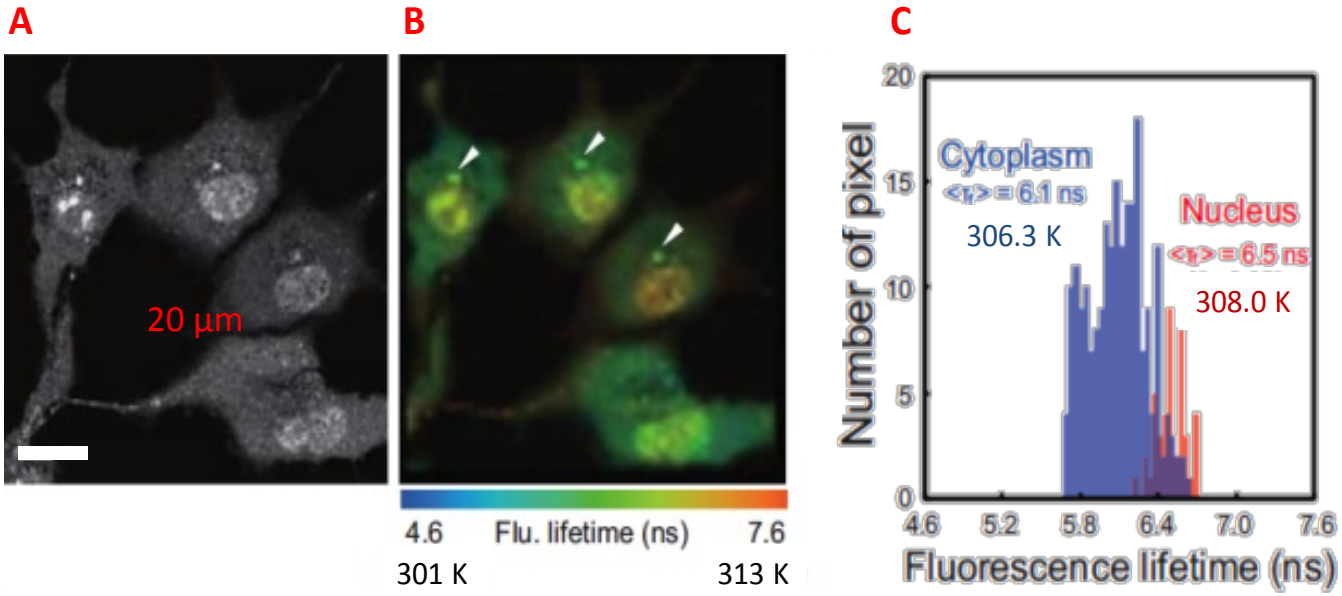

c

- Spatial resolution at the diffraction limit level (200 nm);
- S_m=4.4% K^{-1}, at 311 K;
- Fluorescence lifetime in the nucleus and in the cytoplasm in a representative cell, **mean temperature gradient of 1.9 K**.

K. Okabe *et al.*, **Nat. Commun.** 2012, 3, 705

III. Eu/Tb luminescent nanothermometer

The breakthrough…

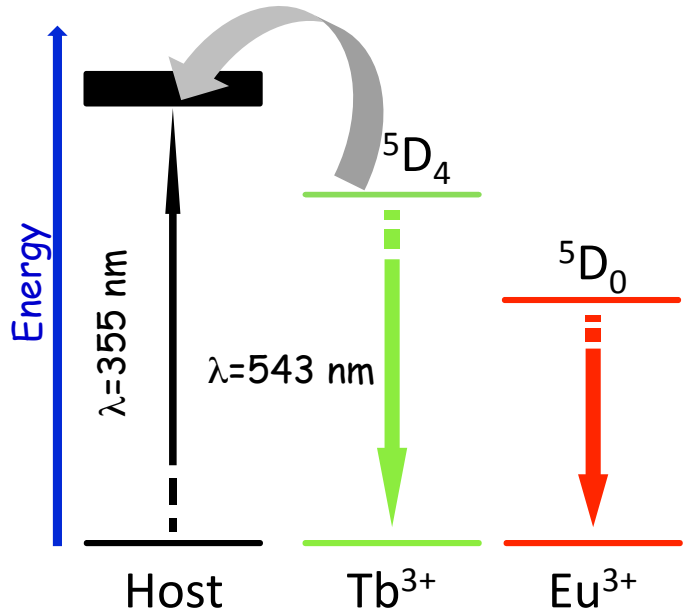

Patent
Spain – P200930367, 2009
EP 10791650.4, 2011
USA – 13380671, 2012

- ***Host rational design***; an excited triplet with energy above that of the Tb^{3+} $^5D_4$ state, thus warranting the occurrence of thermally-driven $^5D_4$⇨host energy transfer
- ΔE between that triplet state and the Eu^{3+} $^5D_0$ emitting level is too large to permit thermally-driven depopulation
- The Tb/Eu relative intensity guarantees **absolute measurement of temperature**
- **The self-calibration** (relative intensities) overcomes the well-known drawbacks of intensity-based measurements (*e.g.* sensor concentration and drifts of the lamp and detectors)

C.D.S. Brites *et al.*, **Adv. Mater.**, 2010, 22, 4499; **New J. Chem.**, 2011, 35, 1177; **Nanoscale**, DOI:10.1039/C2NR30663H

Thermometer design

- $[Ln(btfa)_3(MeOH)(bpeta)]$ (Ln=Eu & Tb) β-diketonates

- Organic-inorganic hybrid NPs formed by a maghemite (γ-Fe_2O_3) magnetic core coated with a tetraethyl orthosilicate/ aminopropyltriethoxysilane ***(TEOS/ APTES)*** organosilica shell (modified Stöber method)

- Eu/Tb co-doped NPs with Eu:Tb ratios of 2:1 **(NP3-2.1)**, 1:1 **(NP3-1.1)**, 1:2 **(NP3-1.2)**, 1:3 **(NP3-1.3)** and 1:10 **(NP3-1.10)**

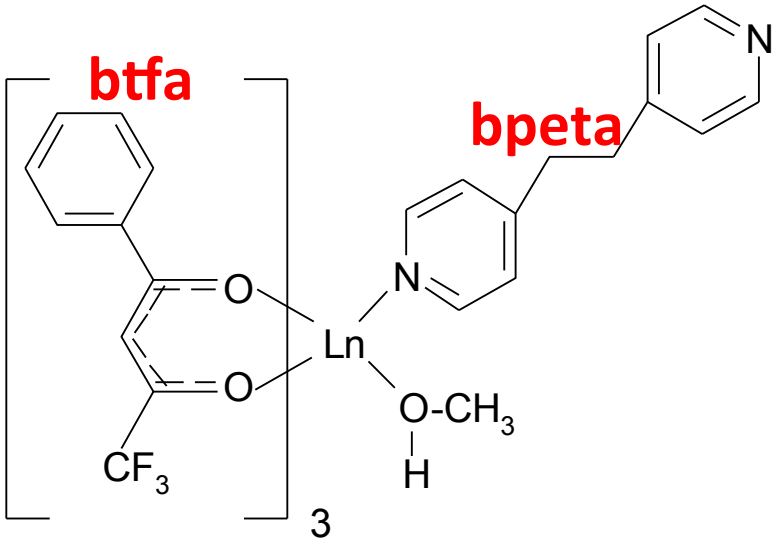

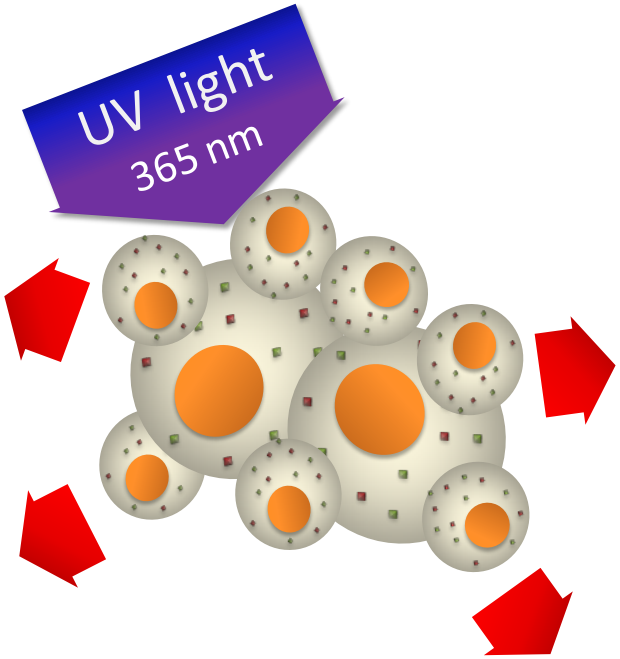

Nanoparticles characterization

DLS: NPs (dispersible in H_2O) diameter distribution

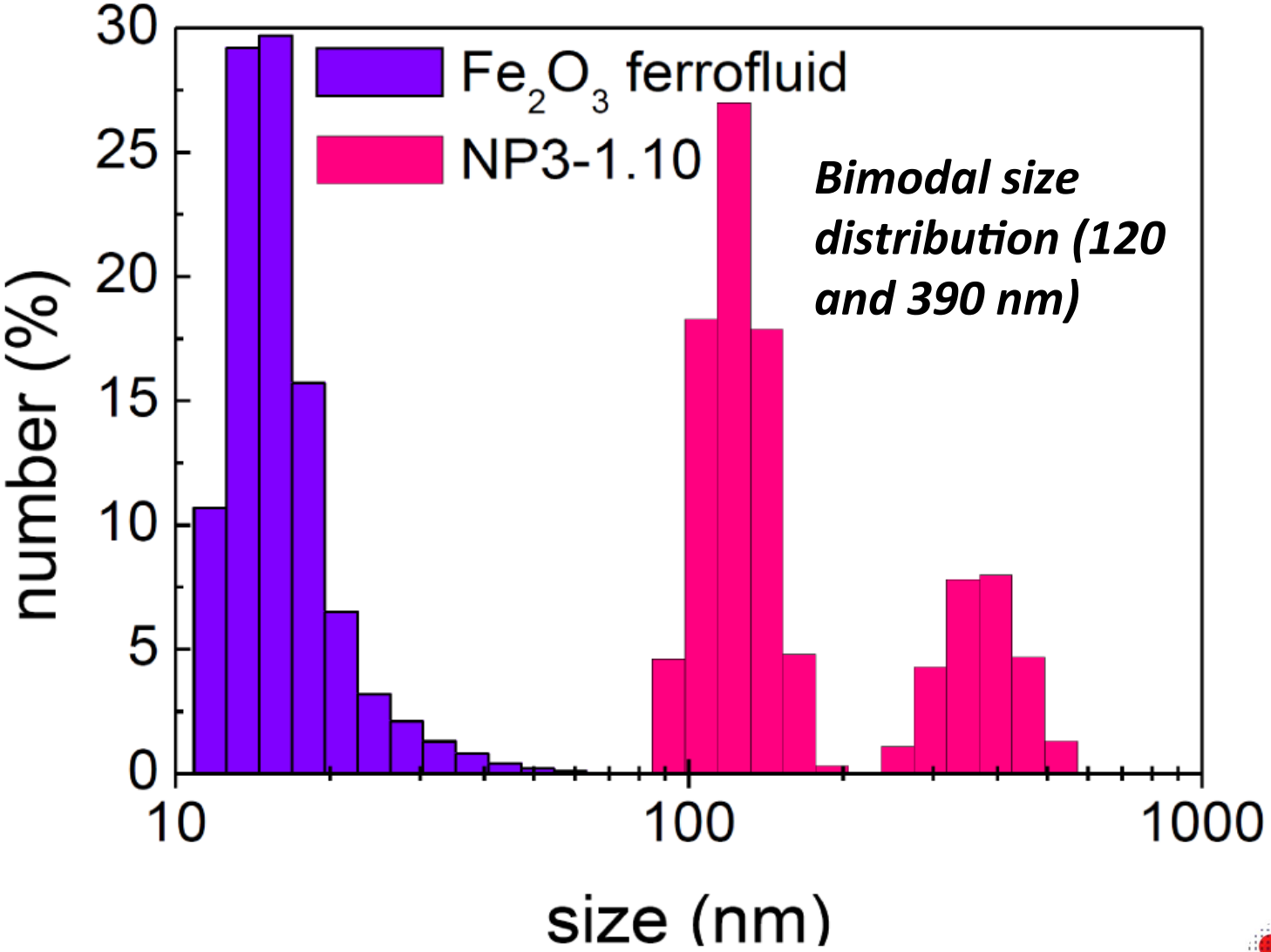

SEM & TEM (NP3-1.3)

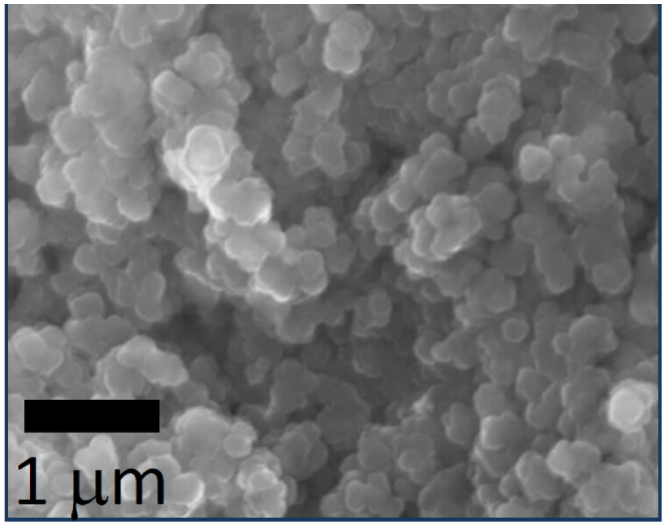

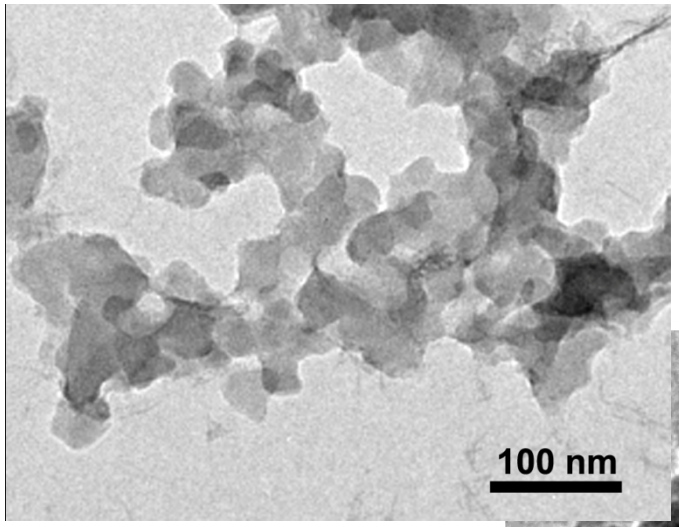

- High contrast: **Eu^{3+}/Tb^{3+}**
- Low contrast: **APTES/TEOS**

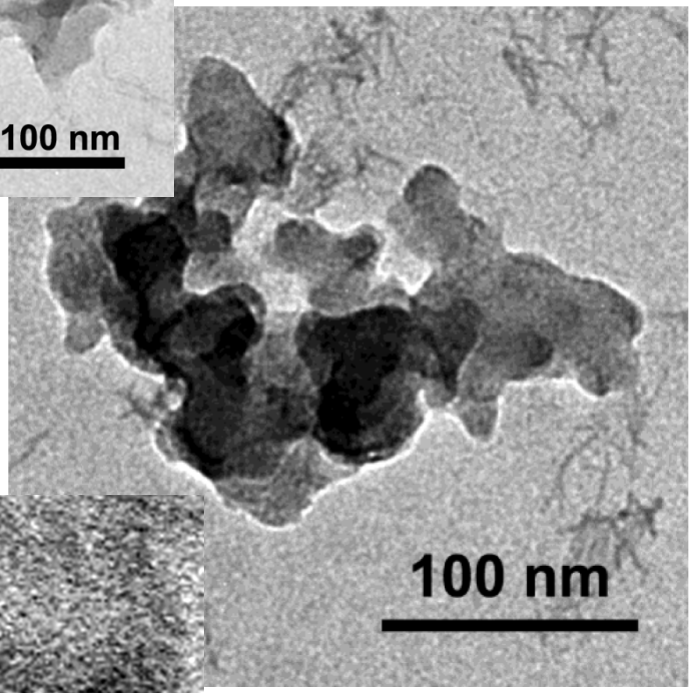

- NPs aggregation occurs during evaporation of the dispersions

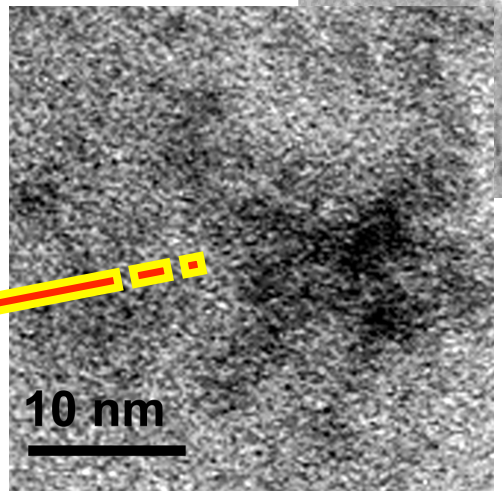

- **γ-Fe_2O_3**

EDS mappings

EDS mappings show Eu^{3+} and Tb^{3+} distributions with contours and shapes similar to those of the NPs

The NPs contain both Eu^{3+} and Tb^{3+}

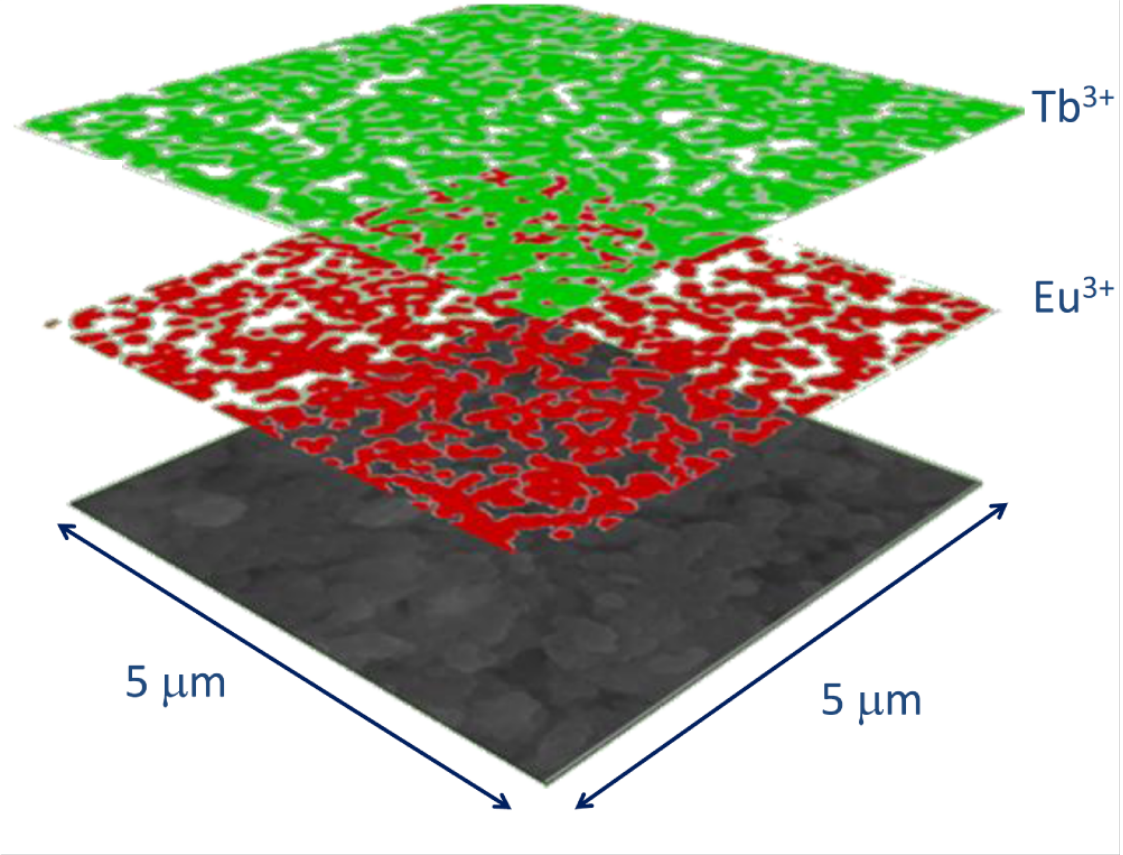

Photoluminescence

γ-Fe_2O_3@TEOS/APTES **NP3-1.3**

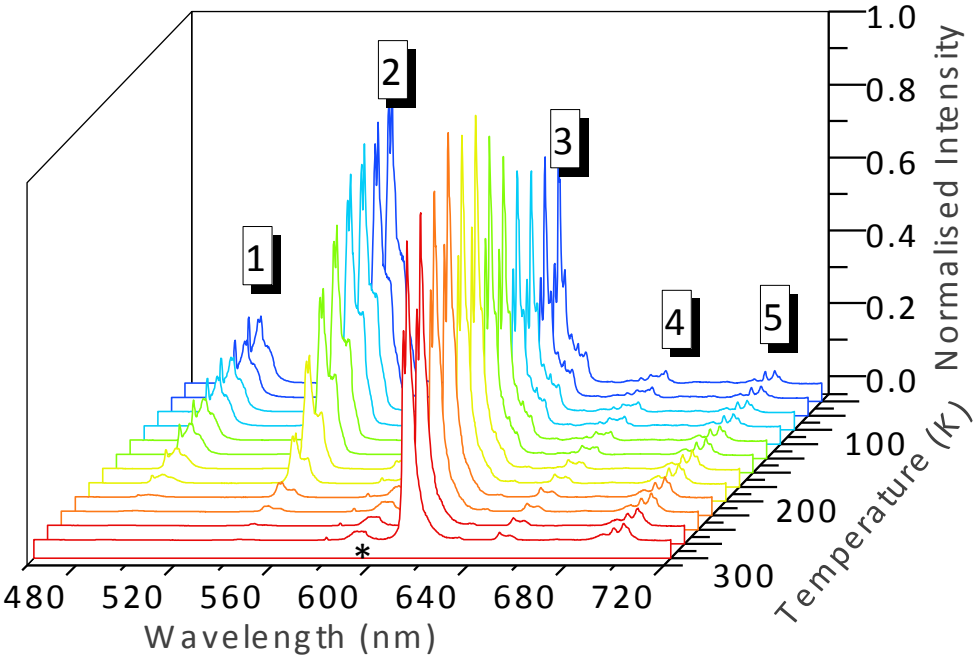

- **1** & **2**: $^5D_4 \Rightarrow {}^7F_{6,5}$ (Tb^{3+})
- **3**, **4** & **5**: $^5D_0 \Rightarrow {}^7F_{2\text{-}4}$ (Eu^{3+})
- Area marked with an asterisk: Eu^{3+}/Tb^{3+} ($^5D_0 \Rightarrow {}^7F_{0,1}$)/($^5D_4 \Rightarrow {}^7F_4$) overlapping

Commission Internacionale d'Éclairage (CIE) (x,y) color coordinates illustrates the dependence on T:

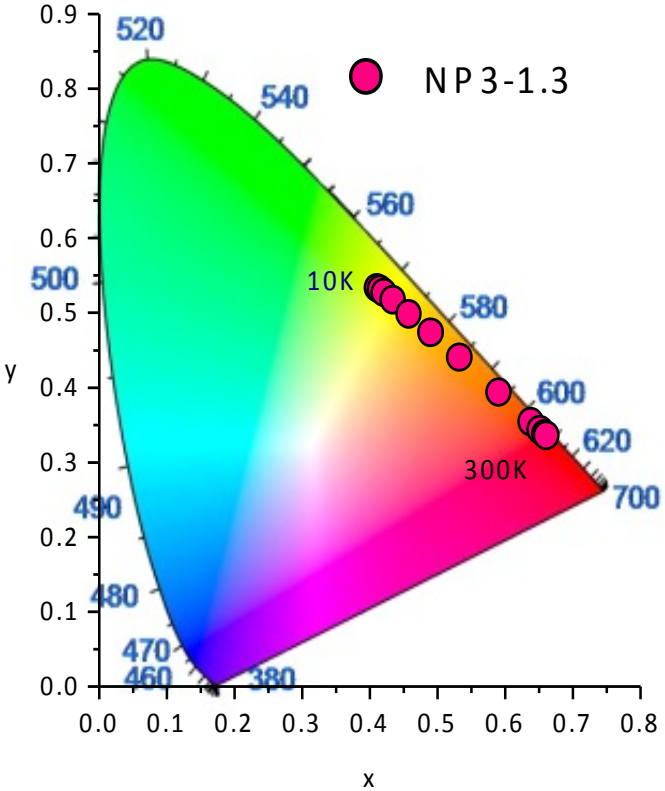

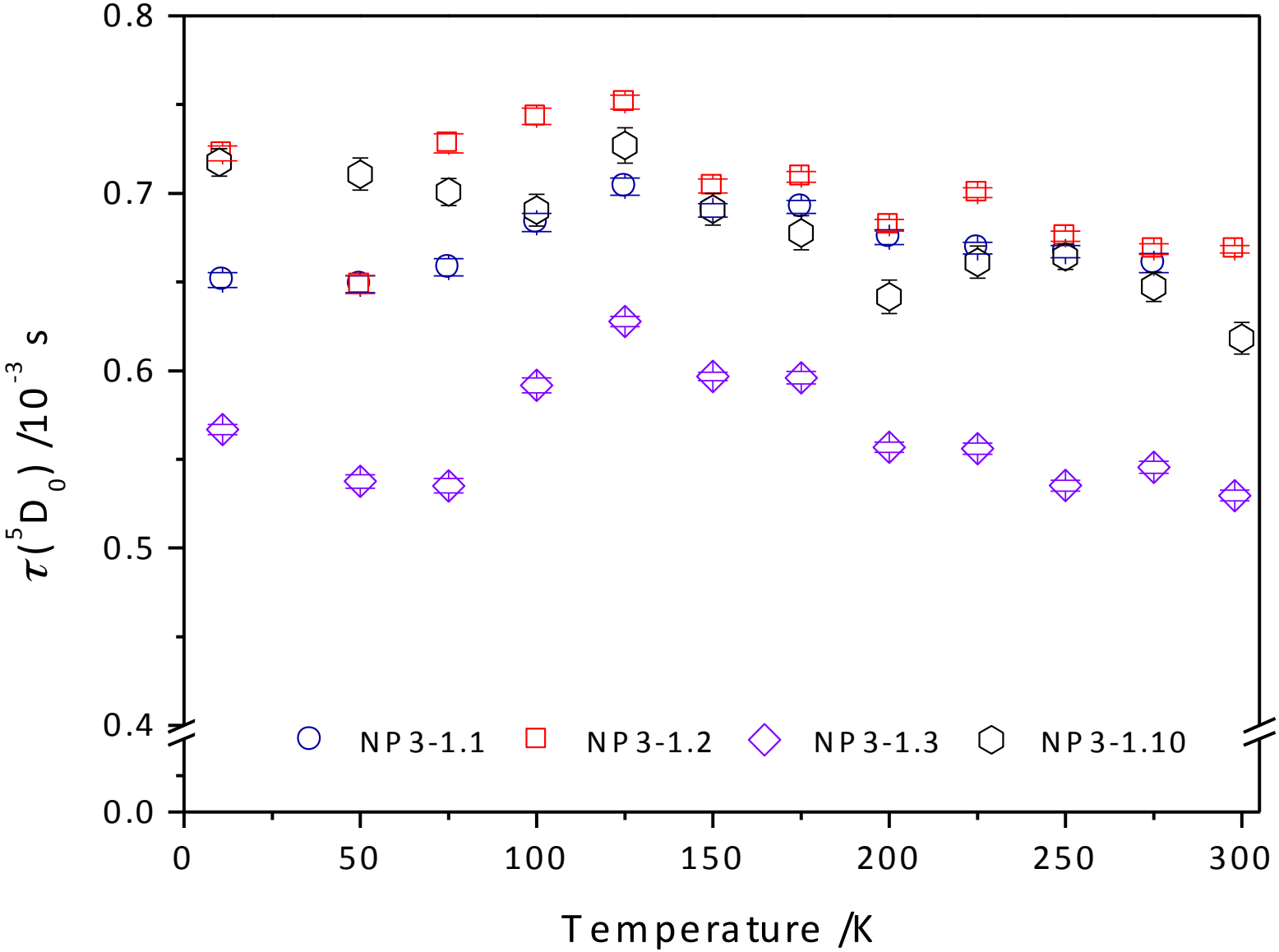
0.8
0.7
0.6
0.5
0.4
0.0
0
50
100
150
200
250
300
$\tau(^5D_0)$ /10^{-3} s
Temperature /K
NP3-1.1
NP3-1.2
NP3-1.3
NP3-1.10

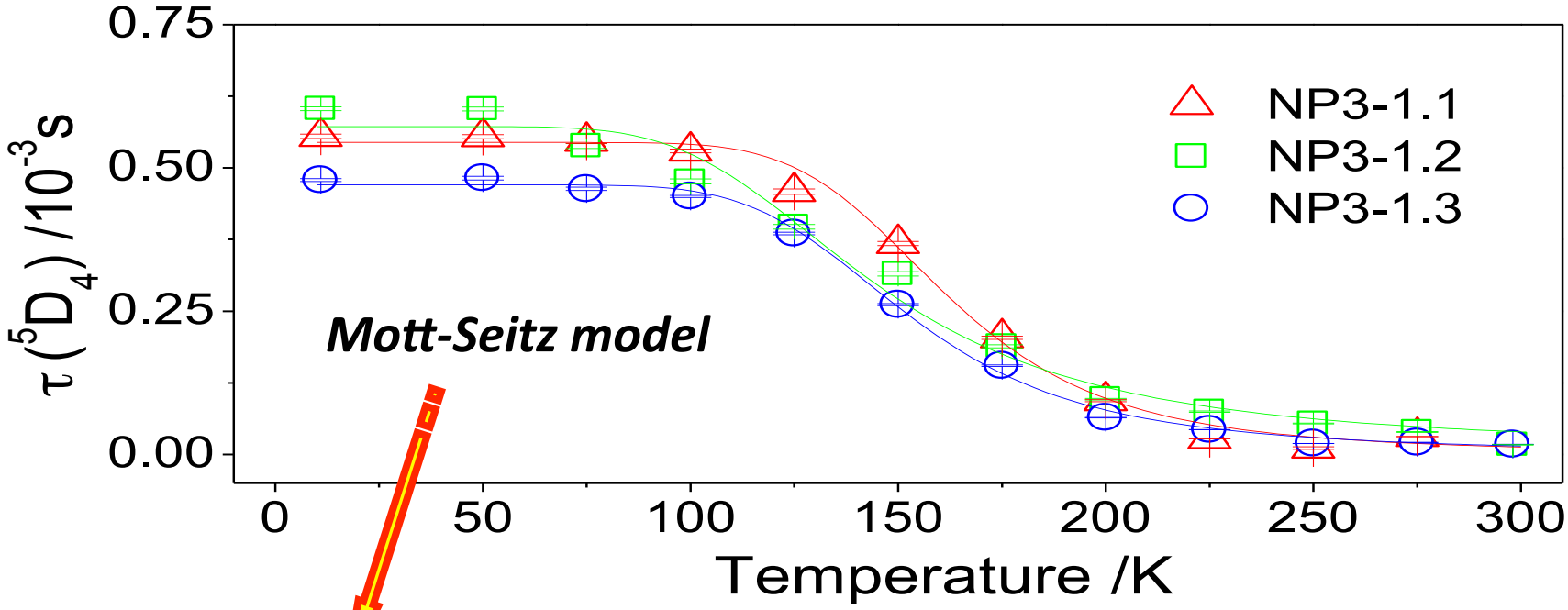

$$\tau^{-1} = \tau_r^{-1} + k\exp\left(-\frac{\Delta E}{k_B T}\right)$$

- τ_r: radiative lifetime
- k: migration energy rate
- ΔE: activation energy between the trap level and the $^5D_4$ state
- k_B: Boltzmann constant

Thermally activated non-radiative mechanism involving *a particular level* located above (500-700 cm^{-1}) the $^5D_4$ level (20590 cm^{-1})

NP3-1.1	**NP3-1.2**	**NP3-1.3**
ΔE=615±19 cm^{-1}	ΔE=521±18 cm^{-1}	ΔE=687±14 cm^{-1}

Emitting levels of the TEOS/APTES layer

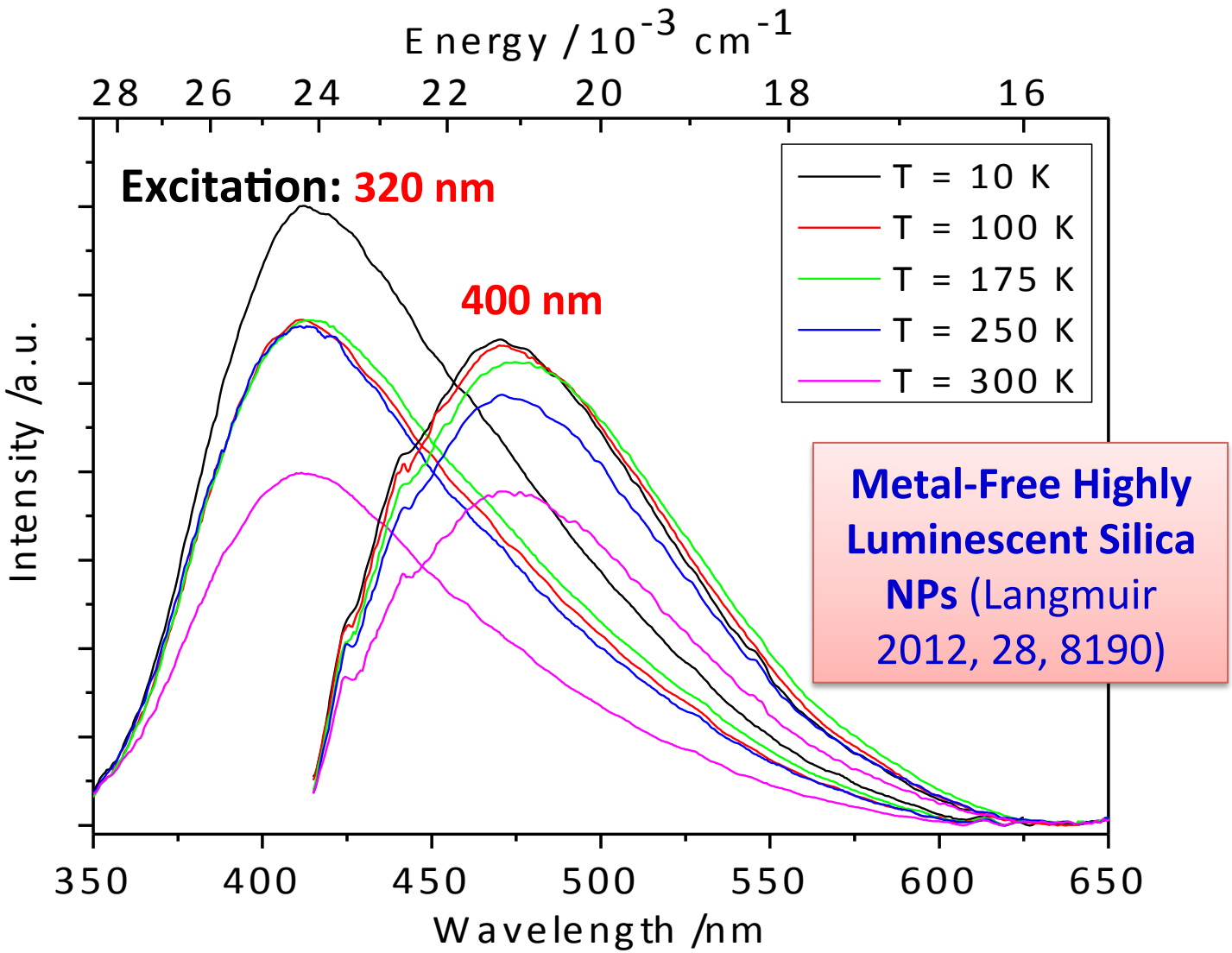

Metal-Free Highly Luminescent Silica NPs (Langmuir 2012, 28, 8190)

A. M. Jakob & T. A. Schmedake, ***Chem. Mater.*** 2006, 18, 3173; L. Wang *et al.*, ***Langmuir*** 2008, 24, 1635; A. Zhanbotin *et al.*, **Mater. Lett.** 2011, 65, 10.

Concerted two–step process involving the Boltzmann energy factor

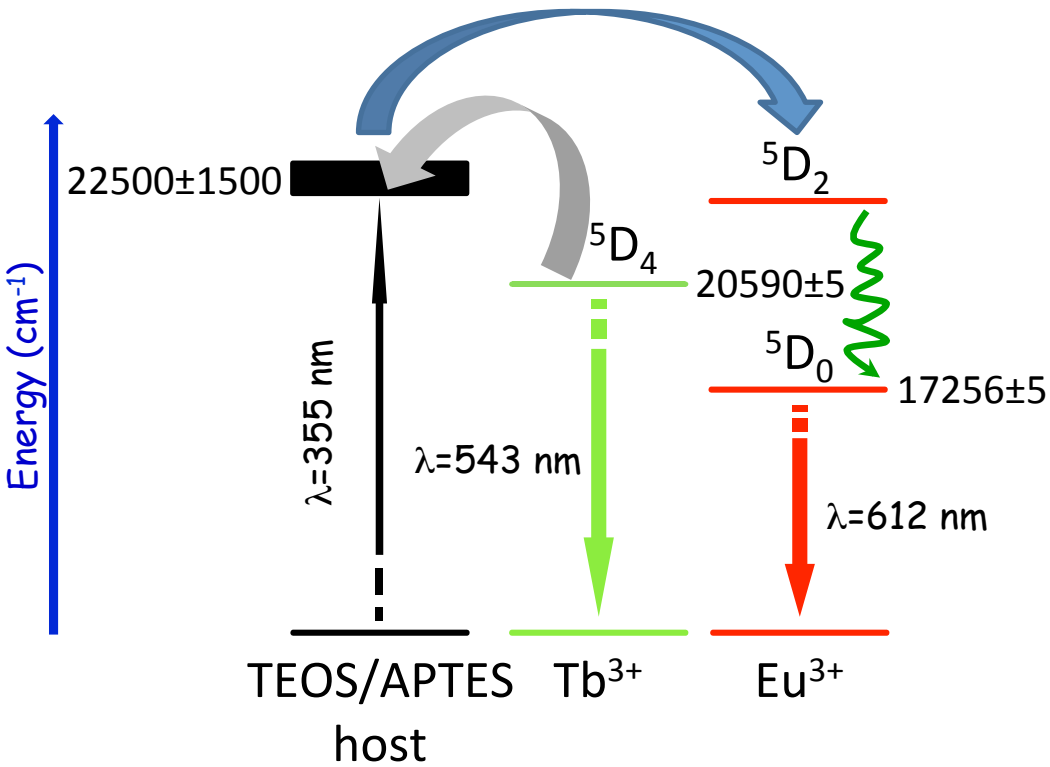

- The excited *T* state of the TEOS/APTES layer is populated through thermally-driven $^5D_4$-to-host energy transfer
- $I(^5D_4 \Rightarrow {}^7F_5) \downarrow$
- The *T* level transfers a fraction of the absorbed energy to the Eu^{3+} ions *via* the btfa/bpeta ligands (through the multipolar and exchange mechanisms)
- $I(^5D_0 \Rightarrow {}^7F_2) \uparrow$

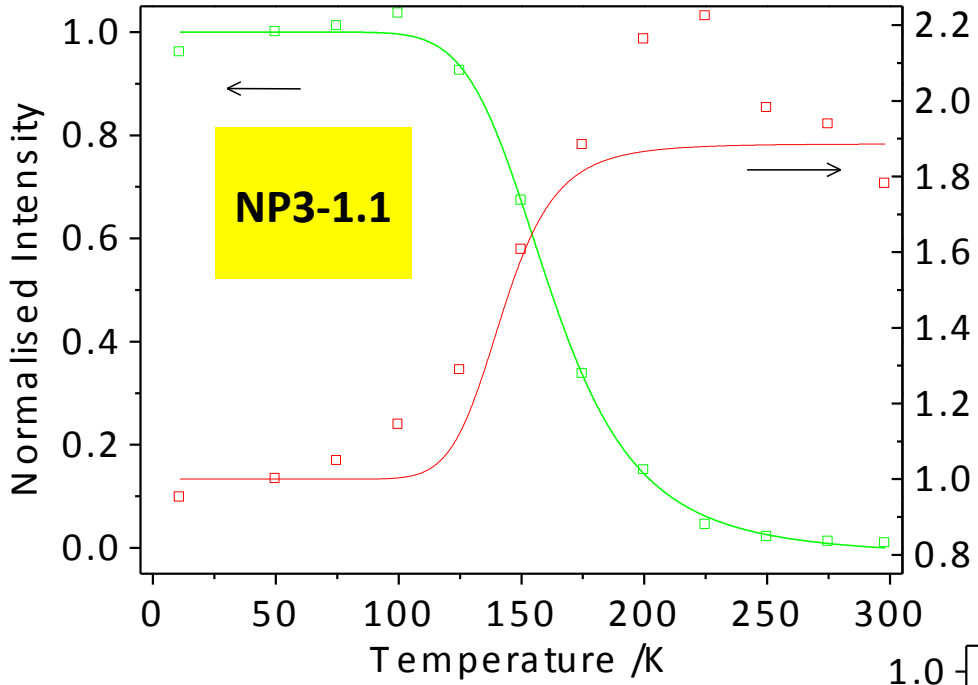

- The Tb^{3+} PL intensity strongly decreases as *T* increases

- The Eu^{3+} PL intensity starts to increase at precisely the same *T* at which the Tb^{3+} emission starts to decrease

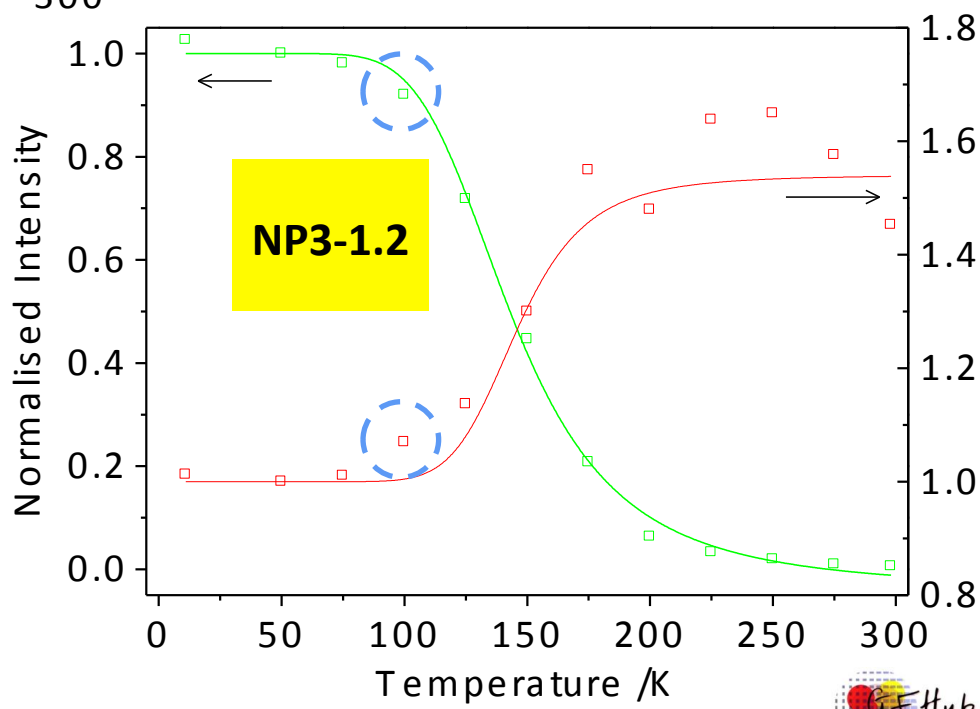

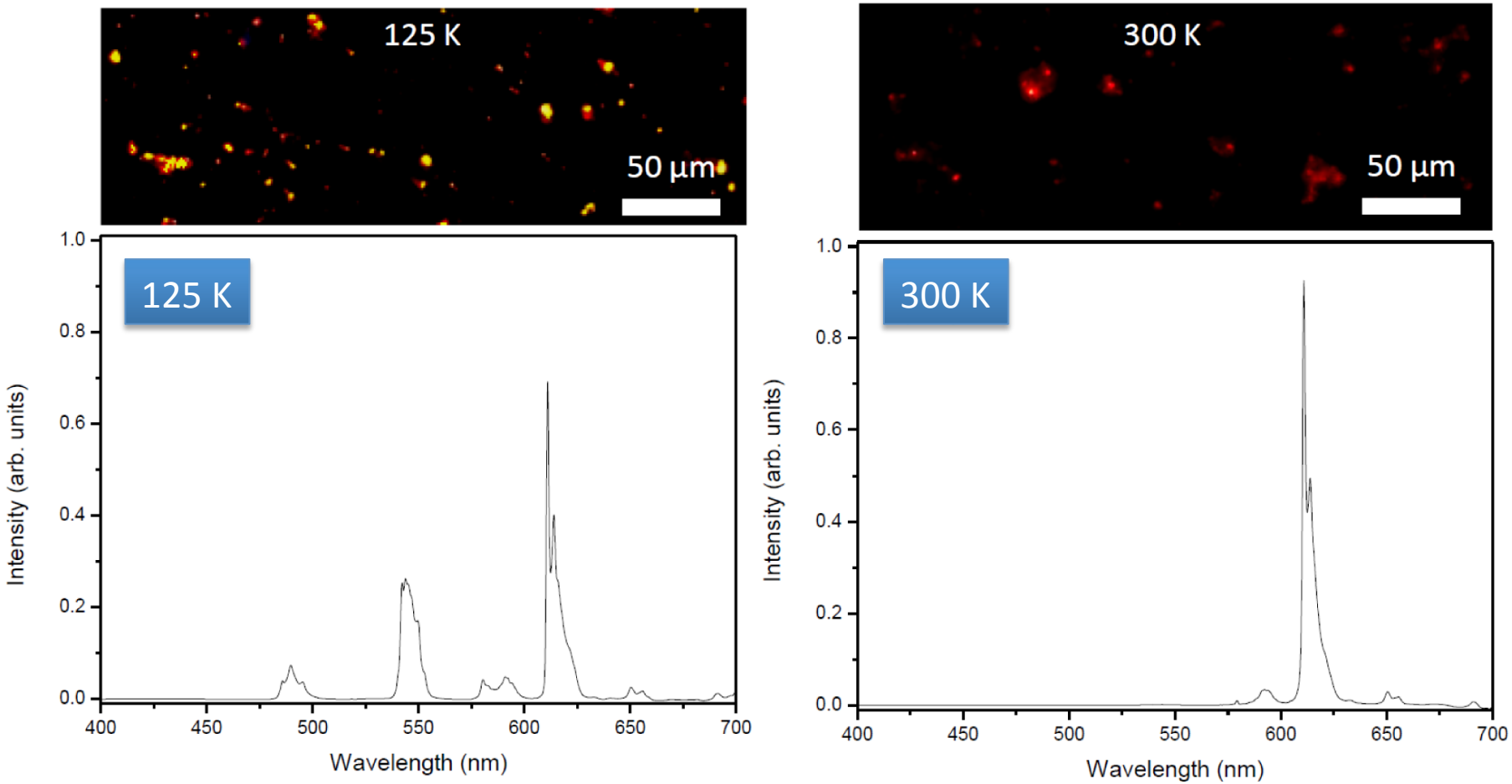

The luminescent molecular thermometer coupled with an OM:

thermometer with micrometer spatial resolution

(larger spot size as compared to the NPs aggregates is direct consequence of the limited space resolution of the instrument)

Nanothermometer performance

Absolute *m*easurements: $^5D_0 \Rightarrow {}^7F_2$ (I_{Eu} at 612 nm) and $^5D_4 \Rightarrow {}^7F_5$ (I_{Tb} at 545 nm) integrated areas

$$\Delta = I_{Eu}^2 - I_{Tb}^2$$

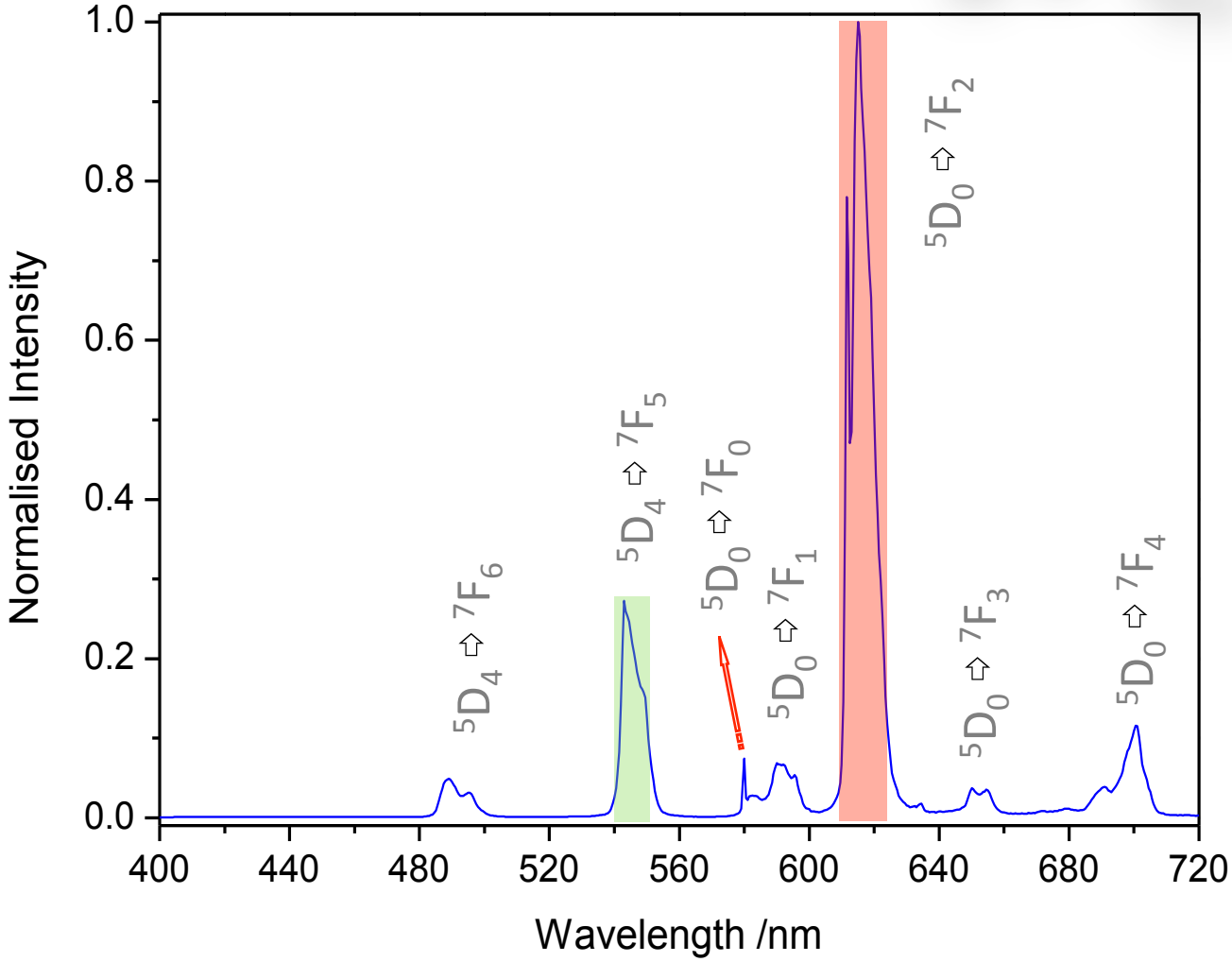

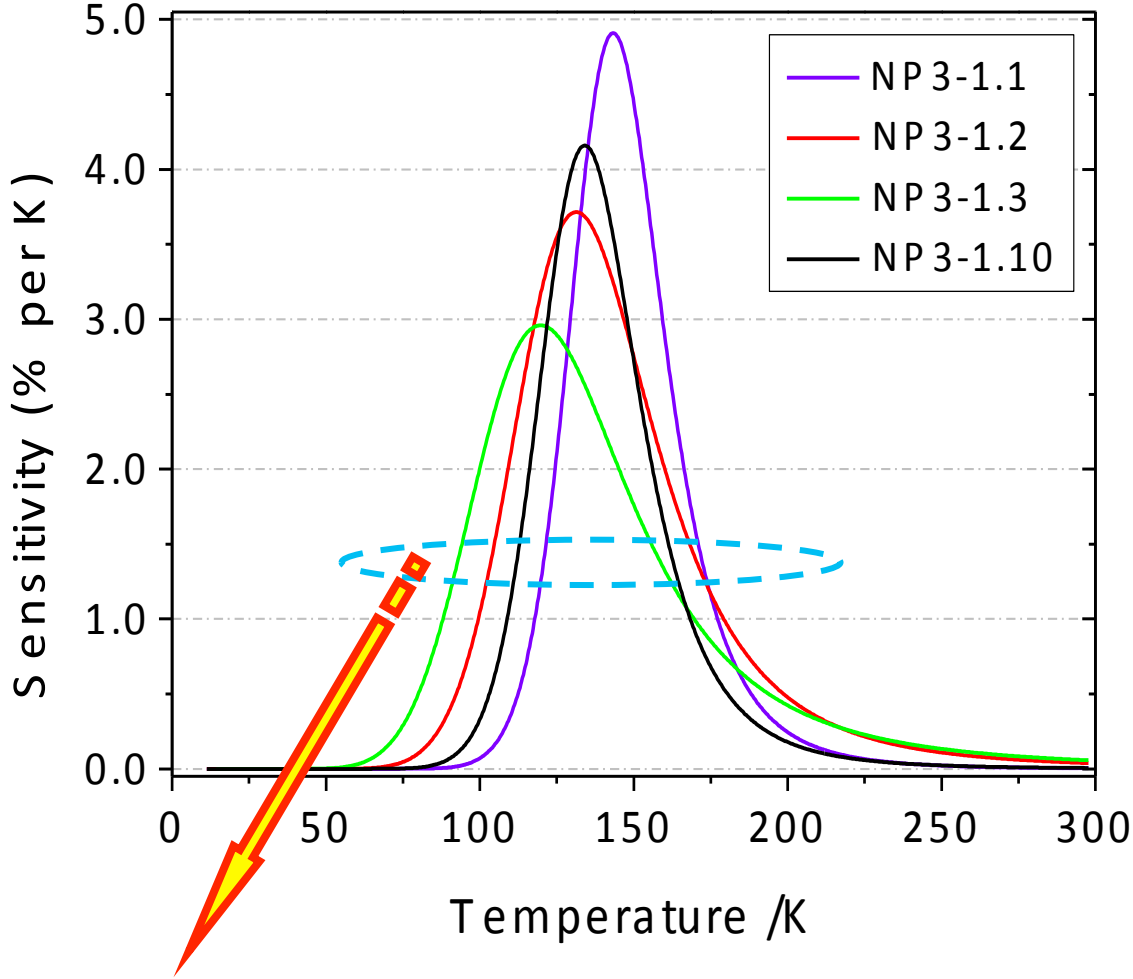

$$S = \frac{\frac{d\Delta}{dT}}{\Delta}$$

Quality limit: S_{min}=1%·K^{-1}

Optimal operation range of 60-80 K around the temperature of S_m (120-190 K

Can the nanothermometer works in solution?

Quenching of Ln^{3+} luminescence: ***nonradiative energy transfer from the Ln^{3+} excited states (e.g. Tb^{3+} and Eu^{3+}) to the OH vibrational manifold***

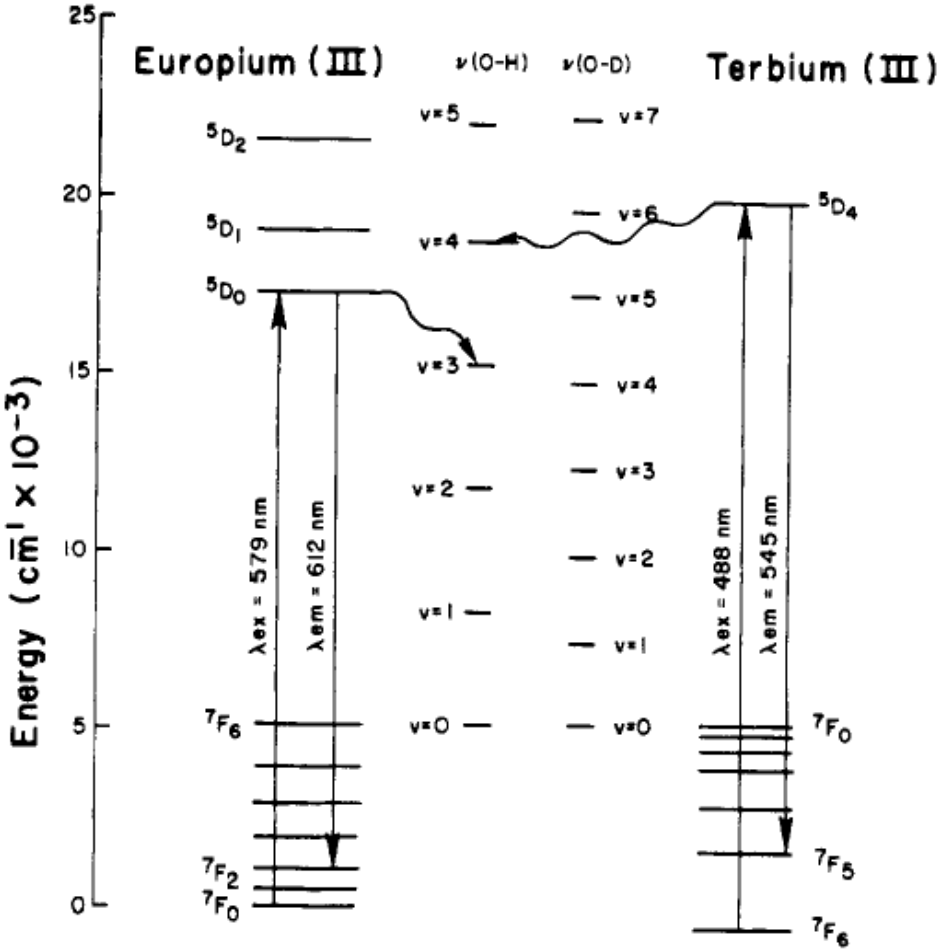

- OH phonons (3700 cm^{-1}) deactivate the electronic levels of Ln^{3+} ions
- The efficiency of this transfer increases as the magnitude of the energy gap between the emissive state and the highest level of the ground manifold decrease (**14800 cm^{-1}**, for Tb^{3+} and **12200 cm^{-1}**, for Eu^{3+})

W. DE W. Horrocks Jr. & D. R. Sudnick, ***Acc. Chem. Res.*** 1981, 14, 384

Working on solutions…

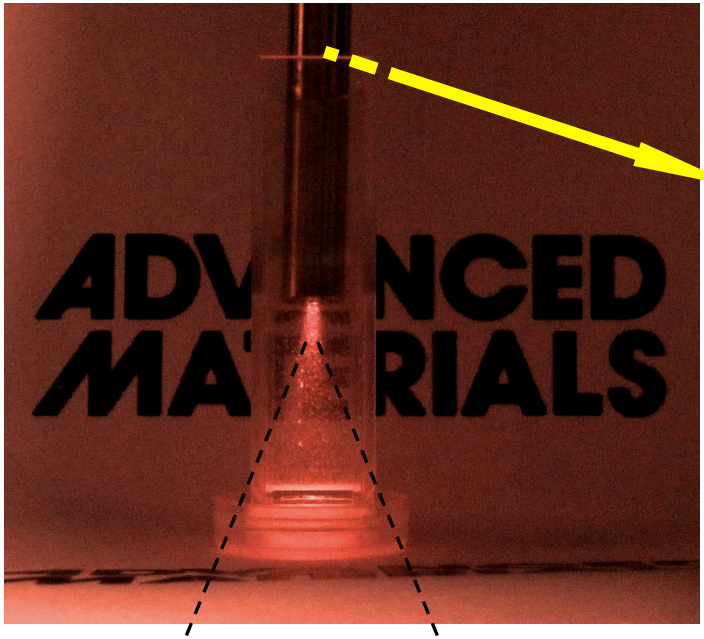

Fibre bundle guiding 365 nm excitation light

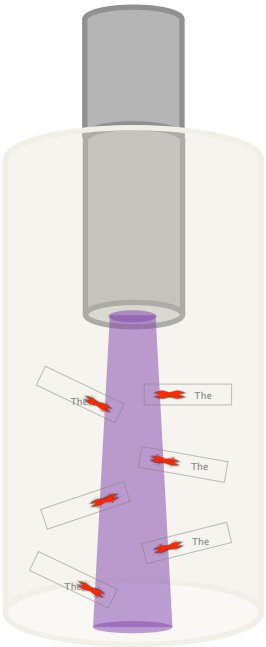

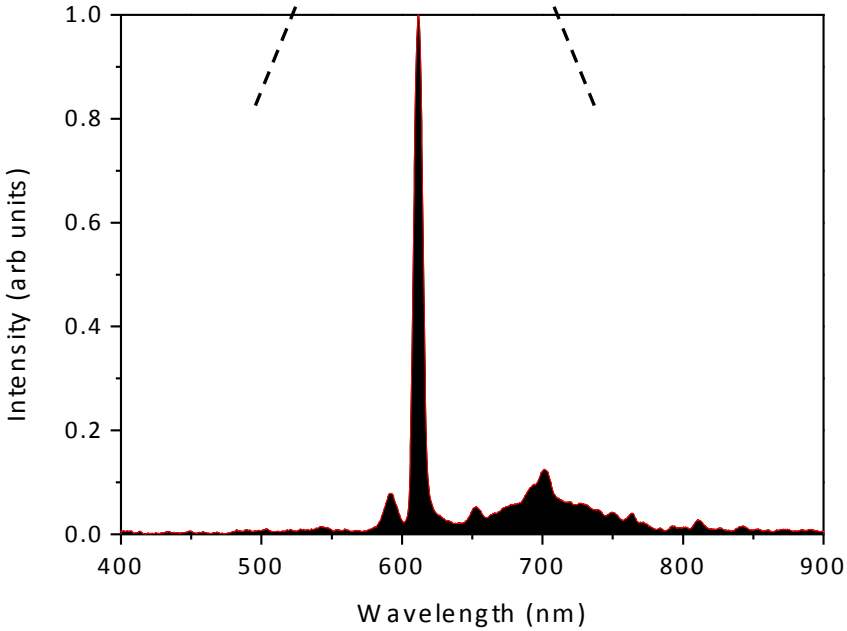

Emission QY

0.38±0.04

Same value than that measured in in solid state

To make absolute measurements at higher temperatures feasible, the activation energy ΔE must increase

- Increasing the TEOS/APTES ratio
- Changing the β-diketonate ligands
- Design of a different host matrix

Excited triplet state located at higher energy (relatively to that of the TEOS/ APTES layer)

IV. Eu/Tb nanothermometer operating at physiological temperatures

- **Different hybrid host (TEOS/TESP), same btfa and bpeta liganfs**

NP4-1.3

N-(triethoxysilylpropyl)-O-Polyethylene Oxide Urethane

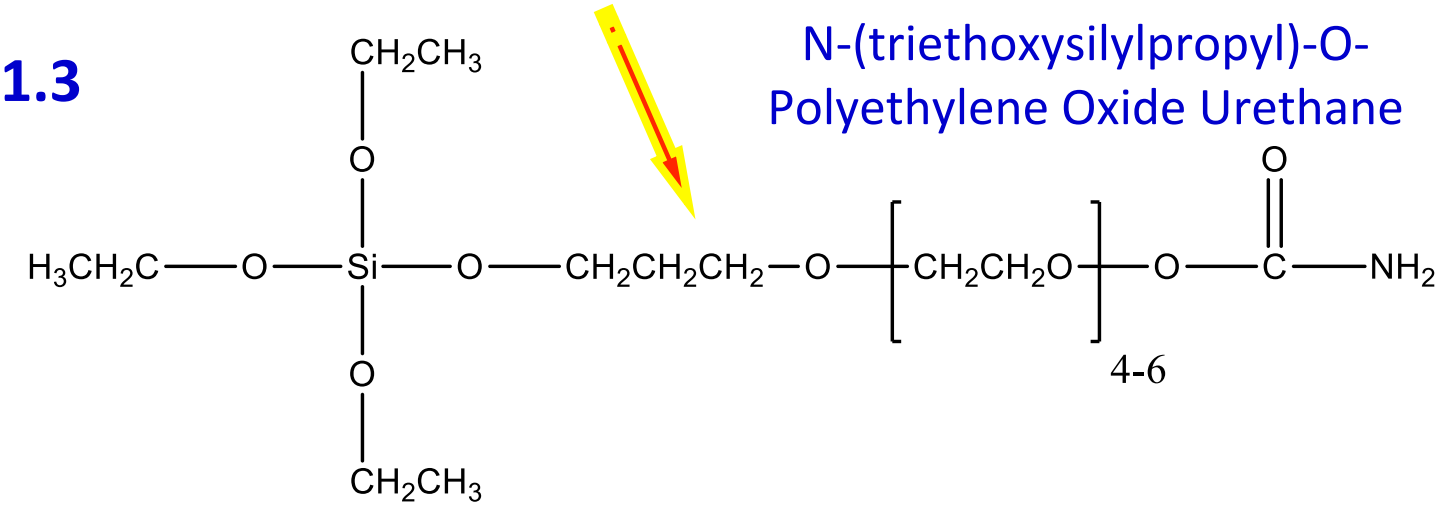

- **Different β-diketonate ligand, same APTES/TEOS hybrid host**

NP5-1.4

$Ln(acac)_3 \cdot 3H_2O$ (Ln=Eu,Tb)

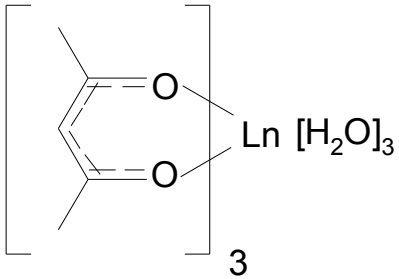

to be published

SEM & EDS

NP4-1.3

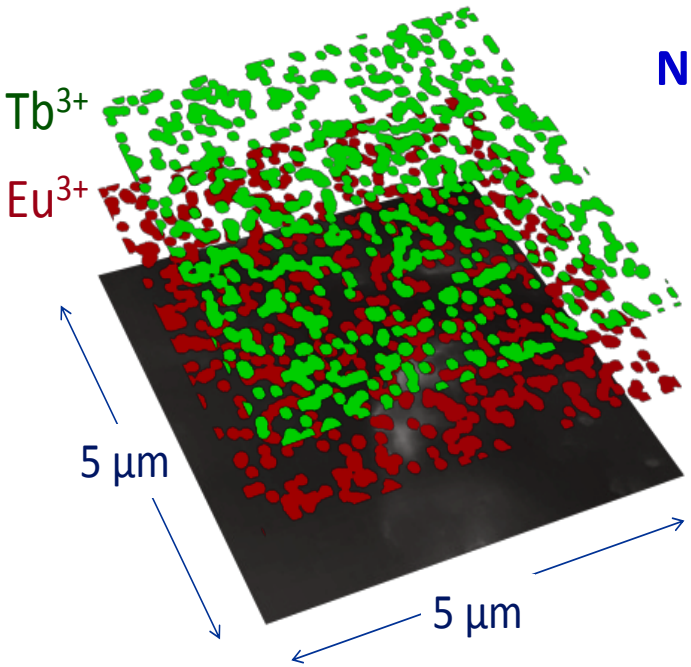

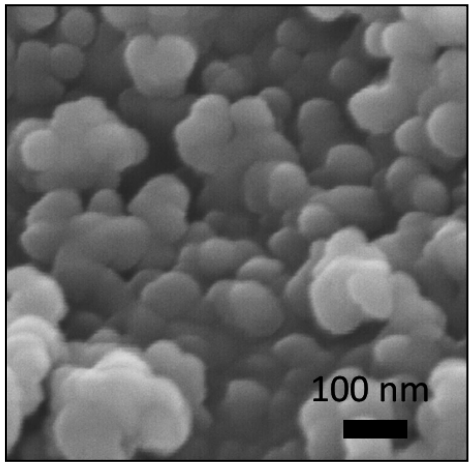

NP5-1.4

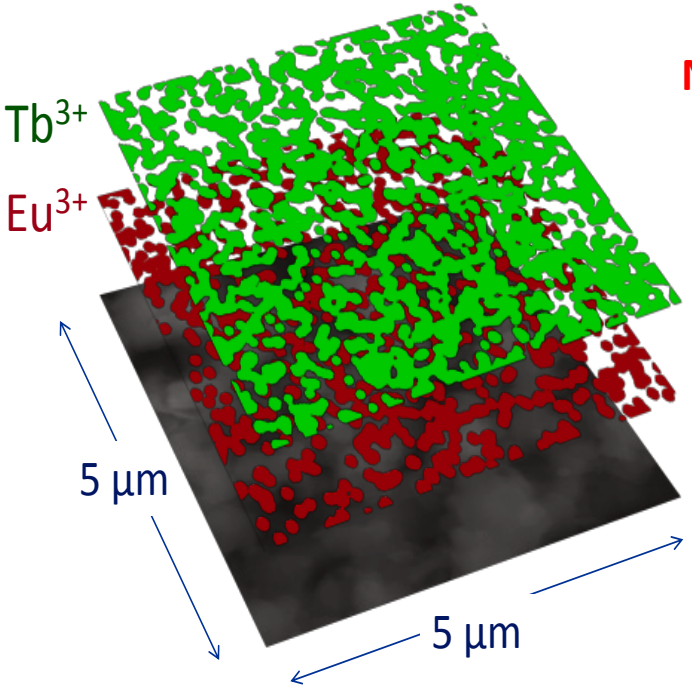

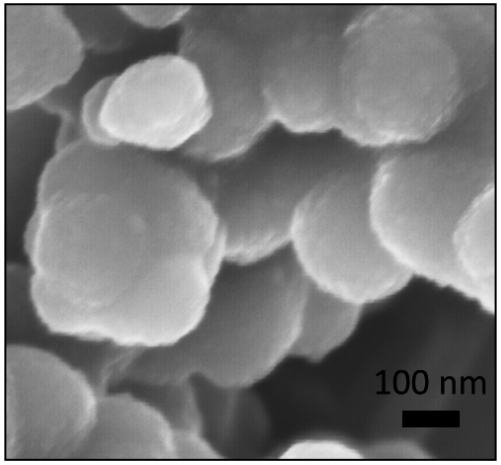

DLS and TEM

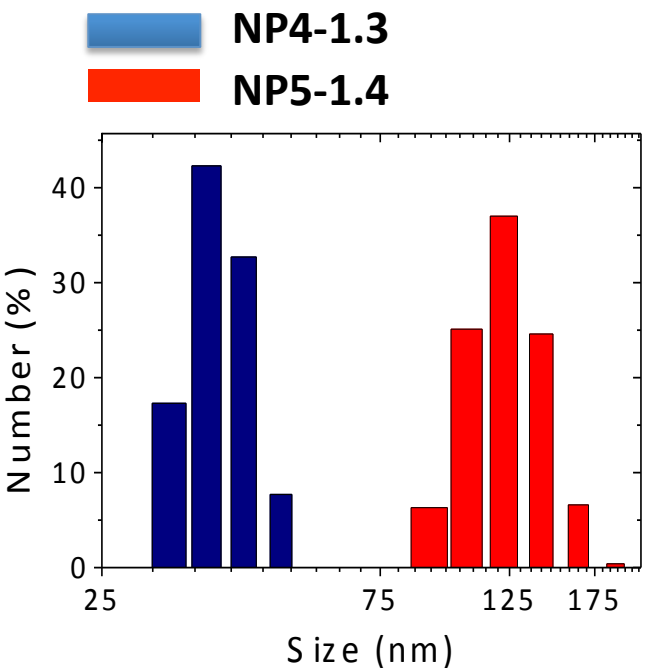
NP4-1.3
NP5-1.4
Number (%)
0
10
20
30
40
25
75
125
175
Size (nm)

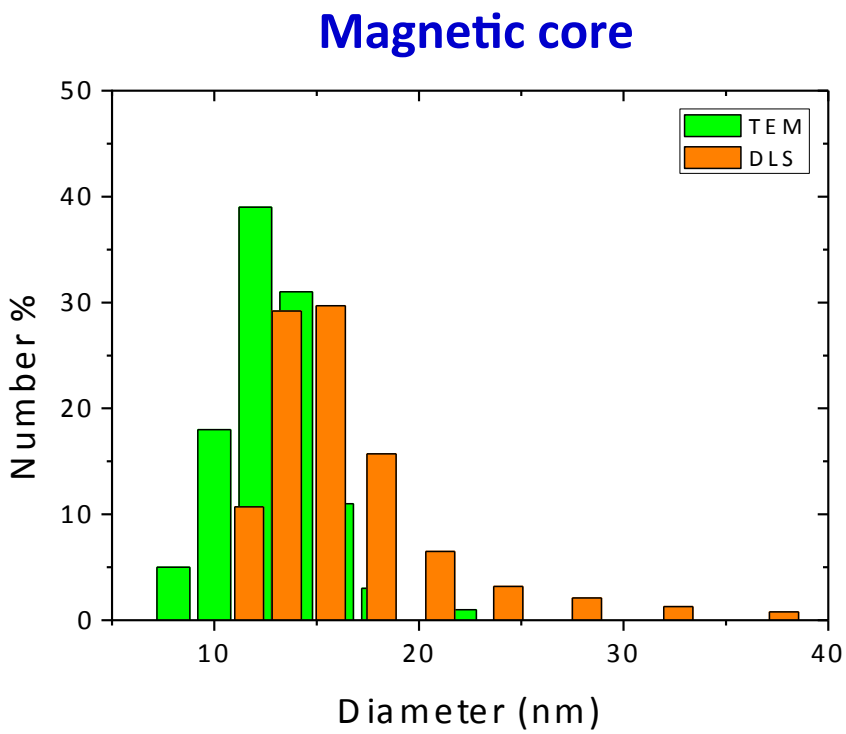
Magnetic core
TEM
DLS
Number %
0
10
20
30
40
50
10
20
30
40
Diameter (nm)

Fluorescence Micoscopy and TEM

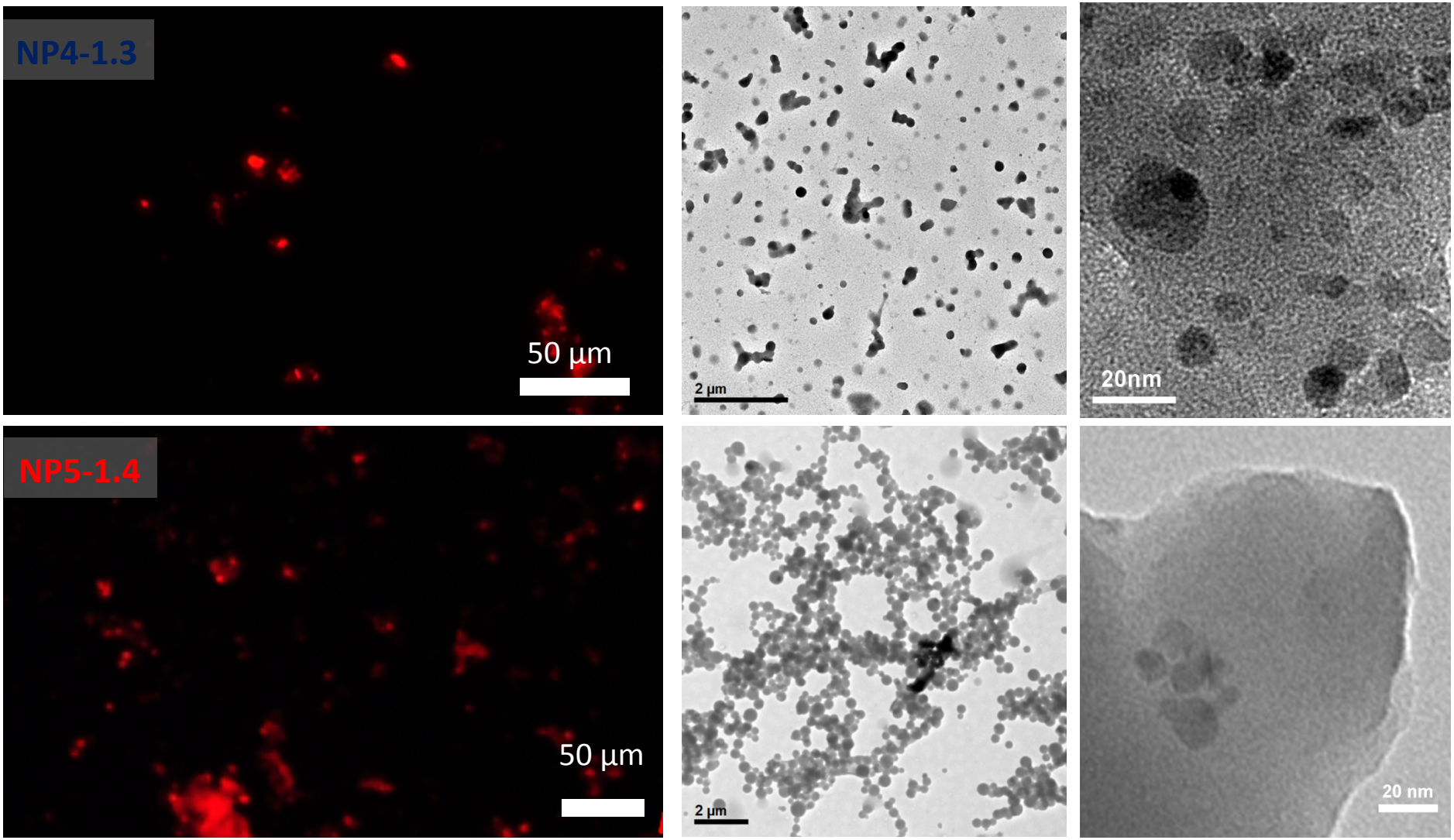

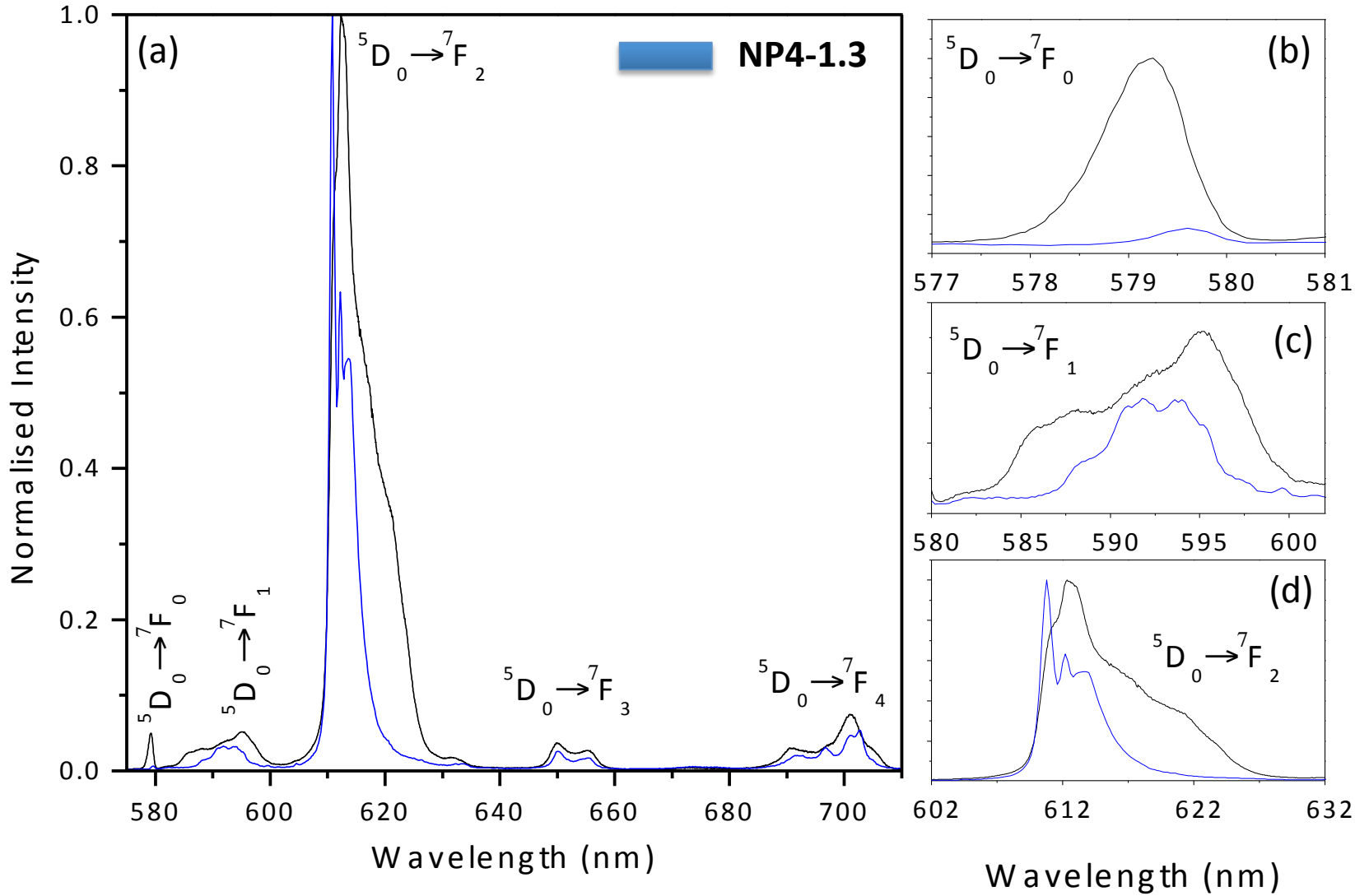
(a)
NP4-1.3
$^5D_0 \rightarrow {}^7F_2$
$^5D_0 \rightarrow {}^7F_0$
$^5D_0 \rightarrow {}^7F_1$
$^5D_0 \rightarrow {}^7F_3$
$^5D_0 \rightarrow {}^7F_4$
Normalised Intensity
Wavelength (nm)
(b)
$^5D_0 \rightarrow {}^7F_0$
(c)
$^5D_0 \rightarrow {}^7F_1$
(d)
$^5D_0 \rightarrow {}^7F_2$
Wavelength (nm)

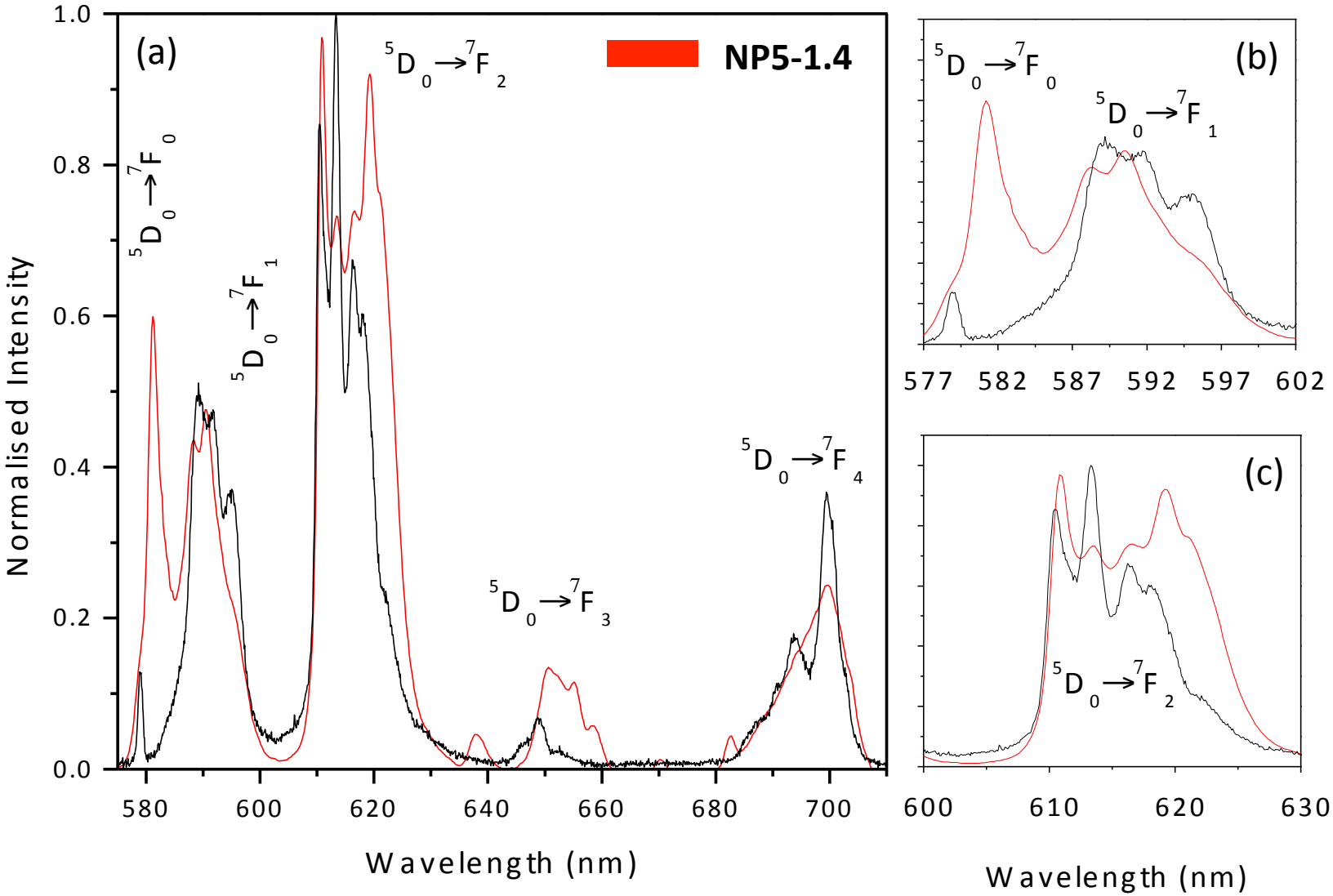
(a)
NP5-1.4
$^5D_0 \rightarrow {}^7F_0$
$^5D_0 \rightarrow {}^7F_1$
$^5D_0 \rightarrow {}^7F_2$
$^5D_0 \rightarrow {}^7F_3$
$^5D_0 \rightarrow {}^7F_4$
Normalised Intensity
Wavelength (nm)
(b)
$^5D_0 \rightarrow {}^7F_0$
$^5D_0 \rightarrow {}^7F_1$
(c)
$^5D_0 \rightarrow {}^7F_2$
Wavelength (nm)

Intensity vs Temperature

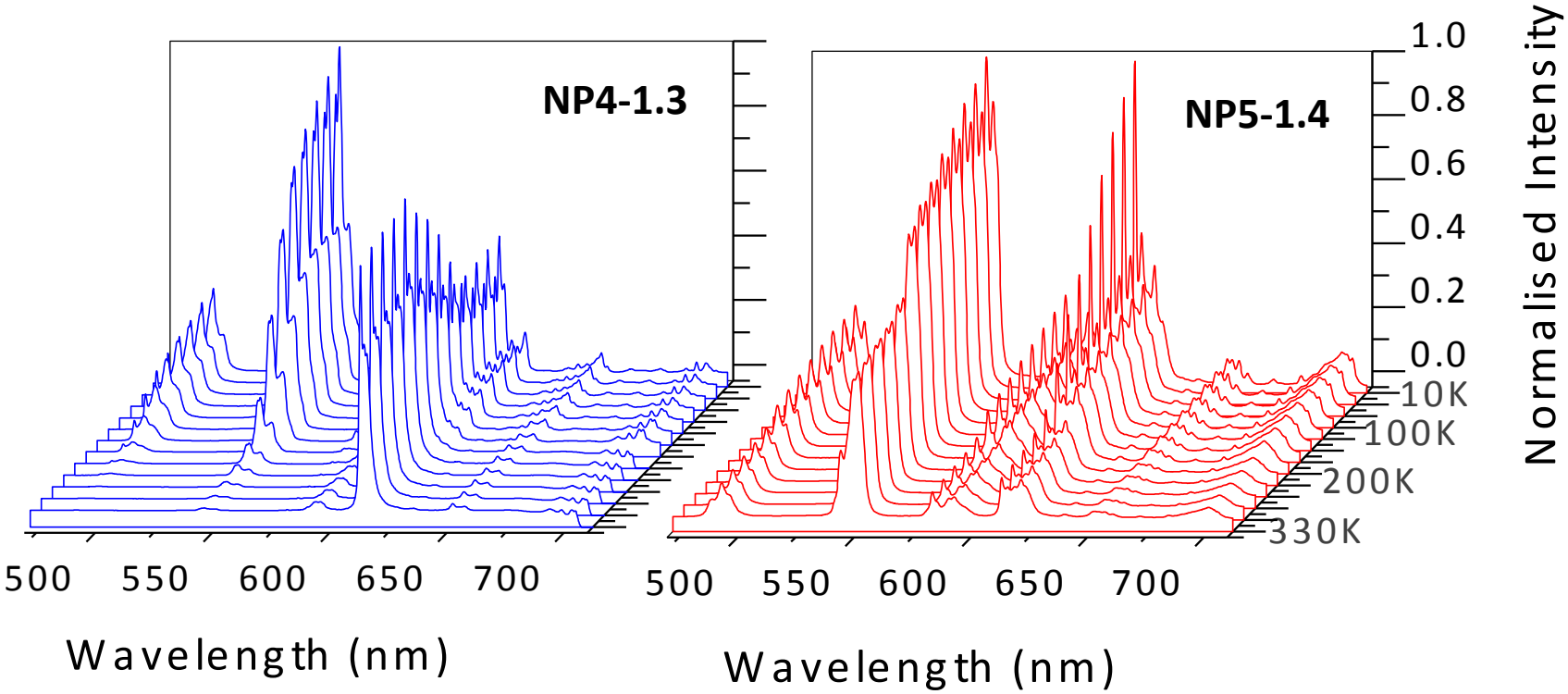

Emission QY at 300 K

NP4-1.3: 0.27±0.03

NP5-1.4: 0.37±0.04

Δ and S parameters

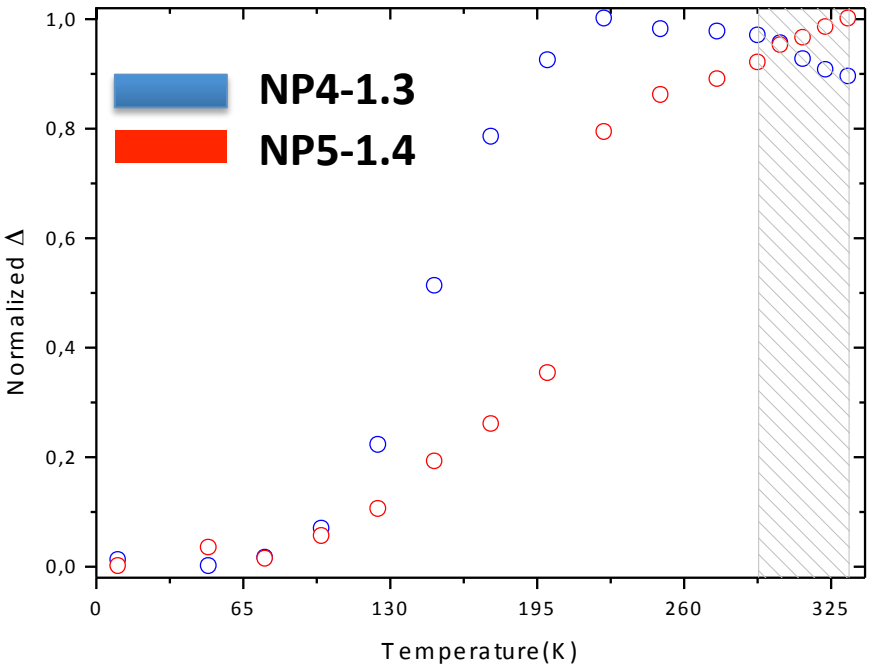

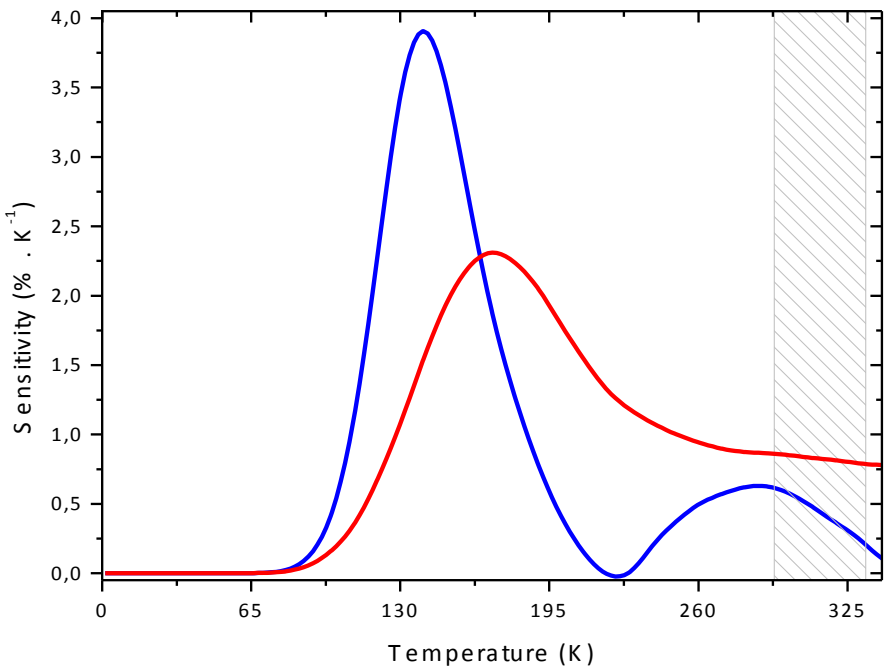

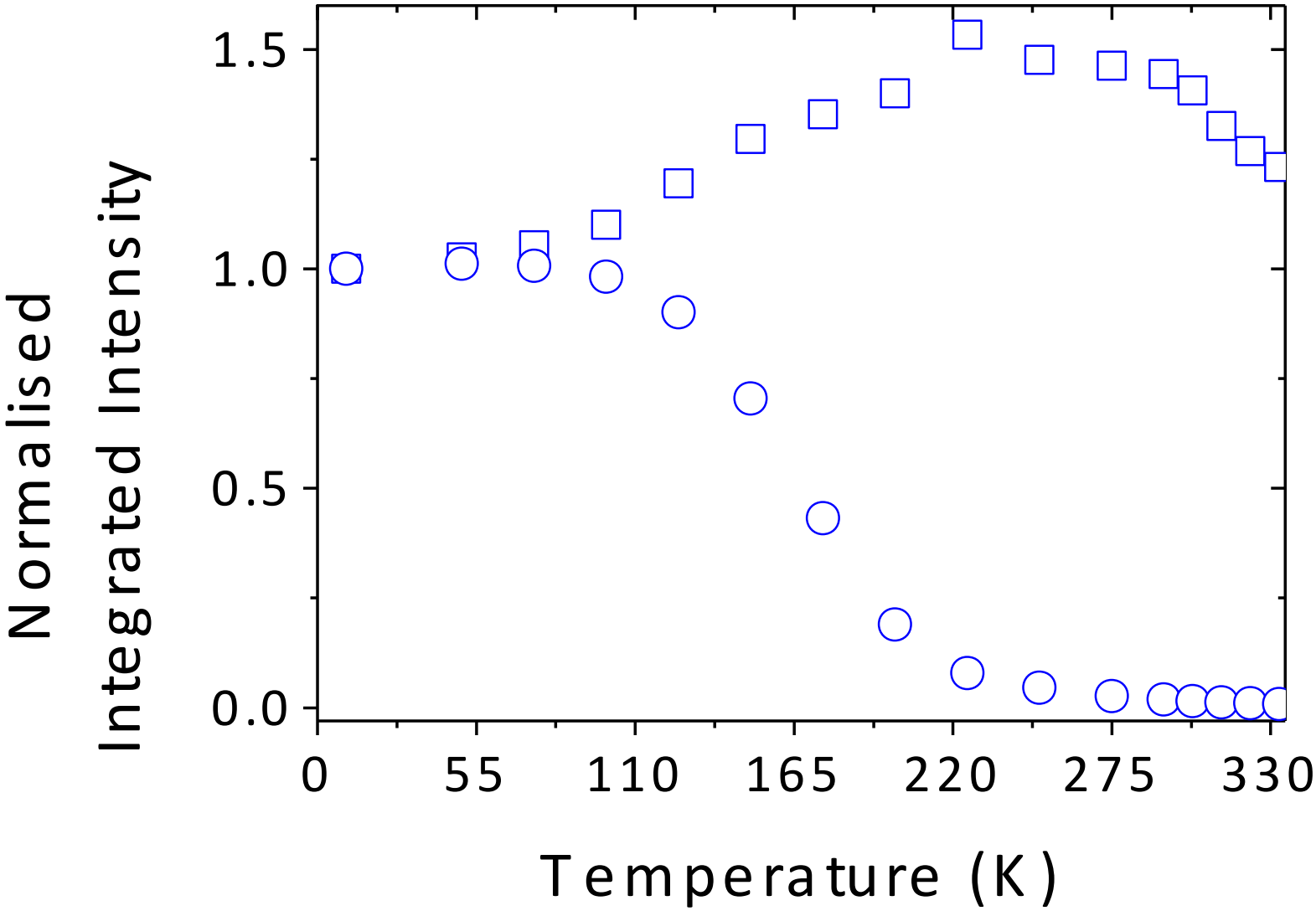
Normalised
Integrated Intensity
1.5
1.0
0.5
0.0
0
55
110
165
220
275
330
Temperature (K)

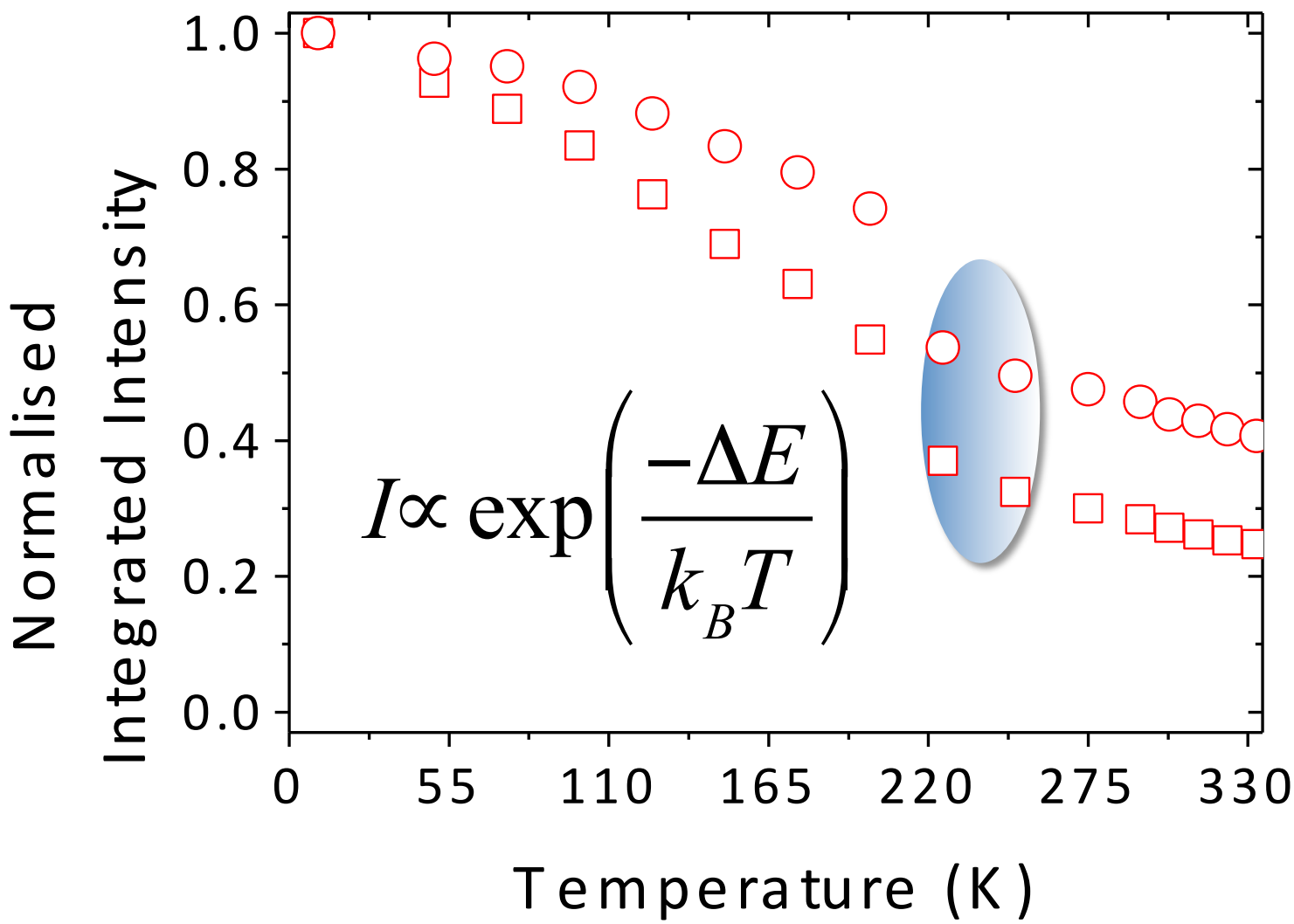
Normalised Integrated Intensity
1.0
0.8
0.6
0.4
0.2
0.0
0
55
110
165
220
275
330
Temperature (K)
$I \propto \exp\left(\frac{-\Delta E}{k_B T}\right)$

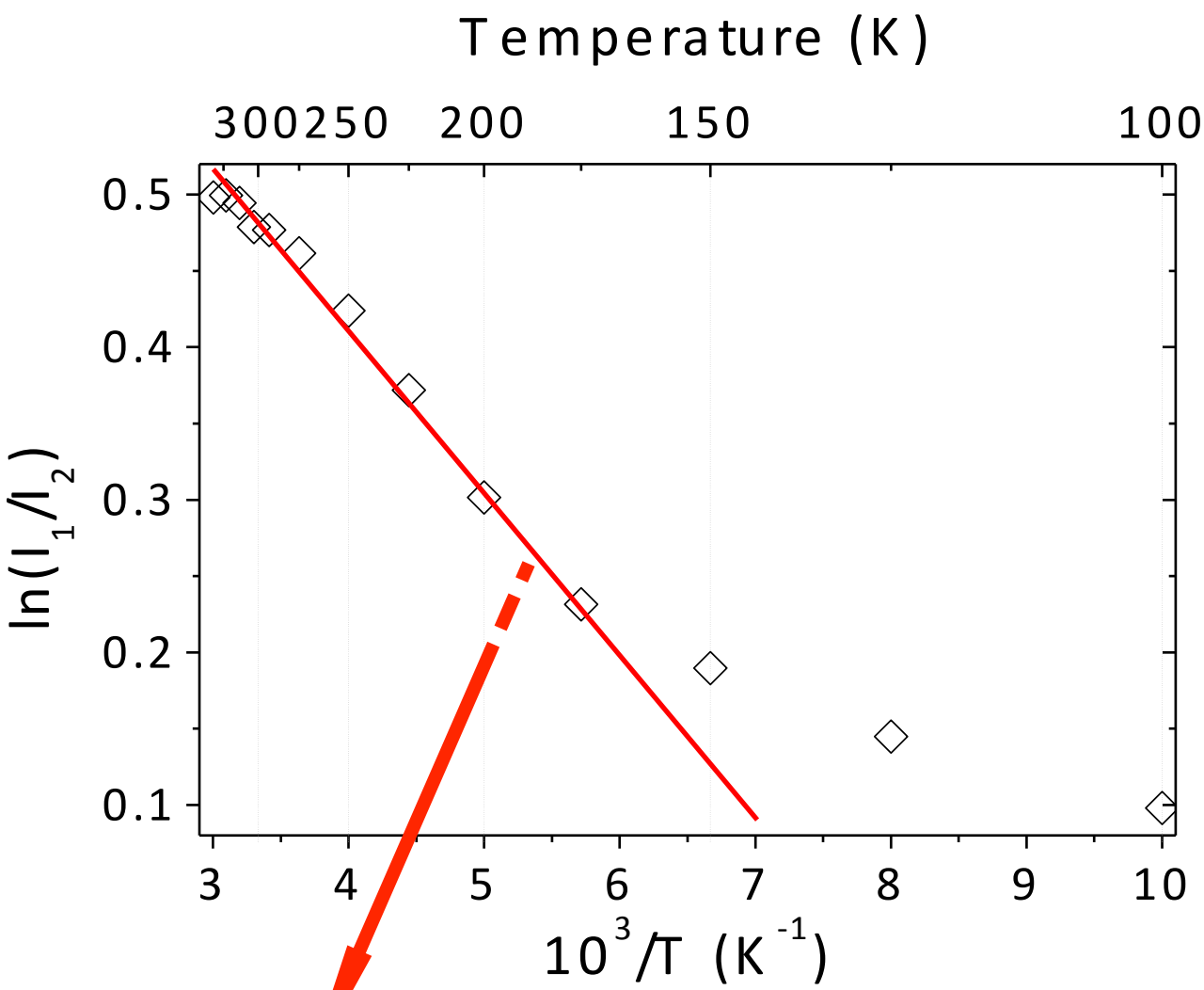

$$\ln\left(\frac{I_{Tb}}{I_{Eu}}\right) \equiv \ln\left(\frac{I_1}{I_2}\right) \propto \exp\left(\frac{\Delta E_2 - \Delta E_1}{k_B}\right)\frac{1}{T}$$

$$\Delta E_1 = E_1 - E(^5D_4)$$

$$\Delta E_2 = E_2 - E(^5D_0)$$

Energy Scheme (above 200 K)

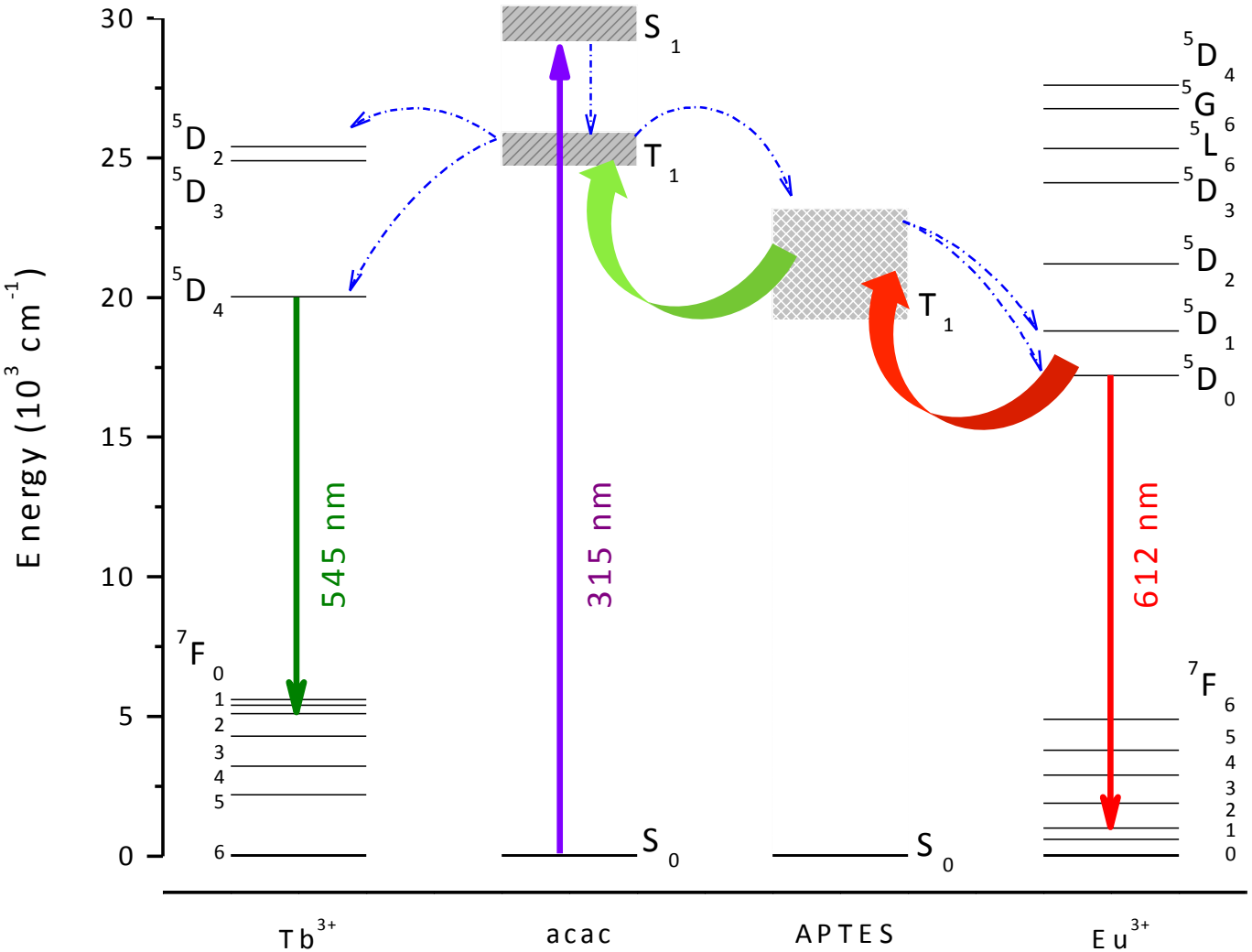

Microfluid Setup

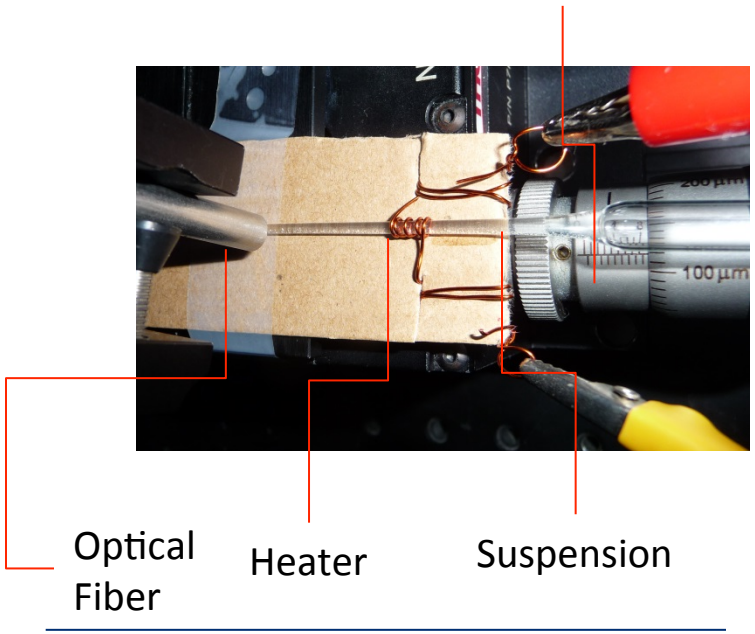

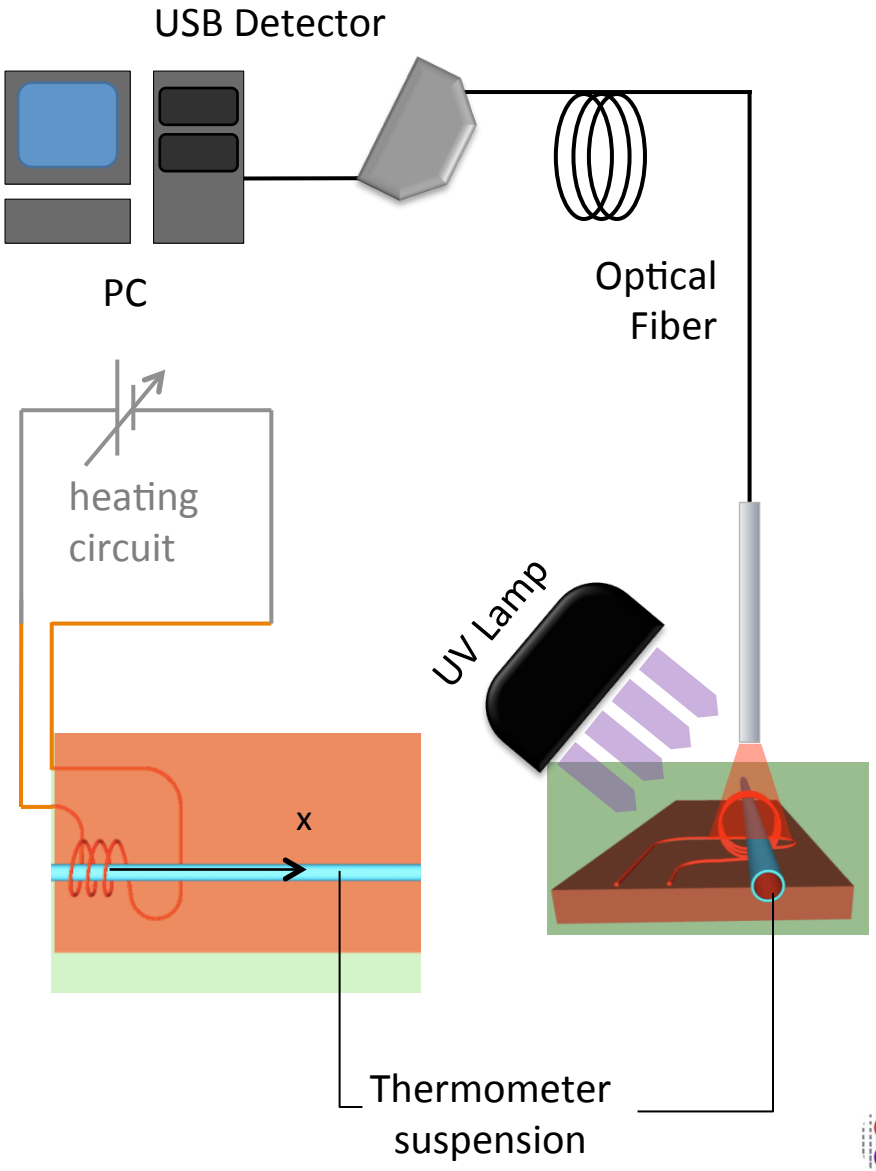

Inner Diameter=1 mm
Total Scanning Length =20 mm
Total Volume scanned= 15.7 µL

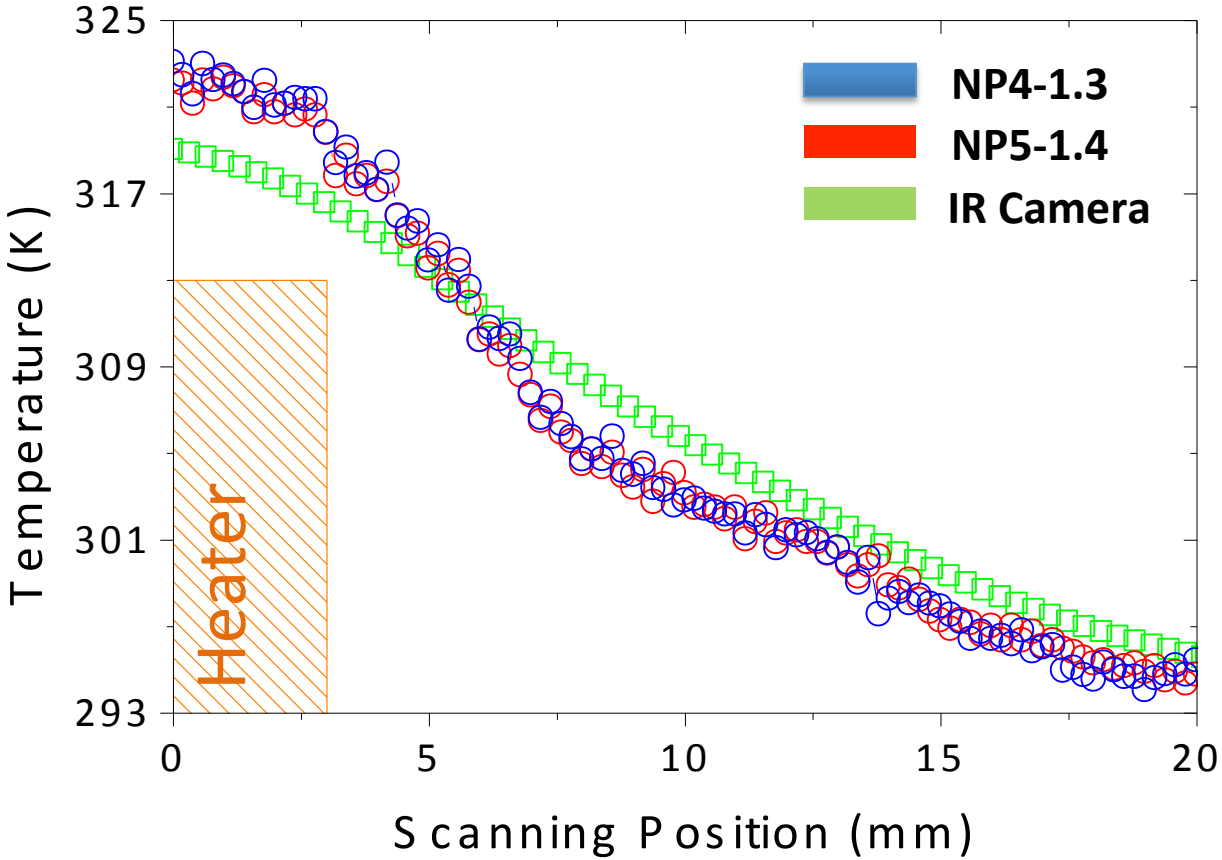

Spatial Resolution

NP4-1.4: 65 µm
NP5-1.3: 67 µm
IR camera: 160 µm

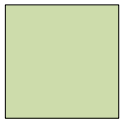

Pixel Size

Spatial Resolution

Fibre Field of View

Spatial Resolution

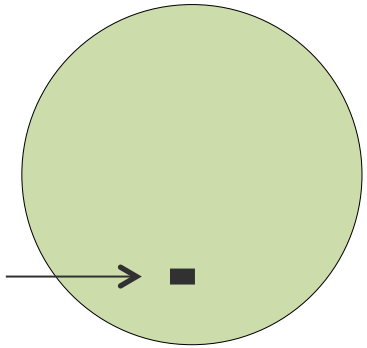

Comparision with literature examples

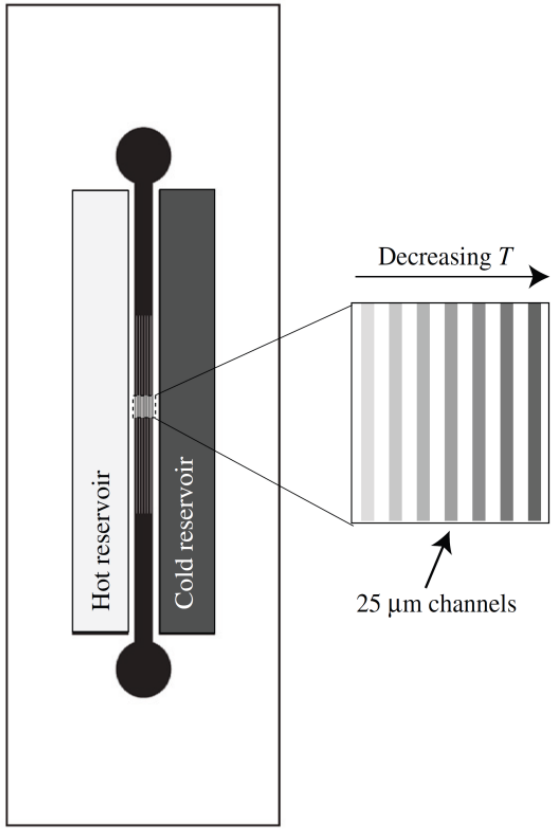

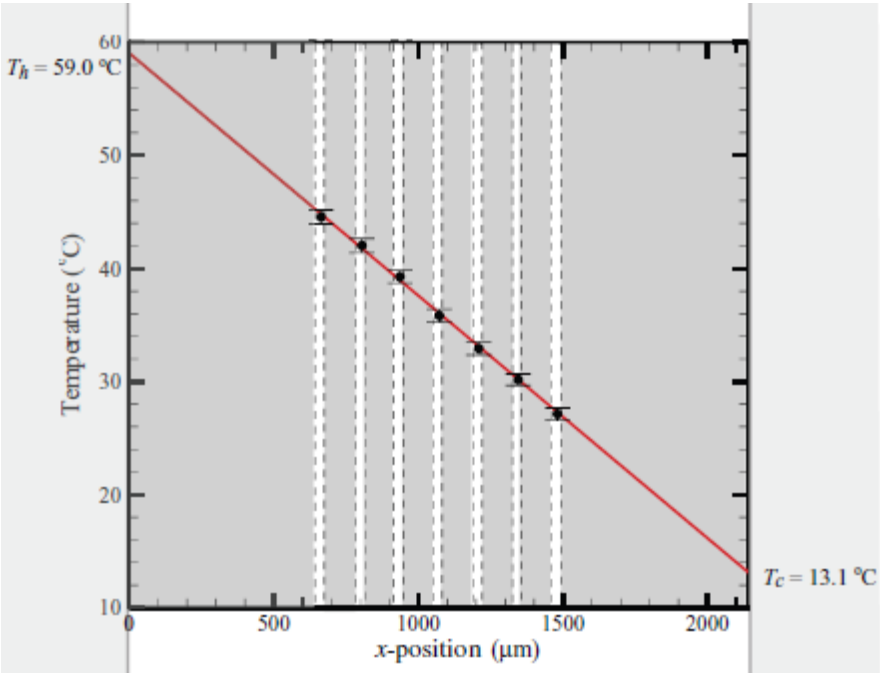

spatial resolution of ~69 µm

V. K. Natrajan & K. T. Christensen, ***Meas. Sci. Technol.*** 2009, 20, 015401

Eu/Tb co-doped di-ureasil hybrids

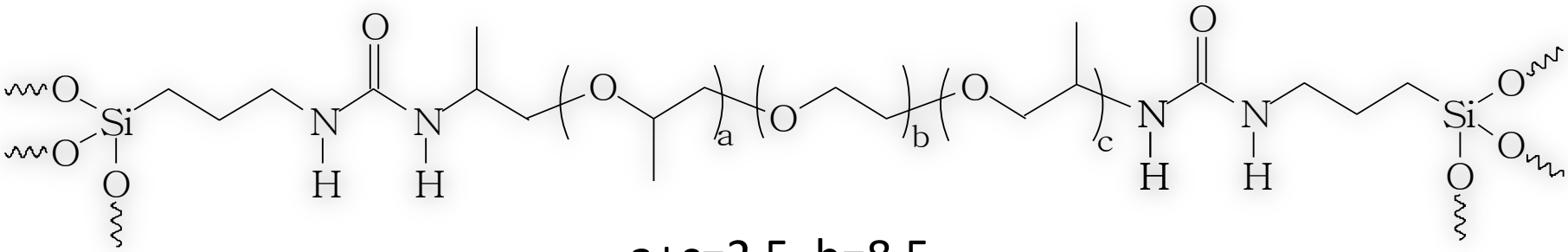

a+c=2.5, b=8.5

- Eu/Tb molar ratio is 1:3 (***U-1.3***)
- Processability as transparent films (≈10 µm) and monoliths
- (a) undoped di-ureasil hybrids
- (b) Eu-doped hybrids
- (c) Tb-doped hybrids

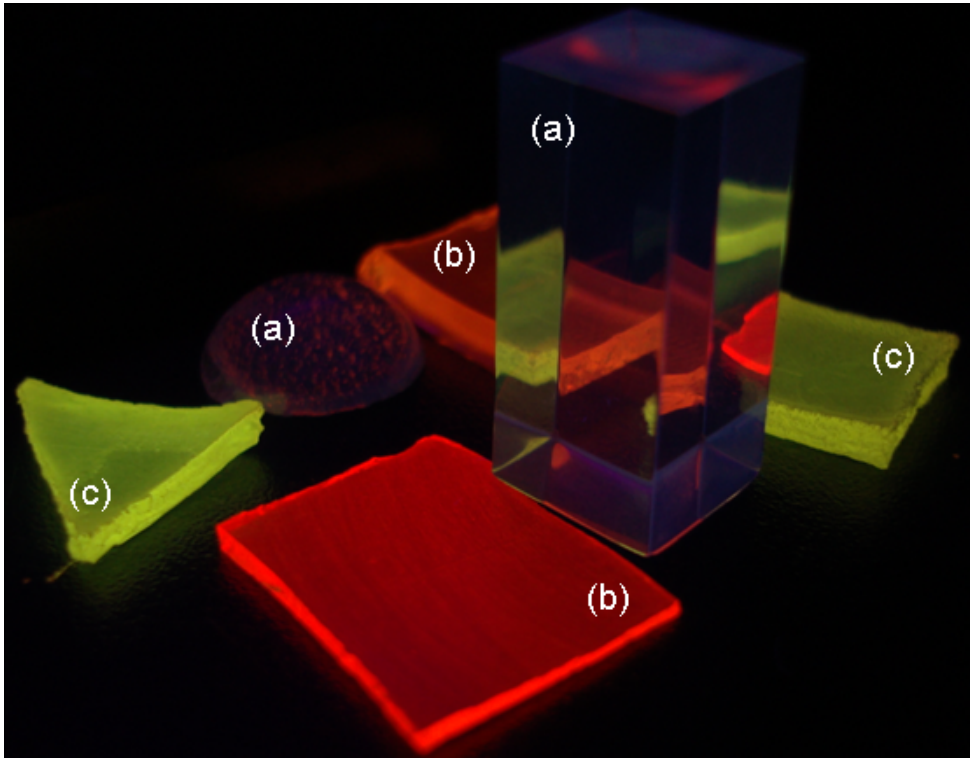

V. D. Bermudez *et al.*, ***Chem. Mater.*** 1999, 11, 569; L. D. Carlos *et al.* **Adv. Mater.** 2009, 21, 509.

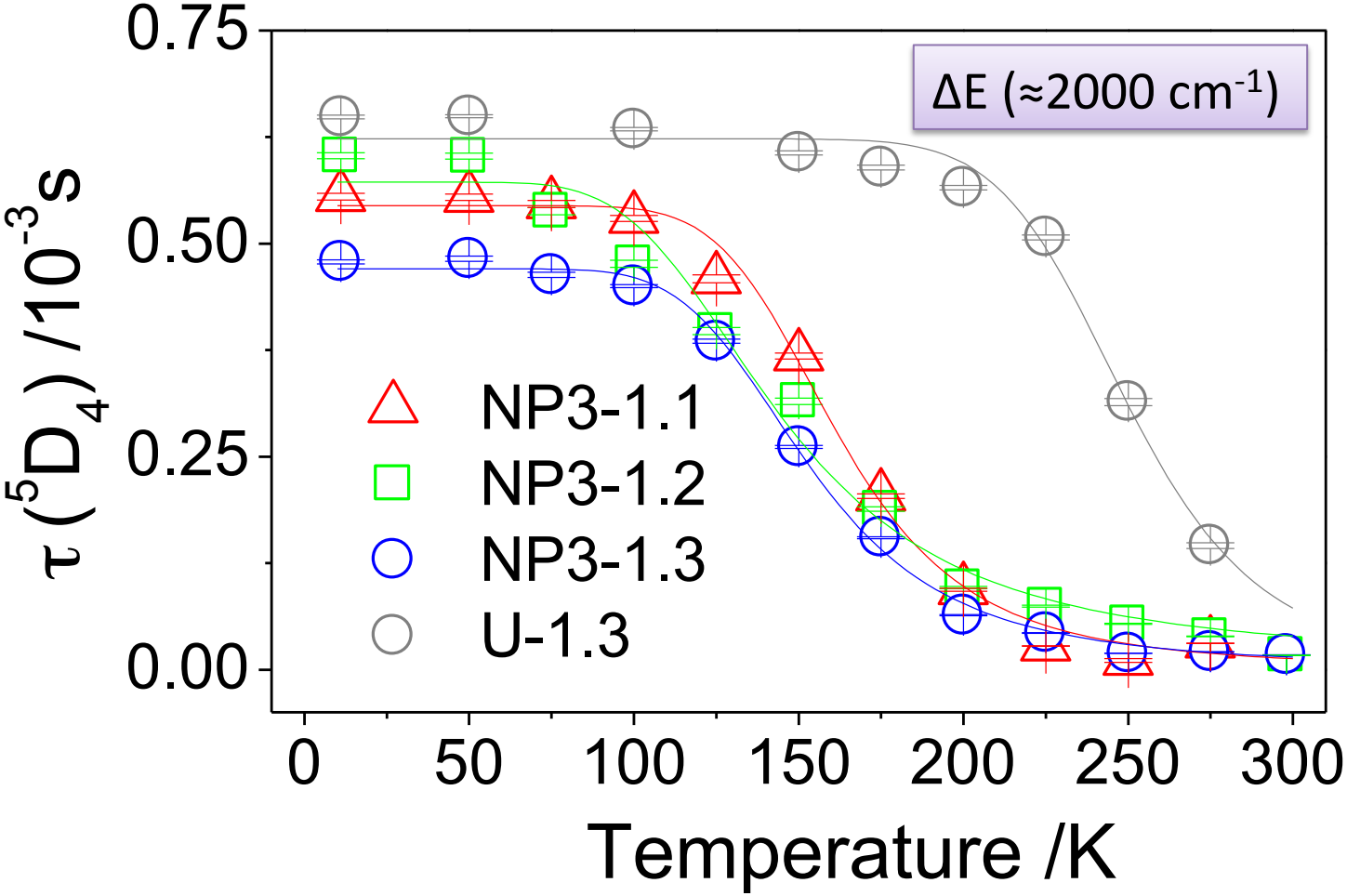

The thermometer range of operation is shifted to room temperature

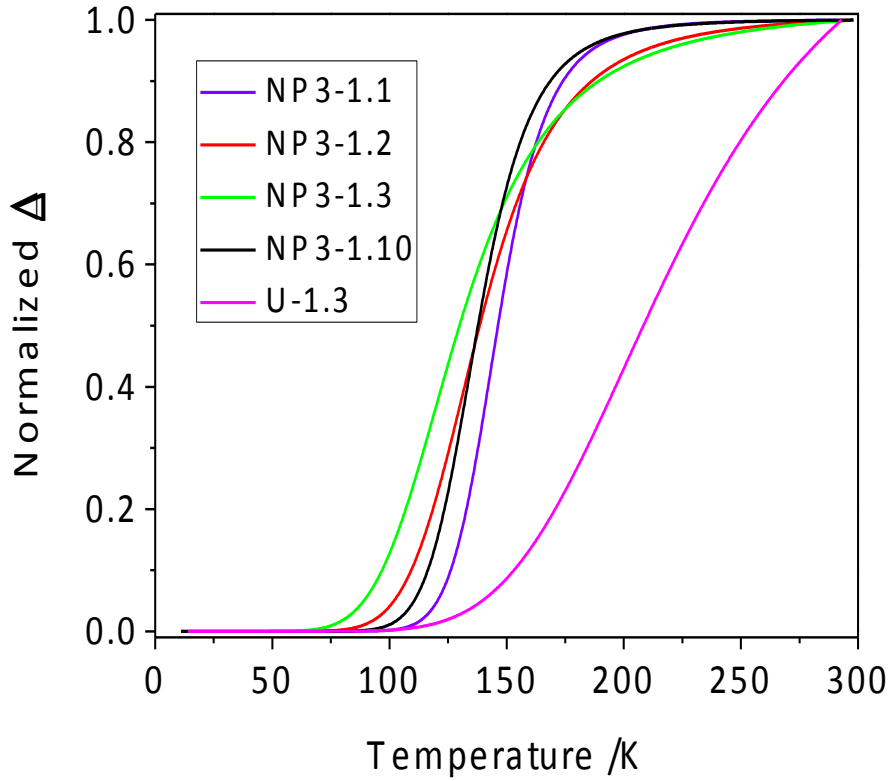

- The maximum absolute emission QY of **U1.3** is **0.16±0.02**
- S_{max}=1.9%·K^{-1} (at 201 K)

The Eu/Tb co-doped di-ureasils are sufficiently sensitive to be used in the physiological temperature range

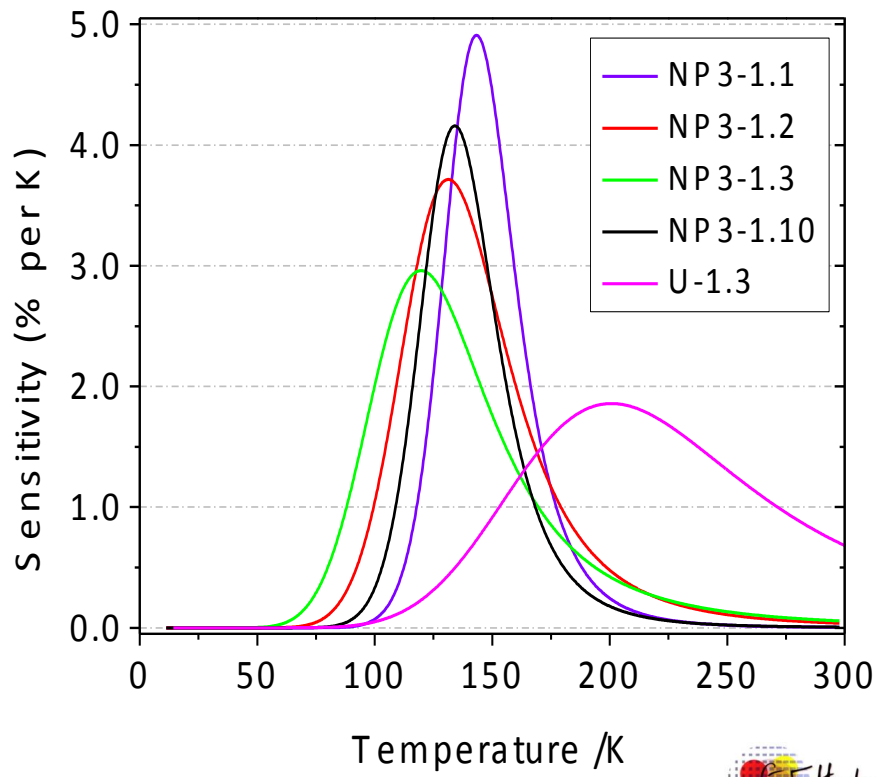

Spatial resolution

Mapping the temperature on a integrated circuit, with tracks of different widths (<200 µm), covered with a **U3-1** layer (10 µm)

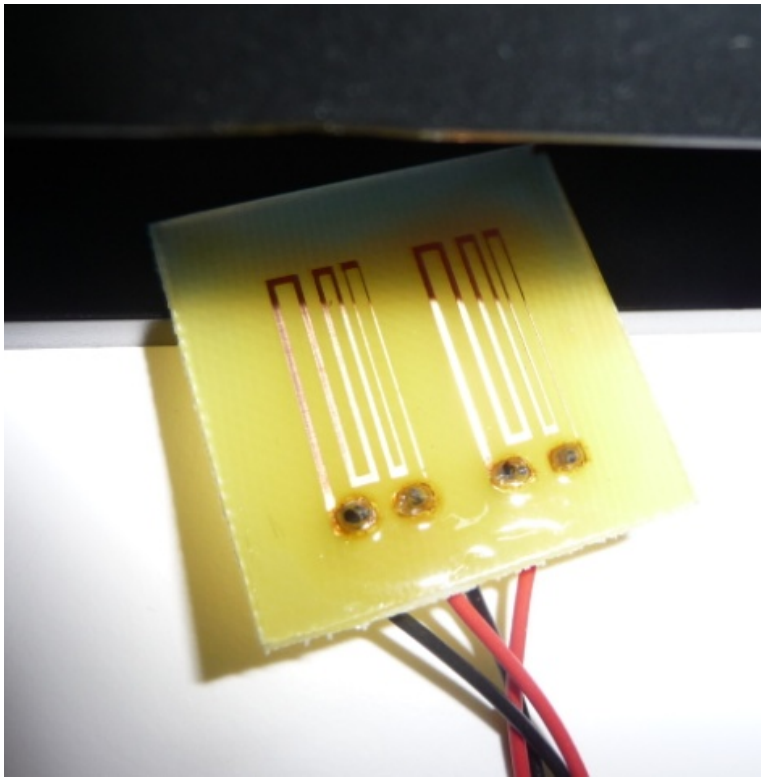

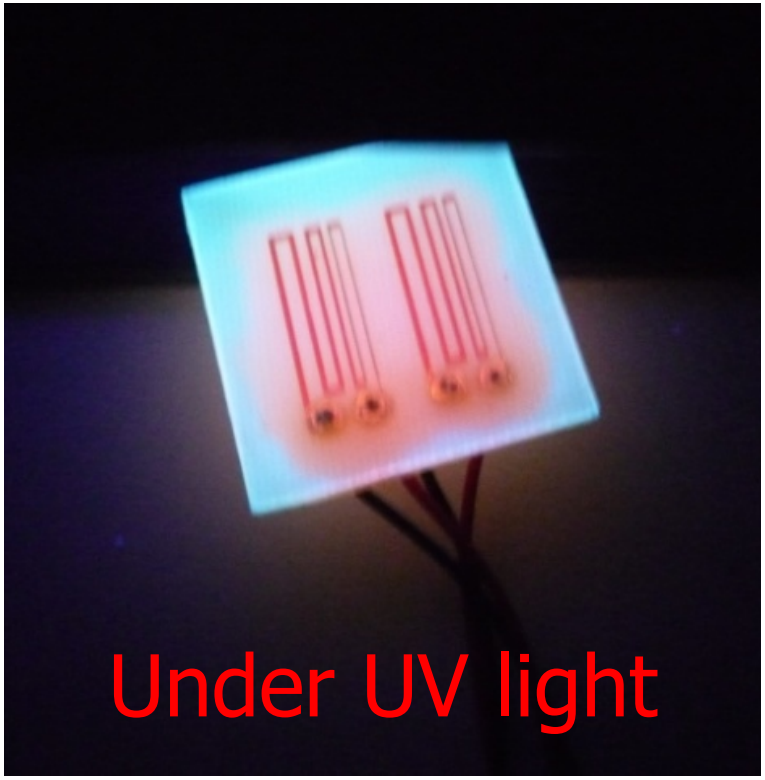

Temperature gradients up to 0.03 degree·µm^{-1}

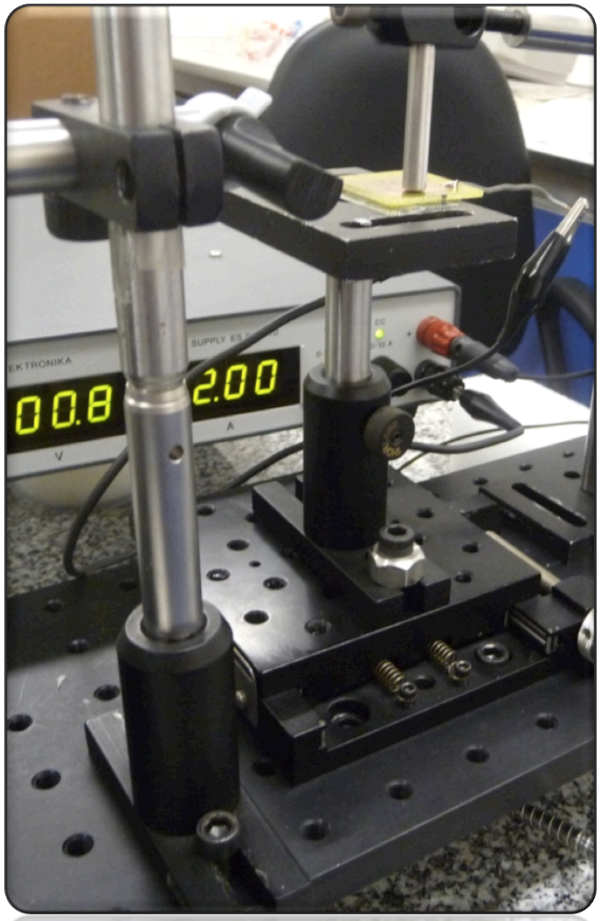

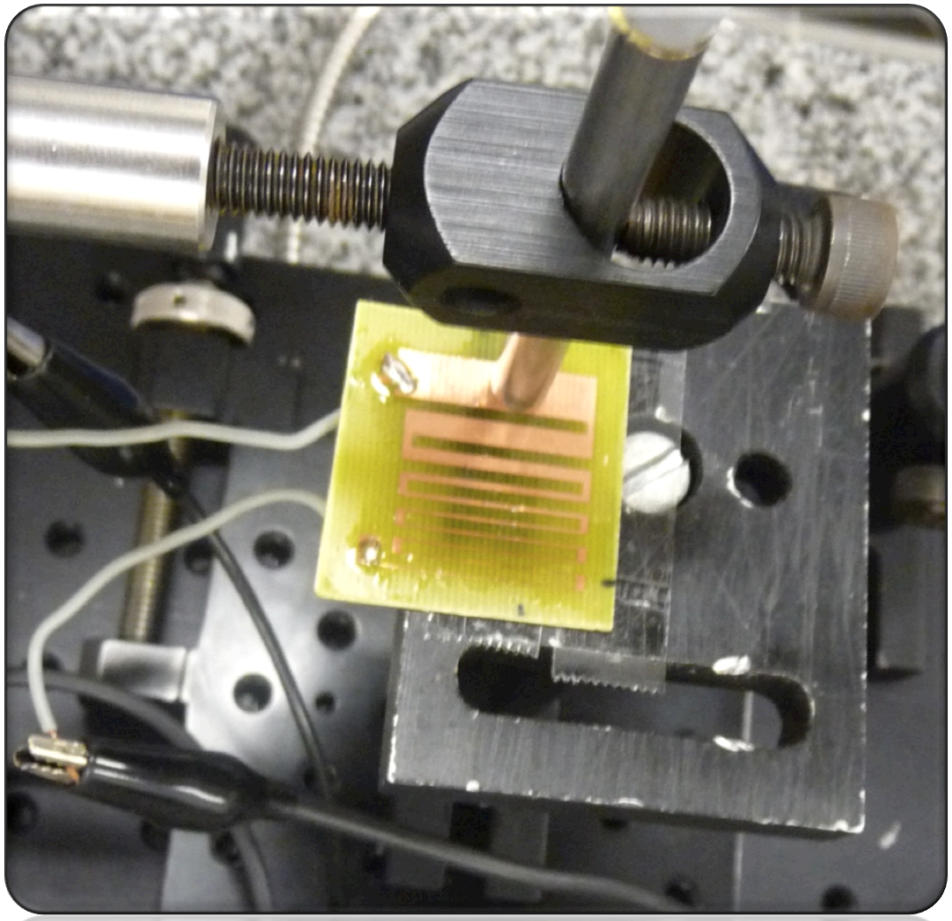

to move the circuit with a precision of 100 µm

M – Monocromator C – Colimating Lens
F – Optical Fiber D – Detector

(precision of 100 µm)

Fiber Tip

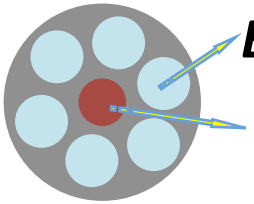

Excitation (355 nm)

Detection (inner diameter 450 µm)

State-of-the-art commercial infrared camera (thermal image)

- Flir i50
- Pixel ≈350 µm
- Thermal sensitivity of 0.1 degree

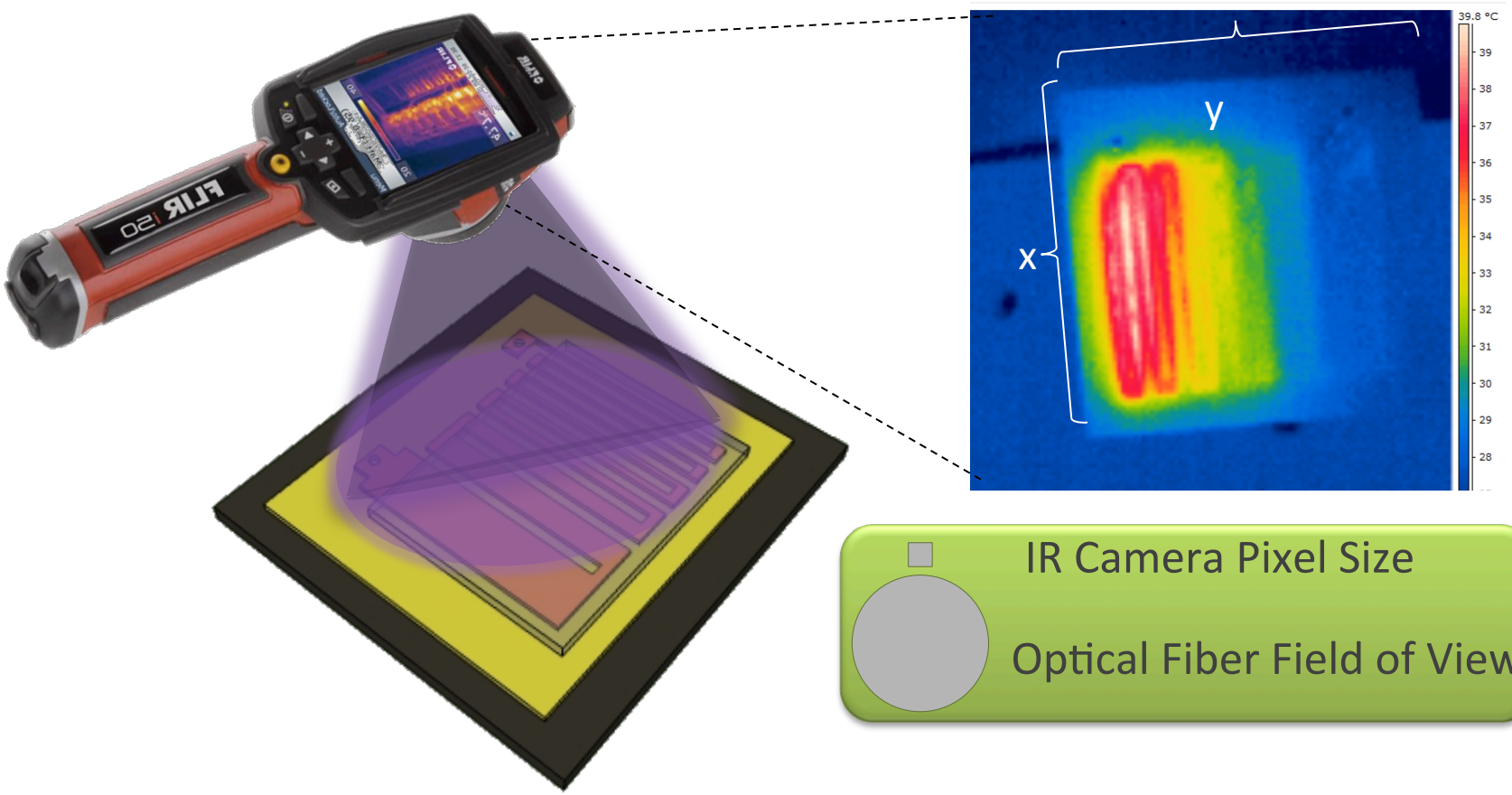

Comparing Measurements

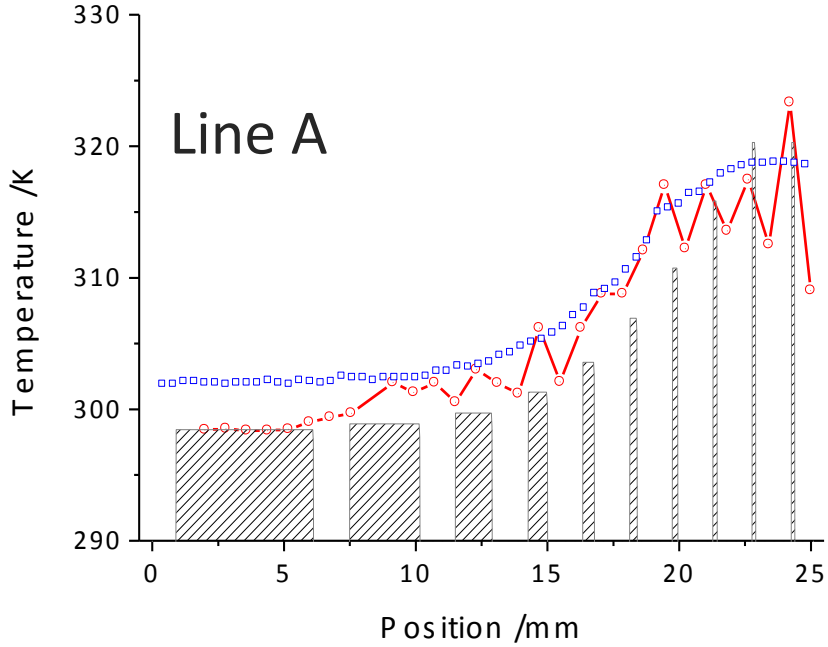

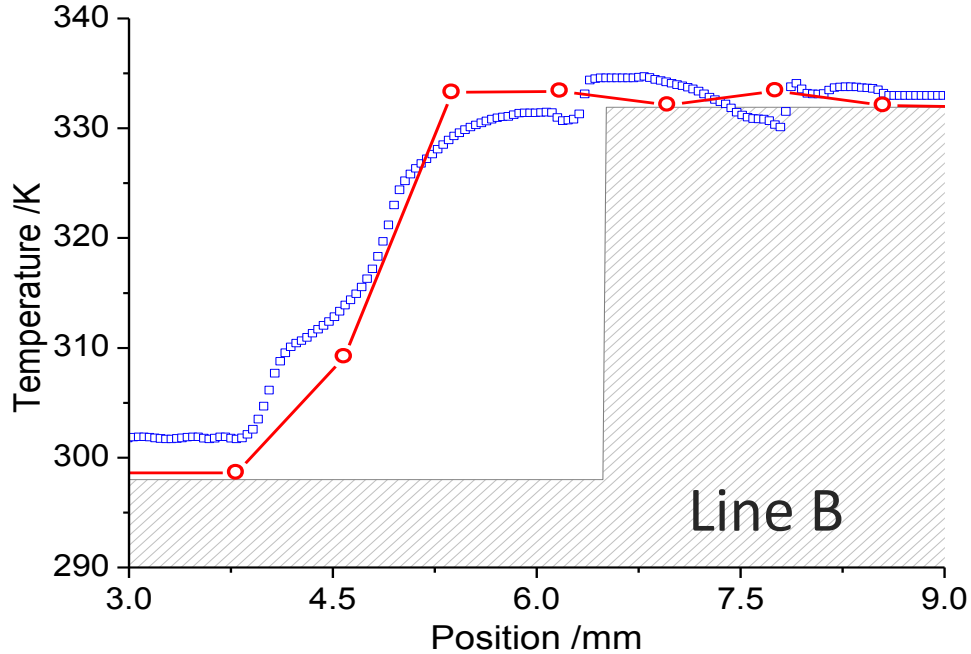

IR camera temperature profile

Spectral extrapolated temperature

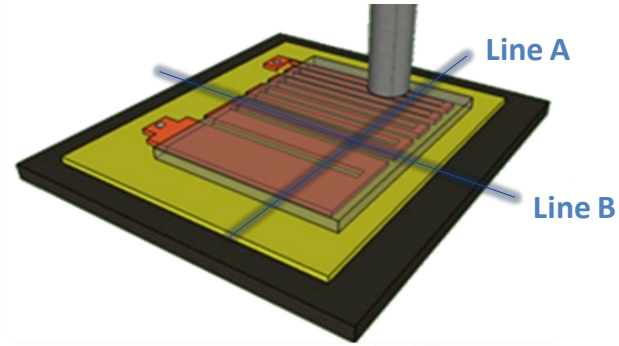

- Spatial resolution (line B, **step: 793 µm**): ***35 µm***, estimated by the minimal distance resolved by the thermometer when *T* changes above 0.5 K (*T* uncertainty)

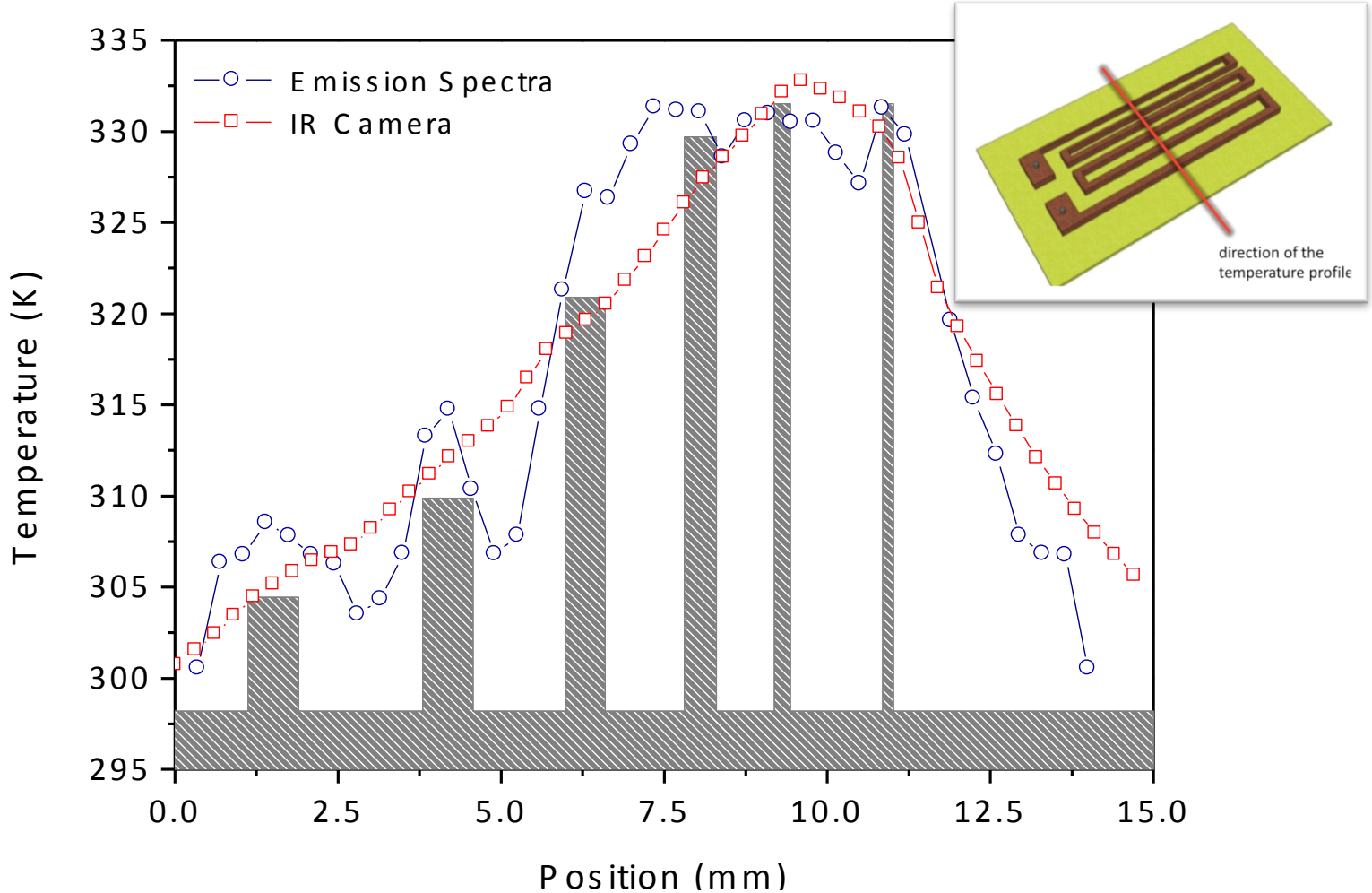

- Step between two consecutive measures of the translation stage: 350 µm (< diameter of the detection fibre)
- Spatial resolution: 3.42 µm (0.146 °C/µm)
- Spectral resolution (or resolving power) of our device (measure of the ability to resolve T in the T map) ≈100 (350/3.42)

- Good agreement between IR camera results and the spectroscopic extrapolated *T*
- Spatial resolution of the molecular thermometer limited by the optical fiber numerical aperture (area < 1 mm^2)
- Measure *T* gradients and discern *T* changes much better than the IR camera:
  - The camera cannot resolve *T* in 0.7 mm range
  - The field of view of the optical fiber can be reduced using lower numerical apertures

Varying the step with the 450 μm fibre

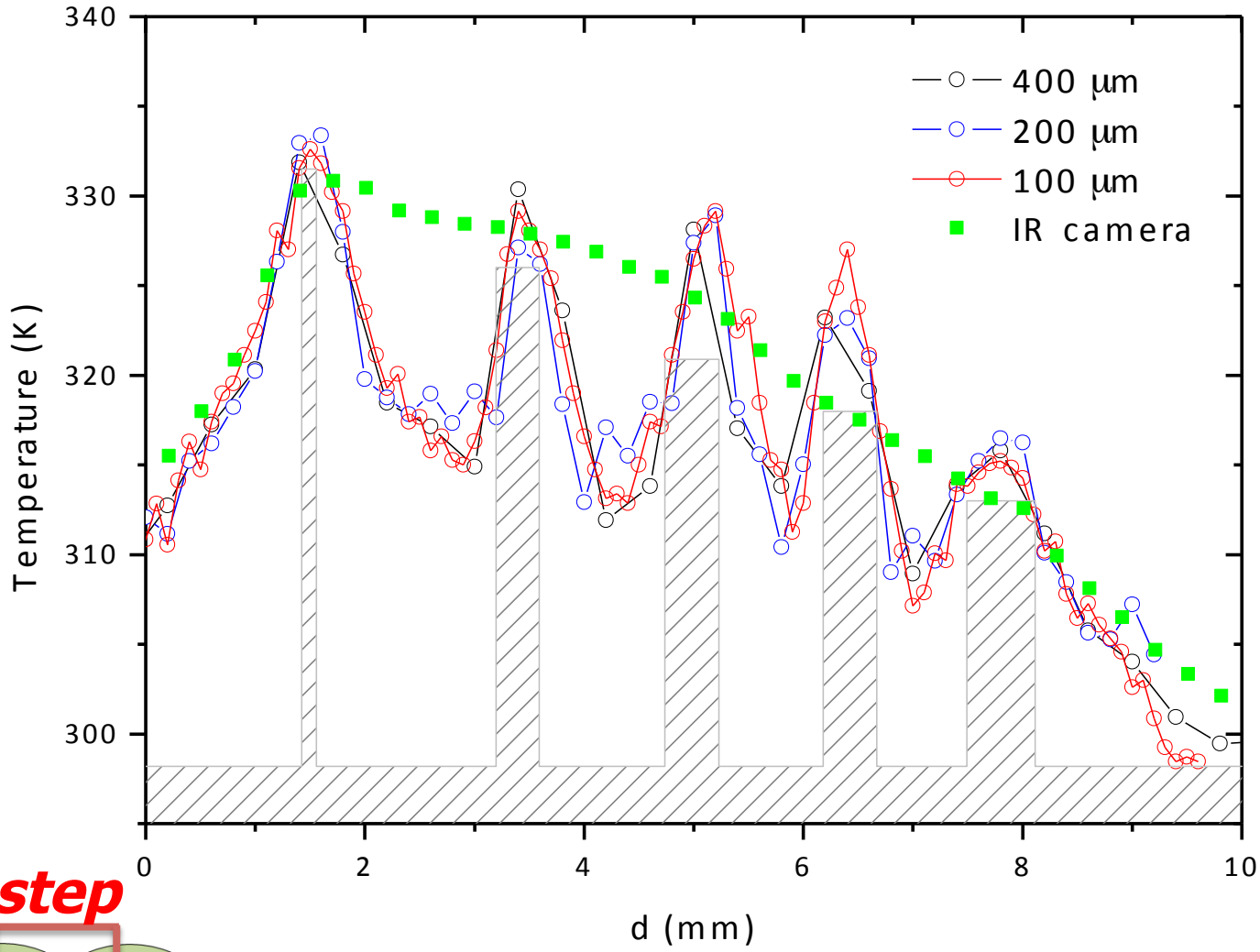

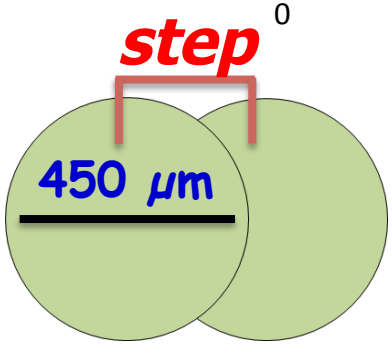

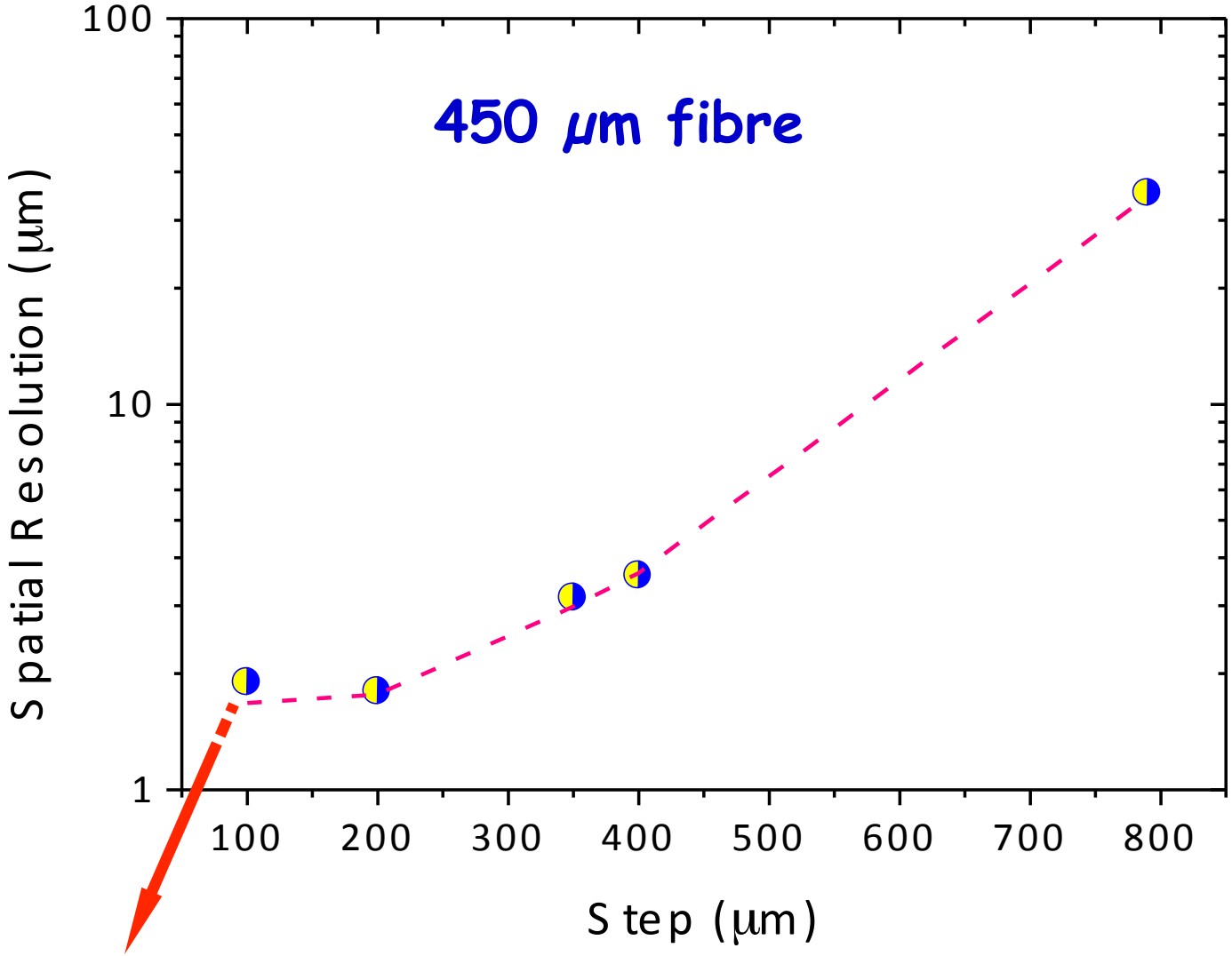

Minimum spatial resolution

Maximum slope on the temperature changes

A

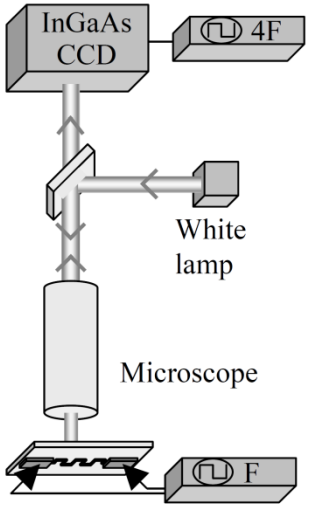

B

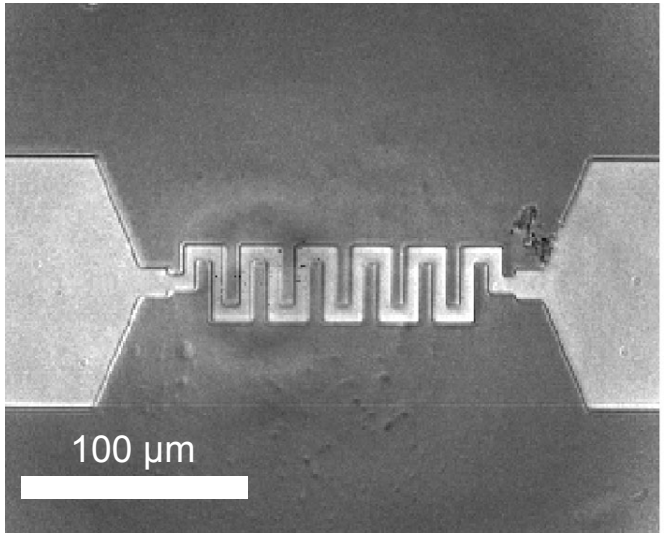

Set-up used for thermoreflectance described in the reference [230] for imaging through the substrate with an InGaAs CCD camera (A). The device is powered at a frequency F with contact needles on its active lower side. (B) Thermal image of a gold resistor dissipating 609 mW, obtained through the 500 µm silicon substrate with a ×50, NA=0.6, objective. The resolution measured along the dotted line is 1.7 µm, which is the diffraction limit. In silicon near the resistor the temperature step corresponds to 27 K.

Indeed there are not many examples of references reporting such measurement in a quantitative way. The exception is a report of Tessier *et al.*. The author reports a temperature mapping using a hermoreflectance-based algorithms operating at 536 ± 13nm wavelengths in order to obtain temperature images. The calibration curve uses the relative variation of the reflectance R/R with the temperature, finding a linear relation with slope $(3 \pm 0.5) \times 10^{-5}$ per degree.

G. Tessier *et al.*, ***Appl. Phys. Lett.*** 2007, 90, 171112

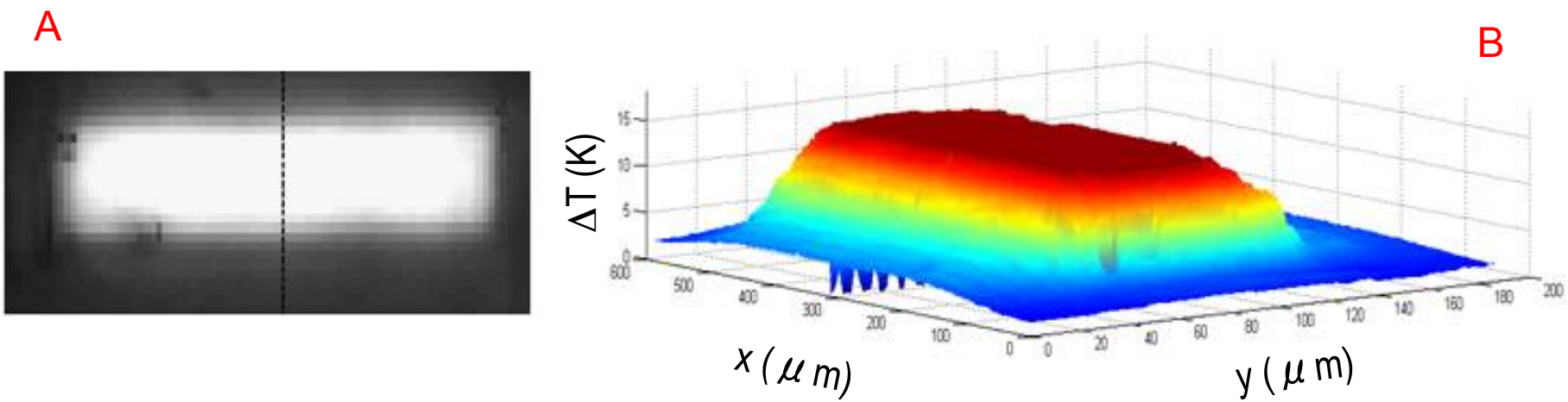

Figure 5.17: Temperature mapping described in reference [230]. The temperature profile (B) is perfectly continuous, unlike what is observed under visible illumination, when several materials are seen under the encapsulation (A)

The 2D temperature mapping reported was imported to MatLab rand the temperature profile presented in figure 5.17. The spatial resolution reported is ~ 1.7 µm, and limited by the diffraction limit that depends on the wavelength used.

This value in good agreement with that obtained for the 450 µm-core fibre diameter.

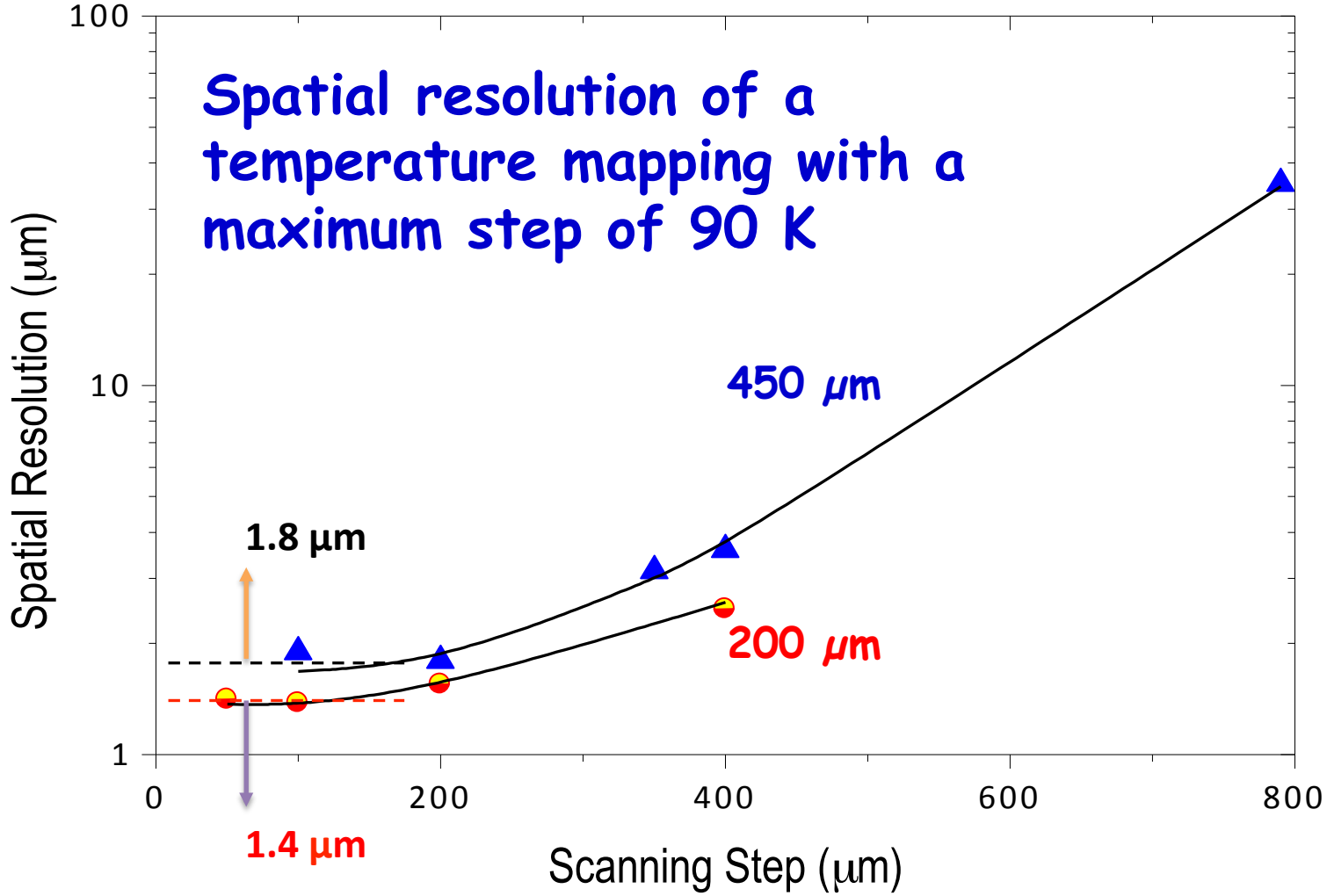

- Spatial resolution on temperature mapping (in units of distance to originate a temperature uncertainly of 0.5 K) using different scanning steps (horizontal axis) for two fibres with different inner diameters.

V. Conclusions and outlook

The luminescent molecular thermometer combines:

- Ability to fine-tune emission color as a function of temperature and Eu^{3+}/ Tb^{3+} proportion
- Self-referencing that allows absolute measurements
- 4.9%·K^{-1} maximum temperature sensitivity (better than 0.5%·K^{-1} in the physiological temperature range)
- High photostability for long-term use
- Flexibility to be processed as thin films for sensing/mapping large areas with a spatial resolution limited by the size of the optical detectors (≈1-10 µm for commercial optical fibers and CCD cameras)
- Temperature uncertainty of 0.5 degree
- Multifunctionality, as it can be hosted in silica-coated magnetic NPs

- The synergetic outcomes arising by combining *T* sensing/mapping and superparamagnetism opens the way for new exciting applications, ***especially in the biomedical field.***

- Such association will provide a unique instrument to map, in a non-invasive way, temperature distributions in biological tissues (*e.g.*, in tumors) during heat release, due to the application of an ac field to magnetic NPs (magnetic hyperthermia), this being, with no doubt, a powerful tool for the study of biochemical micro-processes occurring within a cell.

H. Huang *et al.*, ***Nature Nanotechnology*** 2010, 5, 602–606

ACKNOWLEDGEMENTS

university of aveiro
theoria poiesis praxis

ciceco
centre for research in ceramics & composite materials

Rute Ferreira

Júlio Gonçalves

A.L. L.Videira

Instituto de Telecomunicações (Aveiro)

Carlos Vicente

André Martins

Paulo André

UNIVERSIDAD DE ZARAGOZA

Victor Sorribas

EMMI

enermat
NEW MATERIALS FOR ENERGY

FUNDAÇÃO PARA A CIÊNCIA E TECNOLOGIA

COMPETE and FEDER programs (Portugal)

PEst-C/CTM/LA0011/2011; PTDC/CTM/101324/2008

Nanobiotec-CAPES network (Brazil) for a grant

Integrated Spanish-Portuguese Action PT2009-0131

EUROPEAN MULTIFUNCTIONAL MATERIALS INSTITUTE

ENERMATaa 2009-1/086

FCT
Fundação para a Ciência e a Tecnologia

COMPETE
PROGRAMA OPERACIONAL FACTORES DE COMPETITIVIDADE

GEHybrids
Group of Functional Organic-Inorganic Hybrids